Wind and Solar PV Resource Aggregation Study for South Africa

Final report

RFP No. 542-23-02-2015

Kaspar Knorr, Britta Zimmermann, Dr. Stefan Bofinger, Ann-Katrin Gerlach
Fraunhofer IWES

Dr. Tobias Bischof-Niemz, Crescent Mushwana
CSIR Energy Centre

1st November 2016

Executive Summary

The 'Wind and Solar PV Resource Aggregation Study for South Africa' was carried out to increase the fact base and understanding of aggregated wind and solar photovoltaics (PV) power profiles for different spatial distributions of these renewable energy sources throughout the whole country. Potential to generate electricity from wind and solar PV energy was determined based on data sets for five years covering the whole country with a spatial resolution of 5 km by 5 km and a temporal resolution of 15 minutes. Aggregation effects were investigated for a number of geographical distribution scenarios with varying penetrations of solar PV and wind energy.

The primary findings of the study include the following:

- The wind resource potential is as good as the solar resource. Almost the entire country has sufficient resources with **potential for very high load factors and, thus, profitable wind projects**. It is possible to generate significantly more electricity from wind and solar PV energy than what is needed by the country even when considering spatial exclusion zones.
- While the solar irradiation and electricity generation from solar PV shows nearly **no seasonality,** wind speeds and generation from wind closely follows the demand over the year. In addition the diurnal characteristics of wind feed-in complement the solar PV peak by showing a minimum at noon. Those **complementary effects** enable the integration of wind and solar PV power into the grid to a great extent.
- As determined in [1], at least **20% overcapacity of wind and solar PV power can be installed per substation without any curtailment** of wind and solar PV power.
- **Gradients of the electricity feed-in from wind generation can be reduced** noticeably through aggregation effects (more distributed wind turbines result in reduced fluctuations). A wider distribution of turbines also leads to a significant reduction of forecast errors.
- Finally, up to **20 to 30% energy share of variable renewable energies (wind and solar PV) for the whole country will not increase short-term (15 min) gradients** or ramps significantly if there is a balanced combination of wind and solar PV in the electricity system.

Wind and Solar Resource Aggregation Study
for South Africa

Contents

1. Acronyms

Capex	Capital expenditure
CSIR	Council for Scientific and Industrial Research
EIA	Energy Environmental Impact Assessment
IEC	International Electrotechnical Commission
IWES	Institute for Wind Energy and Energy System Technology
LCOE	Levelised cost of energy
LF	Load factor
NWP	Numerical weather forecast
PV	Photovoltaics
REDZ	Renewable Energy Development Zone
RMSE	Root-mean-square-error
SANEDI	South African National Energy Development Institute
TDP	Transmission development plan
VRE	Variable renewable energies
WASA	Wind Atlas for South Africa
WRF	Weather Research and Forecasting model

2. Introduction

Similar to many countries, South Africa faces an inevitable phase-out of old fossil fuelled power plants (mostly coal based) whilst the electricity demand is expected in the future. The international political willingness for a CO_2-reduction along with significant cost reductions for variable renewable electricity generators like wind and solar PV are often suspected to lead to new challenges regarding grid stability and security of supply. Undoubtedly, a certain amount of flexibility will be needed in a system with increasing shares of weather-dependent renewable energies. However, aggregation effects, which smooth out volatilities in the feed-in of electricity from these resources, occur for spatially distributed installations. This study focuses on the evaluation of aggregation effects by investigating scenarios for the allocation of renewable electricity generators.

In South Africa, it is expected that the major growth in renewable supply will be provided by wind and solar PV energy. Wind and solar PV energy are fluctuating resources and cannot be scheduled like conventional power plants. However, the variability of wind and solar power decreases with increasing scale of the power supply system as many short-term fluctuations are balanced by a spatial smoothing effect. Furthermore, the combination of wind and solar PV energy exhibits potential to further reduce temporal variability on longer time-scale. Obviously, to benefit from the spatial smoothing effect, the large-scale transport of energy is required to ensure the stability of the power system.

The planning of the infrastructure of the future power system can be supported based upon simulations of weather-related wind and solar PV energy generation over a long time in combination with the constraint to meet the demand at any time.

From a relatively low base, South Africa is planning to extend the capacity of wind and solar power as described in the Department of Energy's Integrated Resource Plan (IRP 2010) [2]. Regarding wind conditions and solar irradiation, South Africa is richly endowed. As can be seen from Figure 1, there are only few parts of the world where wind speeds or solar irradiation are as high as in South Africa.

Nevertheless, the installed capacities for electricity generation from renewable energy sources are still low compared to other countries with significantly less wind and solar resources.

The determination of the potentials for electricity generation from wind and solar PV energy in a high spatial resolution is a primary output of this study. In addition, the study has quantified the wind energy resource potential in the whole country, something that had not be done before.

Figure 2 shows the results of a first assessment regarding the feed-in of electricity generated from wind and solar photovoltaics (PV) for single squares of about 25 km² in the area of Port Elizabeth (Eastern Cape) and for a whole supply area in comparison (see chapter 9.1 and [3]). On the September day depicted, a sound smoothing of the fluctuations of both wind and PV feed-in is clearly visible. For a comprehensive planning of the future of renewable energies in South Africa and their efficient integration into the grid, a further investigation and a deep understanding of the aggregation effects is necessary.

The Council for Scientific and Industrial Research CSIR of South Africa in collaboration with the South African National Energy Development Institute (SANEDI) and Eskom undertook a study with the overall objective to increase the fact base and the understanding of aggregated wind and solar PV profiles in South Africa for different spatial distributions and penetration levels of wind/ PV, in order to serve as an input for South African energy planning processes. This includes an improvement of the data for wind power, a transfer of knowledge and skills to South Africa, and the illustration of the possible contribution of wind power to a secure and affordable electricity supply in South Africa.

Wind and Solar Resource Aggregation Study
for South Africa
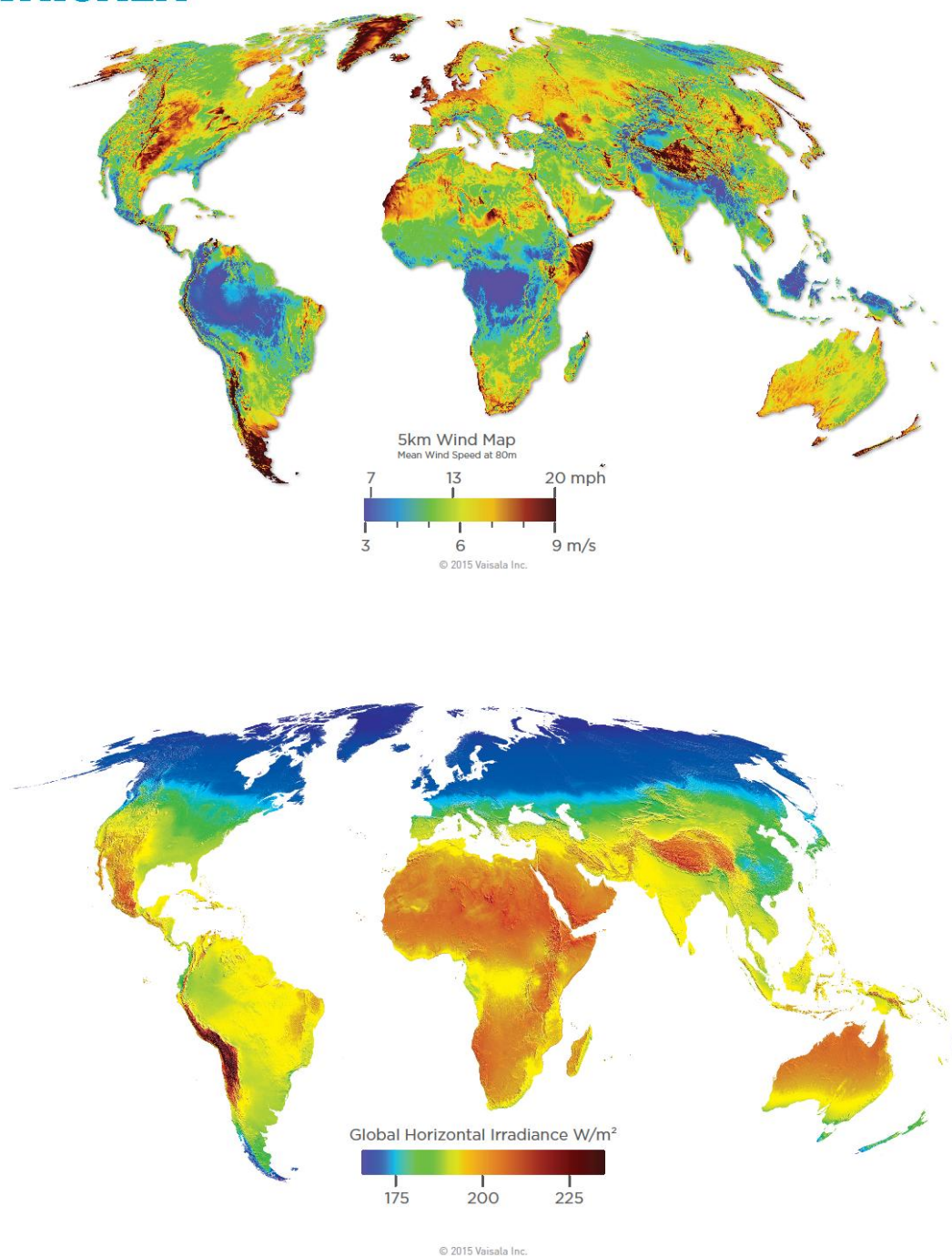
Figure 1: Global maps of wind speed (top) and solar irradiation (bottom)

Wind and Solar Resource Aggregation Study
for South Africa
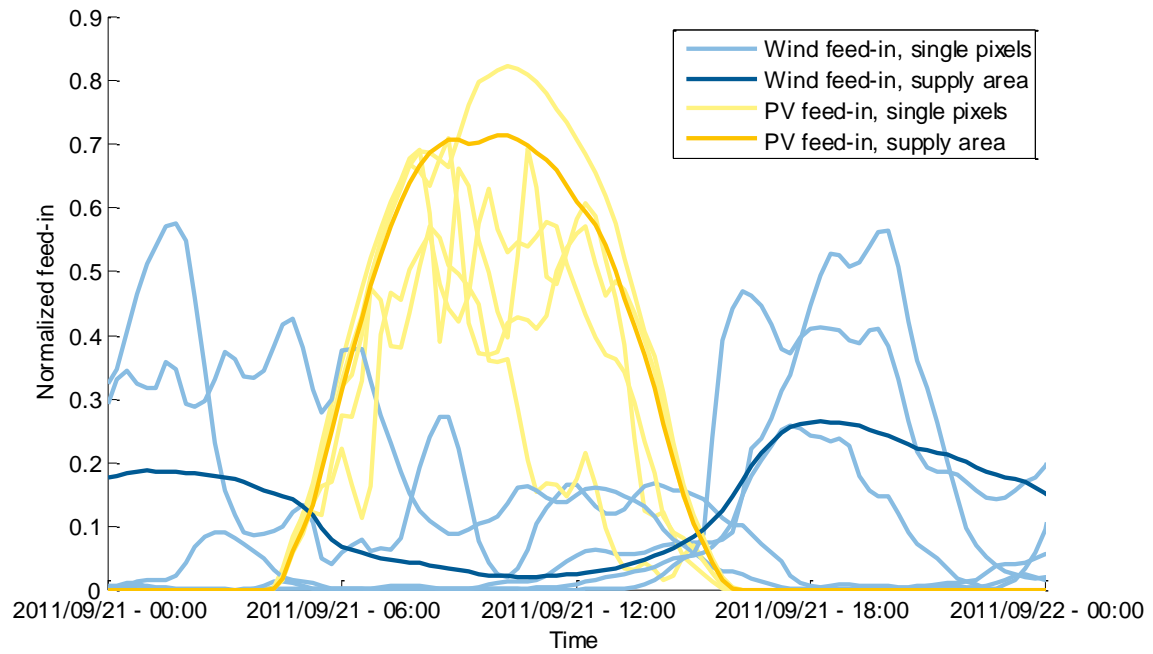
Figure 2: Wind and PV feed-in of single squares and of Port Elizabeth supply area on September 21, 2011

Wind and Solar Resource Aggregation Study
for South Africa

3. Methodology

For this study, wind speeds and solar irradiation were generated for a high spatial resolution with the help of numerical weather models. Theoretical and actual potentials for electricity generation from wind and solar PV energy in South Africa were determined, the latter considering areas to be excluded for structural, scenic or administrative reasons. A future electricity demand was estimated based upon information on historical demand. Different scenarios regarding the spatial distribution of wind turbines and solar installations in South Africa were developed. Some scenarios can be called 'scientific' as the distribution of turbines is assumed to follow rather academic and unrealistic rules which, nevertheless, provide useful results because they show extreme or ideal view. This set includes a uniform wind turbine distribution across the whole country in contrast to building all wind turbines in one location as well as a distribution according to wind speeds and an allocation of turbines optimised in order to result in minimal ramps of the residual load (demand less the feed-in based on wind and solar PV). Other scenarios consider areas already declared for renewable energy, the so-called 'Energy Environmental Impact Assessment' (EIA) areas and 'Renewable Energy Development Zones' (REDZ). The last set of scenarios was set up to investigate the aggregation effects if locations for wind turbines were chosen to minimize their distance to the current and planned electricity grid. The grid used was the transmission grid as per the Transmission Development Plan (TDP 2014 – 2024) [4].

The scenarios were analysed and evaluated considering the following performance parameters:

- Aggregation effects
- Change in residual load
- Load factors
- Forecasting issues

The methodology, scenarios, and the results are described in detail in the following sub-sections.
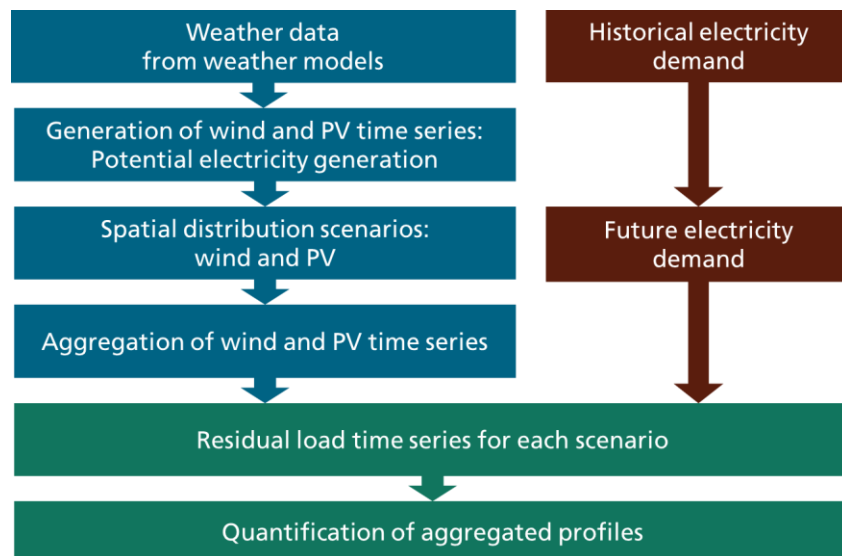

Figure 3: Methodical approach

Wind and Solar Resource Aggregation Study
for South Africa

3.1   Numerical weather models

Measured weather data are available only for certain measuring points. If data for a whole area or, as in this case a whole country, are needed, time-series for high spatial resolutions can be calculated with the help of numerical weather models. For this study, two different weather models were applied, i.e. Wind Atlas for South Africa (WASA) [5] for wind-related time-series and temperatures, and SODA [6] for modelling the solar-related time-series.

The WASA model uses the mesoscale downscaling method presented in [5] to generate time-series of wind speed and other meteorological fields for Southern Africa. It uses the Weather Research and Forecasting model (WRF) [7], a widely-used open-source mesoscale modeling system.

The global irradiation data used are derived from satellite-based images according to the Helioclim model. The time-series were adapted to 5 km by 5 km matching the resolution of the wind time-series.

The most relevant characteristics of the two models are listed in Table 1.

Model name	WASA	SODA
Variables	v, T	I
Height	2 m (T) 50 m, 80 m, 100 m, 150 m (v)	2 m
Temporal coverage	2009 to 2013	2010 to 2012
Temporal resolution	15 min	15 min
Spatial coverage	South Africa	South Africa
Spatial resolution	5 km x 5 km	0.2° x 0.2°

Table 1: Characteristics of the applied numerical weather models

As shown in Table 1, the wind-related data and temperatures were modelled for five years (2009 to 2013) while the solar-related data cover three years (2010 to 2012), each for a temporal resolution of 15 min. The temperature and solar irradiation data are available for a height of 2 m, and the irradiation data are valid for a 0.2° by 0.2° latitude vs. longitude grid.
The WASA model delivers wind speed data for the different heights of 50, 80, 100 and 150 m. Wind speeds for other heights were calculated using the log wind profile equation assuming neutral stability conditions. The mean wind speeds at a height of 100 m above ground are shown in Figure 4.

Having a spatial resolution of 5km by 5km, approximately 47 500 grid squares henceforth referred to as 'pixels' are needed to cover South Africa (see Figure 5). Having a temporal resolution of 15 minutes, 175 296 time steps are needed to cover a period of five years. This means that the data basis of wind speeds in a certain height above ground contains approximately 47 500 x 175 296 ≈ 8.33 billion values. The data requirements on weather data used for this study are accordingly even bigger as a result of four heights above ground, the temperature and the solar irradiation data.

Nevertheless, it has to be analysed if this data basis is sufficiently precise to understand the potential for electricity generation from wind and solar PV energy in South Africa. Regarding the spatial precision, a sufficiency analysis is performed in the next chapter. Regarding the absolute values and the temporal behaviour of the wind speeds of the weather model, a comparison with measurements is drawn in chapter 3.1.2.
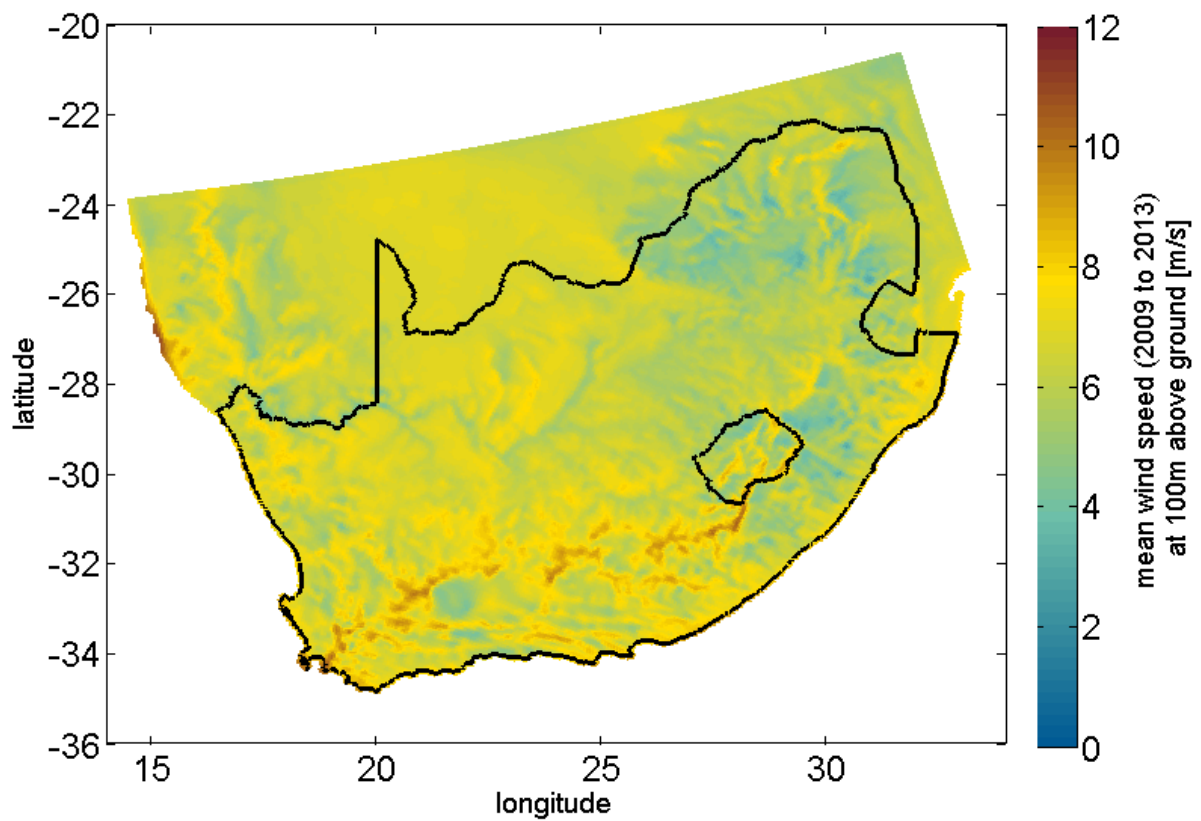
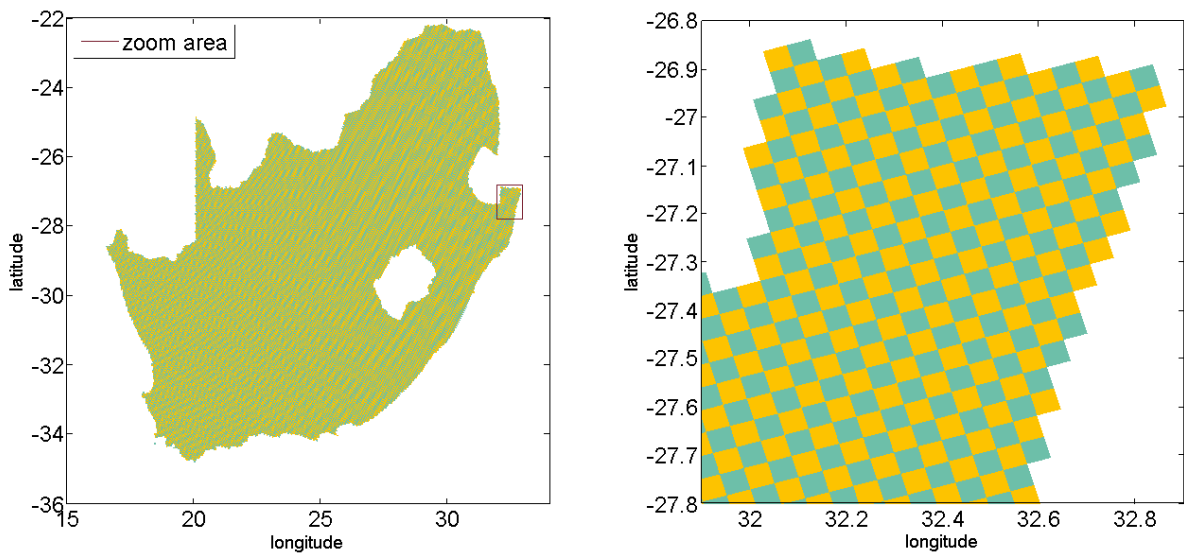**Figure 4: Mean wind speeds in a height of 100 m above ground**

Figure 5: Illustration of the used spatial resolution of the study. The grid squares have an area of 5km by 5km. The left figure shows the whole country. The spatial resolution becomes visible in the zoom-in on the right figure.
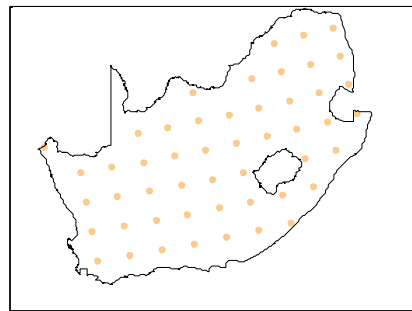
3.1.1 Sufficiency analysis

In order to evaluate the sufficiency of the spatial resolution of the used weather data for the purposes of this study, the wind speeds were transformed to electrical power using the models described in chapter 3.2.3. After doing so, a time series of wind power production of each pixel is produced. In a first step, the time series of all pixels were aggregated to obtain a single time series for the whole of South Africa. In a second step, the time series of every second pixel were aggregated, again in order to obtain a single one for the whole of South Africa. This process was continued for increasing pixel distances (every third pixel, every fourth and so on) until a distance of 70 pixels equivalent to 350km. Figure 6 clarifies this method by the example of four distances.
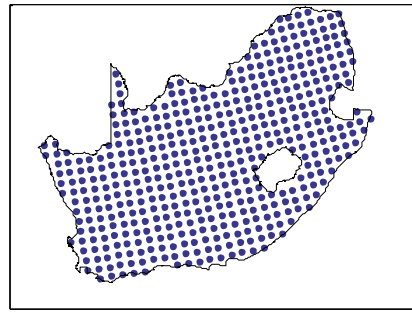
Approximate pixel distance: 50 km
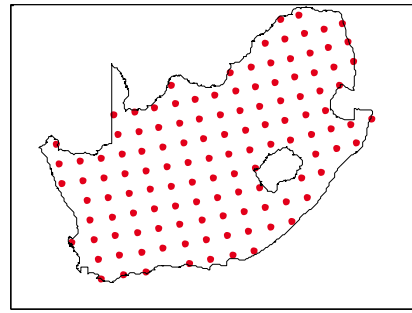
Approximate pixel distance: 100 km

Approximate pixel distance: 150 km
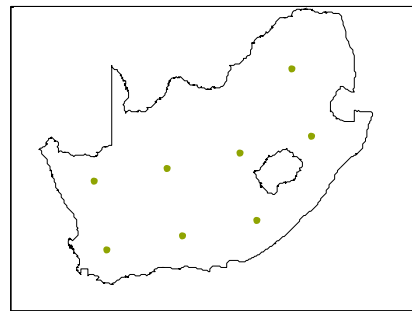
Approximate pixel distance: 350 km

Figure 6: Illustration of pixel selection for the sufficiency analysis

It becomes clear that, for long distances, only a few pixels fall into the boarders of South Africa. Using only few pixels, the aggregated time series strongly depend on their locations. In order to circumvent this dependency, different starting pixels ('layouts') were used for every pixel distance. If possible, sixteen layouts were applied for every pixel distance, as shown in Figure 7 by the example of a pixel distance of 350km.

Wind and Solar Resource Aggregation Study
for South Africa

Approximate pixel distance: 350 km

Figure 7: Illustration of the layouts of pixel selection for the sufficiency analysis

Figure 8 shows the normalised standard deviations of the aggregated time series of every used pixel distance and layout. As mentioned above, the influence of the layouts on the characteristics of an aggregation (measured as the standard deviation of its time series in this case) tends to be larger for long pixel distances as for short. The mean dependence of the standard deviations on the pixel distances is shown as black line. T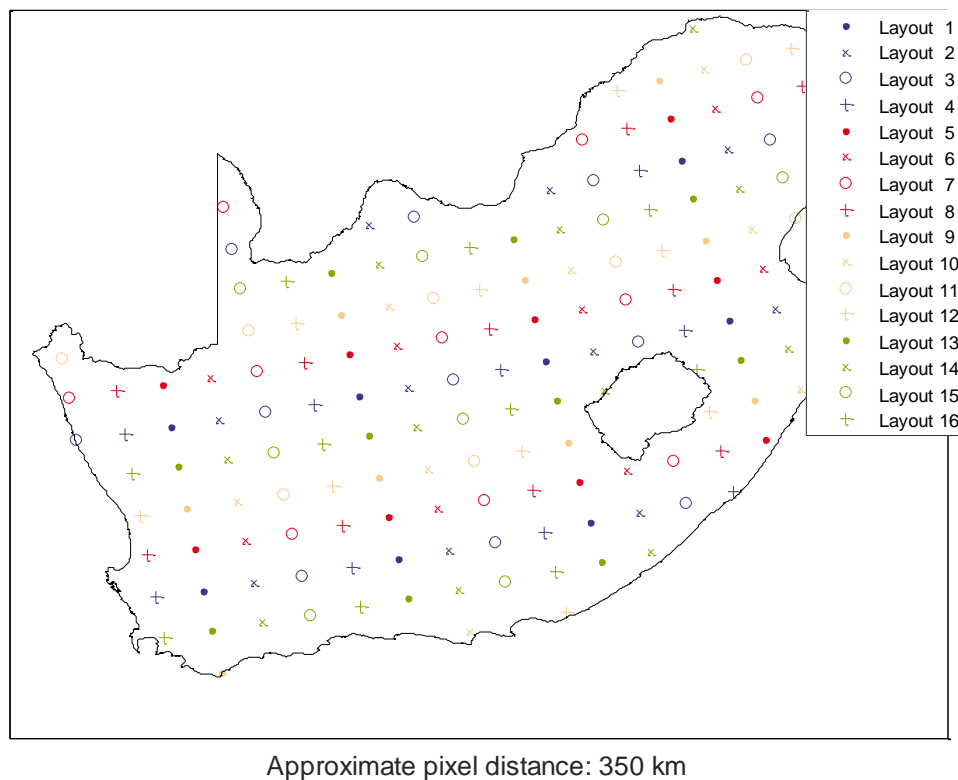he standard deviation increases with increasing pixel distance. This means that an aggregation study based on spatial data with a poor resolution will overestimate the variability of the wind power feed-in. However, the spatial resolution of this study (5km by 5km) is sufficient according to the investigation since there is a stable behaviour of the standard deviation in the range from 5km up to 50 km pixel distance.

Figure 9, which shows the standard deviations of the gradients of the aggregated time series as a function of the pixel distances, has comparable characteristics, albeit the influence of the layouts and the range of a stable behaviour is smaller (approx. 5km up to 20km).

However, even if the spatial resolution of the data basis needed to be higher for a more realistic modelling of the wind power feed-in, a lower resolution would results in higher fluctuations. Higher fluctuations pose greater challenges to the power system. In a power system adapted to fluctuations higher than possibly realistic operational stability related to ramps is ensured.

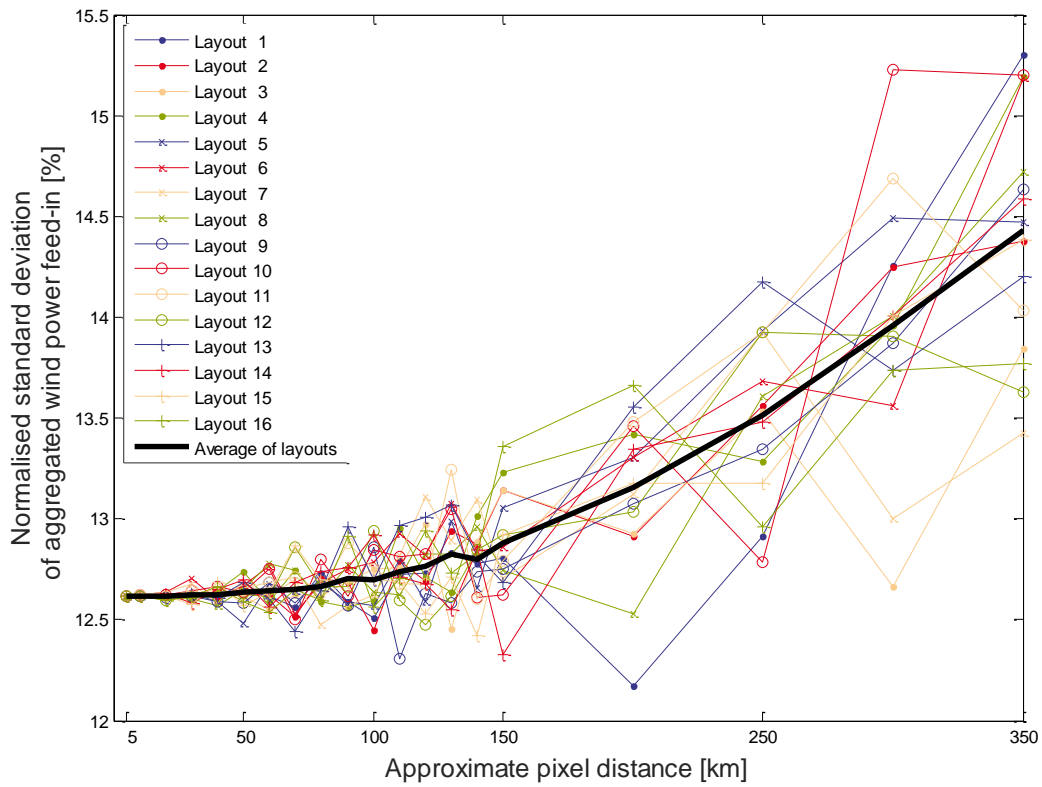Wind and Solar Resource Aggregation Study
for South Africa

Figure 8: Normalised standard deviations of the aggregations
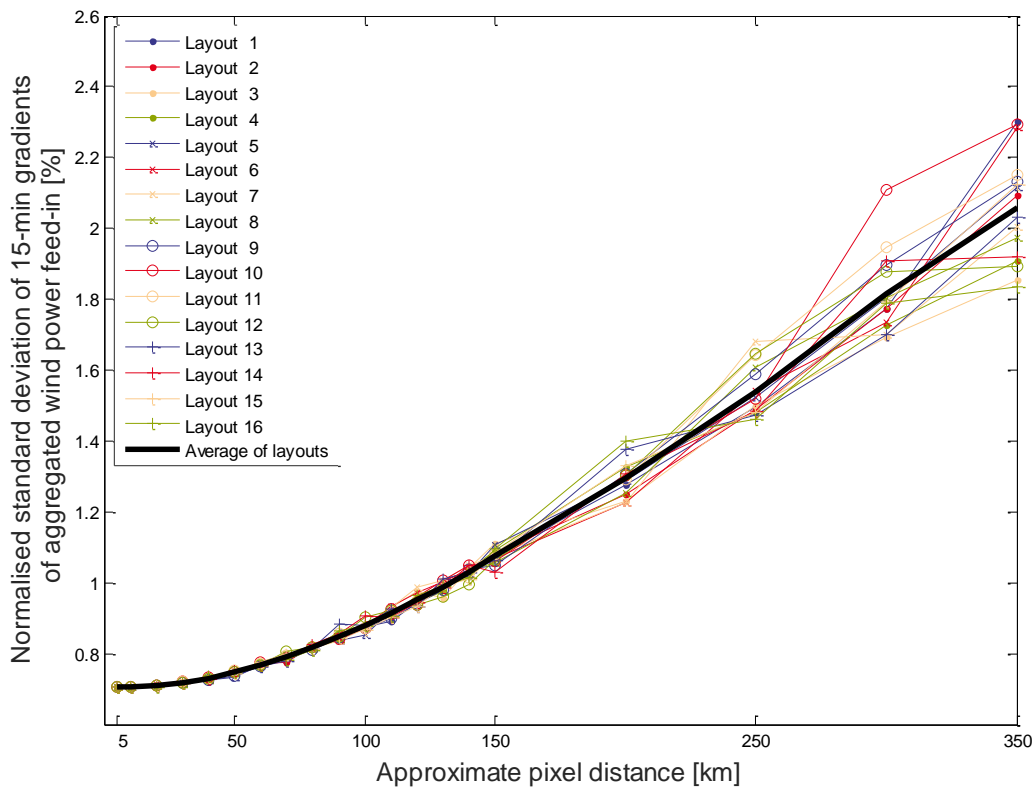
Figure 9: Normalised standard deviations of the aggregations' gradients

Wind and Solar Resource Aggregation Study
for South Africa

3.1.2 Comparison with measured wind speeds

Figure 10 shows the 10 locations of measurement towers used for the WASA Project [8]. On these sites, the wind speeds and directions in several heights up to 60m above ground, the air temperature, the barometric pressure and the relative humidity have been measured since 2010. The measurements are stored as the minimum, mean and maximum values as well as the standard deviation of 10min time steps.
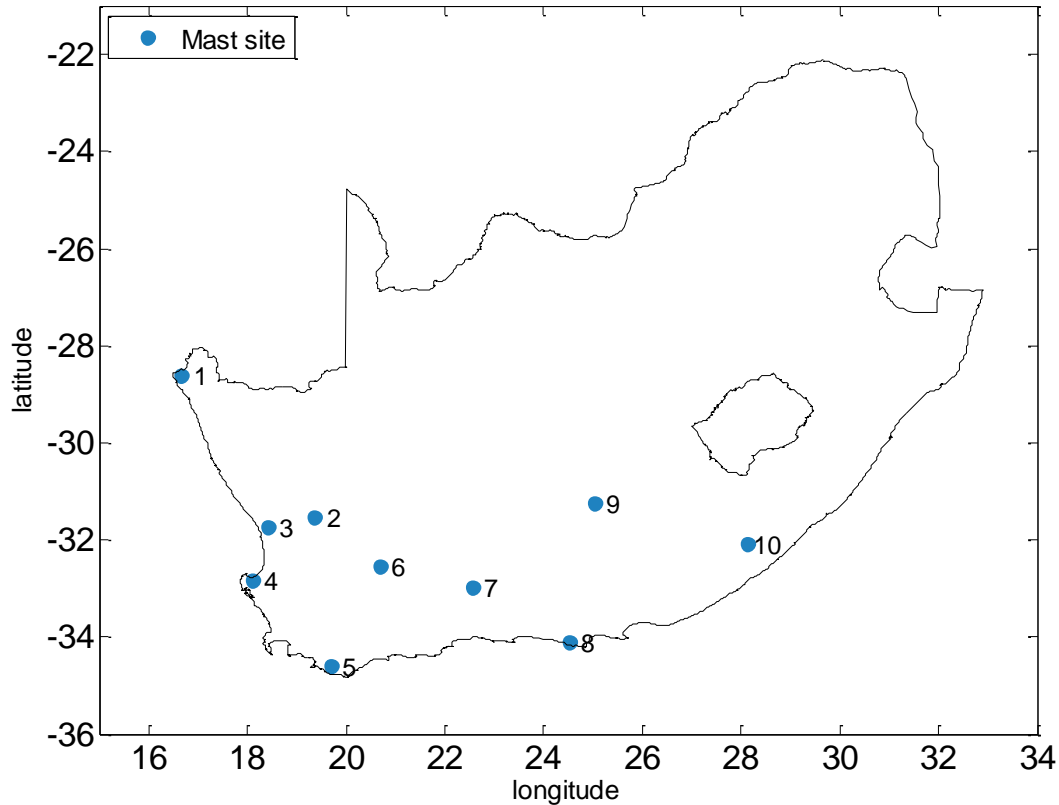
Figure 10: Locations of the WASA masts

For the following analysis, the 10 min mean values of the measured wind speeds at 6m above ground were converted to 15min mean values by a weighted moving averaging. The wind speeds of the weather model were extracted for the 10 mast sites in 50 m and 80 m above ground and logarithmically interpolated to 6om above ground.

Figure 11 and Figure 12 draw comparisons between the characteristics of the wind speeds of the measurements and the weather model using the example of site no.3 and no.7, respectively. Some key metrics, as the mean wind speeds over three years $\bar{v}_{3a}$, the standard deviations over this period $\sigma(v)$, the standard deviation of the increments/gradients of the wind speeds over this periode $\sigma(\Delta v)$, and the correlation coefficient between the wind speeds of the measurements and the weather model r, are stated as well.

Wind and Solar Resource Aggregation Study
for South Africa
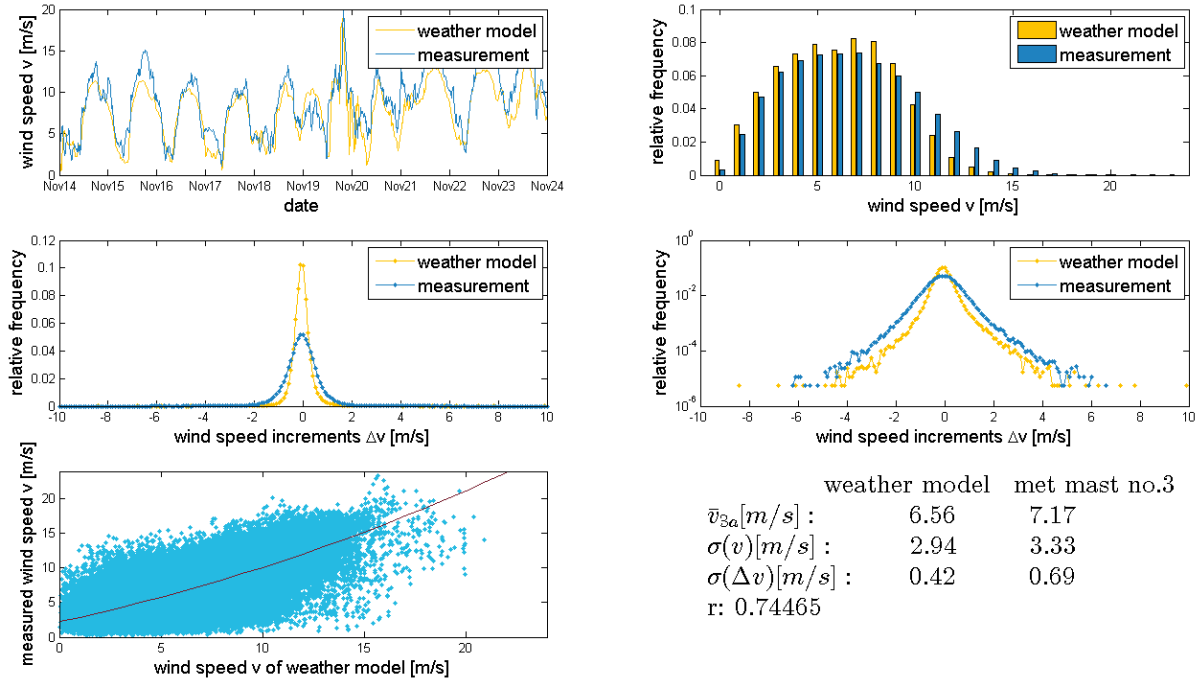
Figure 11: Comparison between the wind speeds of the measurements and the weather model on site no.3
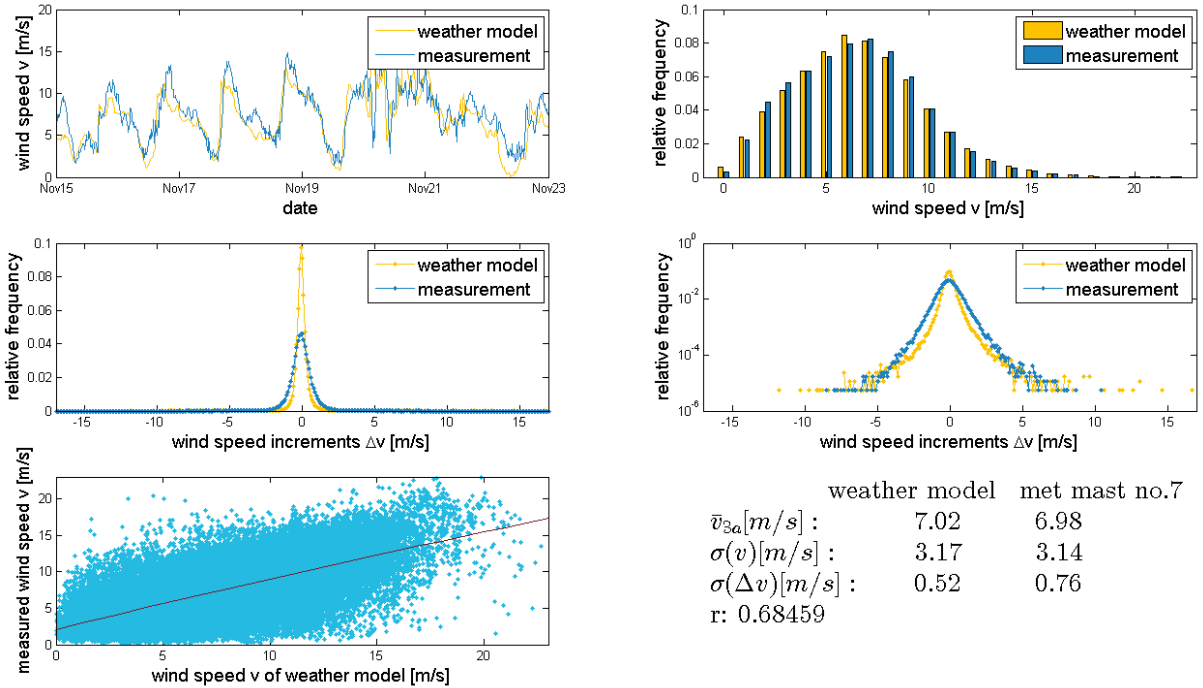
Figure 12: Comparison between the wind speeds of the measurements and the weather model on site no.7

The two chosen examples are representative for all 10 sites. The mean wind speeds $\bar{v}_{3a}$ and the standard deviations $\sigma(v)$ of the measurements and the weather model lie close together. In the case of site no.3 the measured wind speeds and standard deviations are higher on average, in the case of site no.7 it is the other way round. The standard deviations of the wind speed increments are lower for the weather model in both cases. This is a reasonable results as the weather model data is valid for an area, namely the pixels of 5km x 5km while the measurements represent the wind speed of one point in space instead. Thus, the fluctuations of

the weather model (expressed as standard deviations) ought to be lower than the measured ones, since as the area considered becomes larger, there is an increase in the smoothing effect. This correlation is also visible in Figure 13, which shows the comparison between the aggregated wind speeds of the measurements and the weather model. For this analysis, the time series of all 10 sites were averaged for every time step. The standard deviation is consequently lower than for a single site.

	weather model's average	met mast's average
$\bar{v}_{1a}[m/s]$:	7.13	7.13
$\sigma(v)[m/s]$:	1.88	2.00
$\sigma(\Delta v)[m/s]$:	0.19	0.29
r: 0.83903		
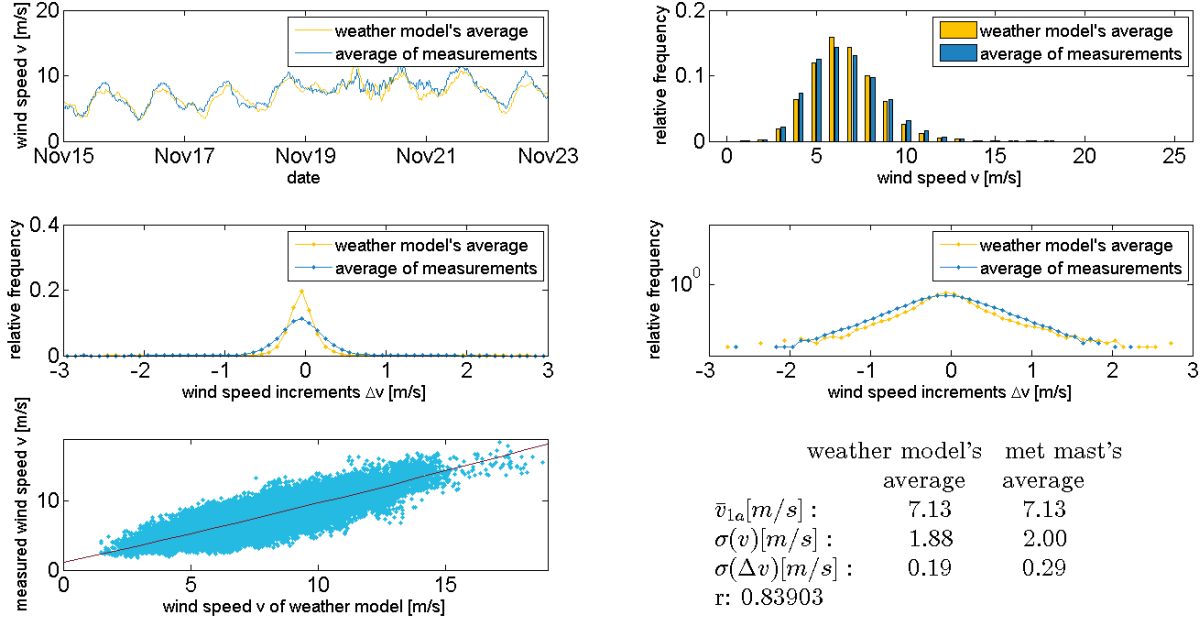
Figure 13: Comparison between the average wind speeds of the measurements and the weather model of all 10 sites

Figure 14 shows the key metrics of all ten sites. As mentioned, the $\bar{v}_{3a}$ of the measurements and the weather model are more or less in balance. The measured $\sigma(v)$ tend to be higher, but there are some sites where the weather model gives higher fluctuations regarding the absolute values of the wind speeds. For $\sigma(\Delta v)$ which is a measure for the fluctuations of the wind speed gradients, the measurements are higher for all sites.

In summary, it can be stated that the weather model give a more or less good representation of the measurements in some aspects, namely the absolute values of the wind speeds and their sequence as can be seen regarding the upper left pictures of Figure 11 to Figure 13. However, it has to be evaluated to which extent this results from a calibration of the weather model to the measurements as part of the WASA project [8]. The correlation coefficients are not very high in all cases (see lower right picture of Figure 14), what might be attributed as well to faults in the measurements. Regarding the metrics for fluctuations, model and measurements differ as a consequence of the areas they represent.

It should be kept in mind, that the purpose of this study is not to precisely model wind speeds of the past, but to understand the possible realistic electricity generation from wind energy in future, based on weather data.

Wind and Solar Resource Aggregation Study
for South Africa

Figure 14: Key metrics of wind speeds of all 10 sites

Wind and Solar Resource Aggregation Study
for South Africa

3.2 Generation of time series
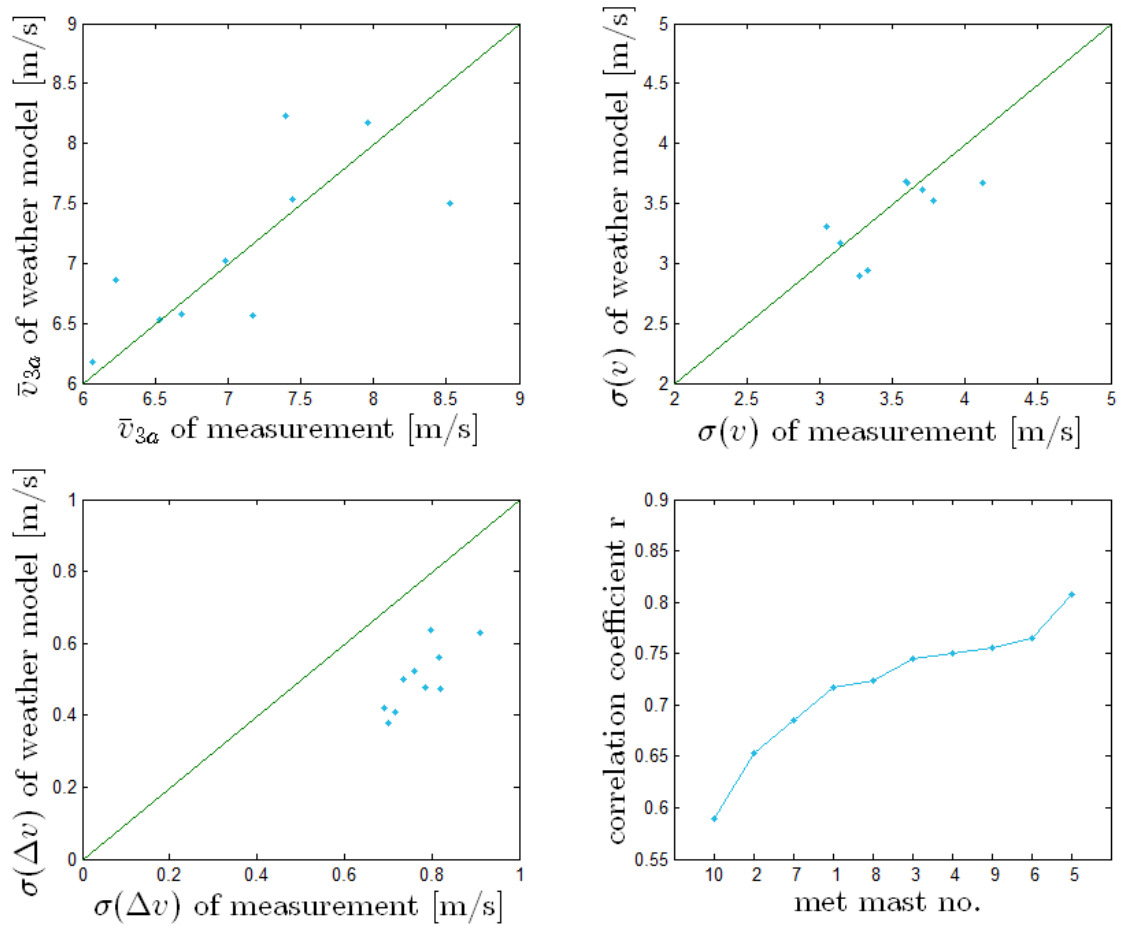
3.2.1 Electricity demand

Recent South Africa's annual electricity demand is ≈225 TWh (average of 2010 to 2012). Time series of the electricity demand were made available for 126 substations throughout the country with a temporal resolution of 30 min [9]. These data were downscaled to 15 min by linear interpolation and aggregated for the whole of South Africa. In this study the demand is expected to rise to about 500 TWh in the future. To reach the future load for every time step, the time series were scaled according to the ratio of recent versus assumed future demand per year. Table 2 shows some characteristics of the electricity demand.

Year	2009	2010	2011	2012	Future
Annual electricity demand [TWh]	216.6	225.9	226.5	221.2	500
Maximum power consumption [GW]	33.18	34.36	34.01	33.5	76.53
Minimal power consumption [GW]	15.58	17.87	17.42	17.06	38

Table 2: Characteristics of the electricity demand

3.2.2 Photovoltaics

The very good conditions for generating electricity from solar PV energy in South Africa are illustrated in Figure 1. A study on solar power in South Africa and aggregation effects has already been conducted [10].

The modelling of solar photovoltaics (PV) is based on assumptions regarding the space requirement of the installations. For PV on rooftops 0.2 km² per MW are defined, while for ground-mounted plants 0.03 km² per MW are estimated. All modelled PV is assumed to be fixed tilted, no tracking PV systems are modelled. The time-series are calculated with a Fraunhofer IWES model based upon the SODA data. For every pixel and every time step of 15 min the model first calculates the irradiance for the inclined module plane using the models of Orgill-Hollands [11] and Klucher [12]. Subsequently the PV output is calculated. For this purpose the inverter and module models of Schmidt and Sauer [13] and Beyer [14] are being applied. Standard polycrystalline modules are being modeled by module type.

To define potential areas with rooftops, data on settlement areas [15] are used (Figure 15). Ground-mounted installations are expected to be built within the 'Energy Environmental Impact Assessment (EIA)' areas (see chapter 4.2.1).

This results in a potential electricity generation from rooftop installations of more than 136 TWh per year with a potentially installed capacity of 72 GW. Just in the EIA areas it is possible to install 220 GW of ground-mounted solar PV which leads to a potential annual electricity generation of 420 TWh.
All in all, almost 292 GW of solar PV could be installed and produce over 550 TWh of electricity per year, i.e. more than twice as much as the current annual demand. Installations at additional locations to the EIA areas could even increase the potential significantly.
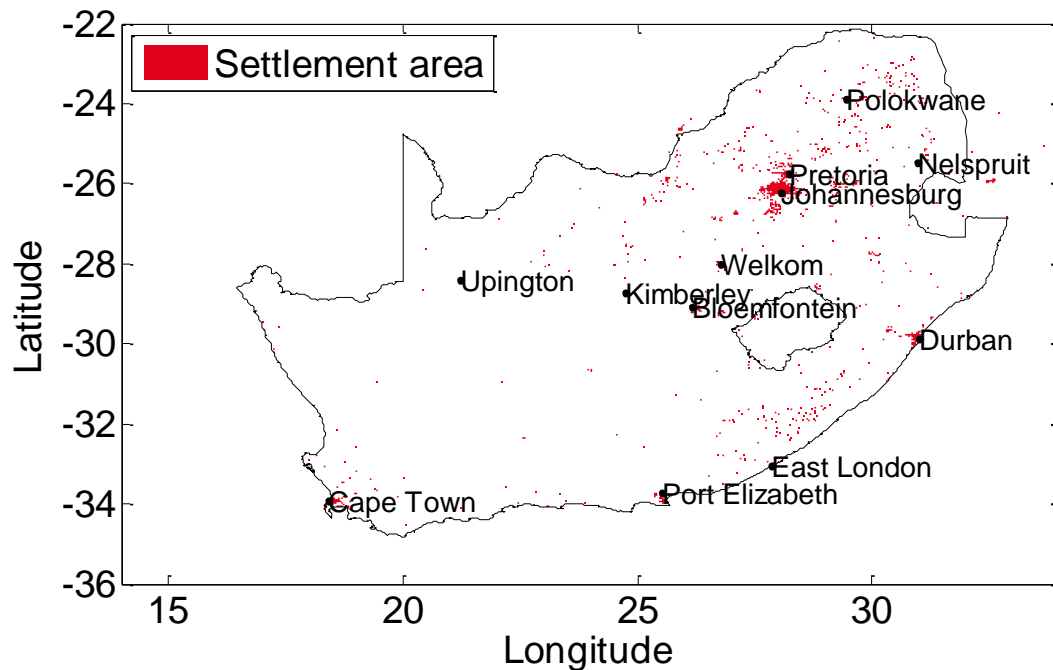
Figure 15: Settlement areas eligible for the installation of solar PV

Considering that wind energy was the focus of this study, for solar PV, a single base scenario was developed and scaled to an annual electricity generation of 40 TWh, 80 TWh and 200 TWh. This scenario with its three levels of electricity generation from solar PV energy (PV scenario 1 to 3) can be combined with any of the wind energy scenarios of chapter 4: Regarding the installation of solar PV, it is likely that in the future most of the capacity will be installed on rooftops. It is therefore assumed that 70% of the installed capacity will be 'distributed' solar PV installations while the other 30% will be large, 'utility-scale' installations. 'Distributed' is a proxy for all PV that is assumed to be distributed according to population density. It represents all PV close to the load which in this study would include only rooftop PV in all sizes. In reality, distributed PV could also include small ground-mounted installations. 'Utility-scale' is a proxy for large-scale PV installations in the multi-MW$_p$-range, for which EIAs (see chapter 4.2.1) have been applied for.
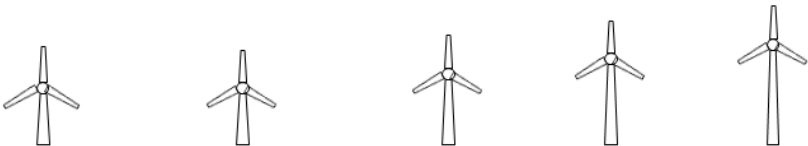
The installed capacities of the PV scenarios are summed up in Table 3. To generate 40 TWh per year of electricity from solar PV, a total installed capacity of 21 GW is necessary. For an electricity generation of 200 TWh per year, roughly 104 GW of PV would be installed.

	PV scenario 1	PV scenario 2	PV scenario3
Annual electricity generation from solar PV energy	40 TWh	80 TWh	200 TWh
Distributed (70%)	15 GW	29 GW	73 GW
Utility scale (30%)	6 GW	13 GW	31 GW
Total	**21 GW**	**42 GW**	**104 GW**

Table 3: Installed capacity of PV by scenario

3.2.3 Wind energy

As it is impossible to foresee which exact wind turbines would be installed in the future, three different example turbines with representative characteristics were chosen, among which turbines for areas with low wind speeds, moderate wind speeds and high wind speeds. The selection of turbines follows the definition of the IEC classes [16].

Turbine type no.	1	2	3	4	5
Nominal power	3 MW	2.2 MW	2.4 MW	2.4 MW	2.4 MW
Rotor diameter	90 m	95 m	117 m	117 m	117 m
Swept rotor area	6362 m²	7088 m²	10750 m²	10750 m²	10750 m²
W/m²	442	310	223	223	223
Hub height	80 m	80 m	100 m	120 m	140 m
Selection criterion	øv at 80 m > 8.5 m/s	øv at 80 m < 8.5 m/s and øv at 100 m > 7.5 m/s	øv at 100 m < 7.5 m/s	øv at 120 m < 7.5 m/s	øv at 140 m < 7.5 m/s
Turbine type	High wind speed	Medium wind speed	Medium low wind speed	Low wind speed	Low wind speed

Table 4: Representative wind turbines and their characteristics

Wind turbine type 1 with a nominal power of 3 MW, a rotor diameter of 90 m and a hub height of 80 m is assumed to be installed in pixels with high average wind speeds øv. Wind turbine type 2, with a nominal power of 2.2 MW, a rotor diameter of 95 m and also a hub height of 80 m is selected for pixels with moderate average wind speeds. Wind turbine type 3 with a nominal power of 2.4 MW and a rotor diameter of 117 m is supposed to be installed with a hub height of 100 m for medium low wind conditions. The same turbine can be installed on higher towers of 120 m and 140 m in pixels with low wind speeds. This leads to the five different turbine types displayed in Table 4. All turbines selected are based on current off-the-shelf technology
The assumptions described above lead to a potential distribution of turbines as shown in Figure 16.

The wind turbine power curves of the turbines are shown in Figure 17. Here, the actual power curves of the turbines (top of the figure) are drawn as well as smoothed power curves which account for the behaviour of hypothetic wind farms built on a 5 km by 5 km pixel (bottom) assuming a space requirement of wind power of 0.1 km² per MW. Wake effects, turbines availability and grid losses within wind farms are also taken into consideration.

For simulating the feed-in of electricity generated from wind energy for every 15 min and every pixel, the method and parameters of [17] are applied on the WASA data, using a Fraunhofer IWES software tool.
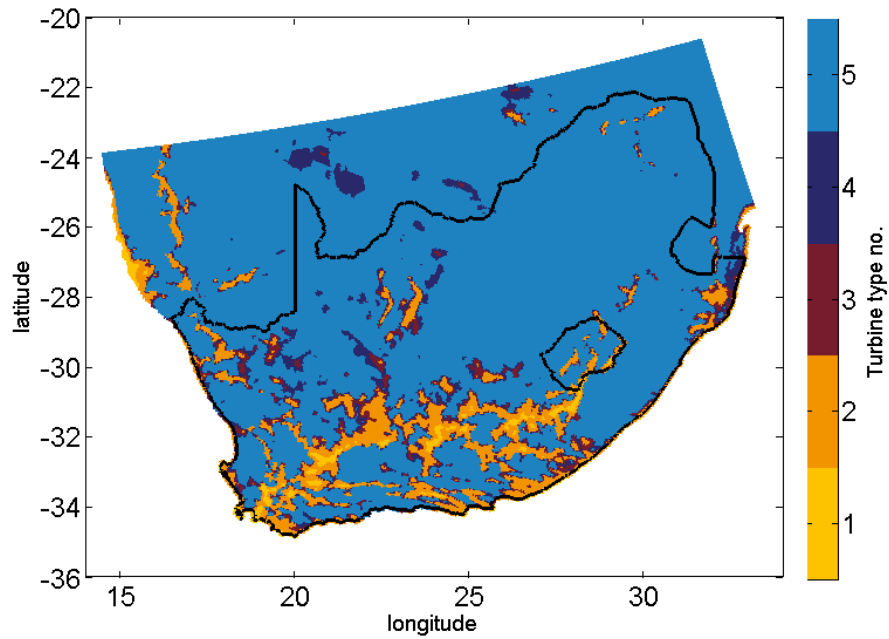
Wind and Solar Resource Aggregation Study
for South Africa

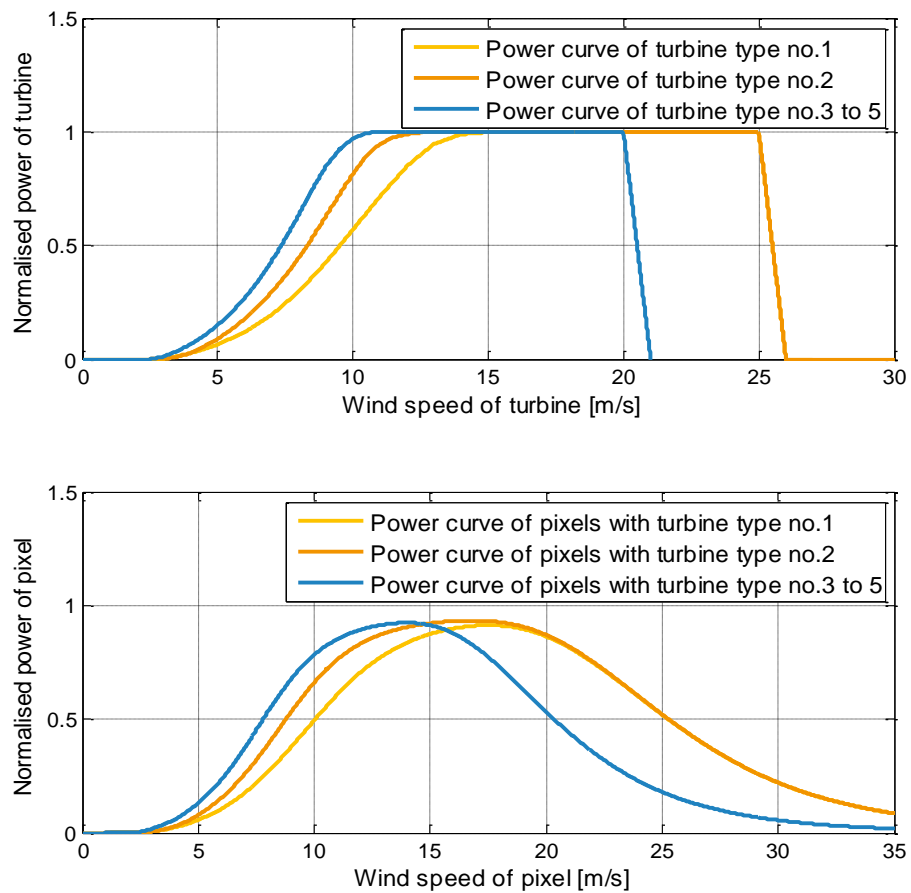**Figure 16: Turbine types – distribution according to mean wind speeds**

Figure 17: Power curves of single turbines (top) and for wind farms on 5km x 5km squares (bottom) by type

4. Study scenarios

The simulation and modelling methods described in the previous chapter result in time series of potential electricity production from wind energy in a spatial resolution of 5km by 5km covering the whole of South Africa. This corresponds to approximately 47 500 time series (one for every pixel). This spatially inclusive and comprehensive data basis offers the possibility to distribute renewable applications in many different ways and various locations. This is formidable and and results in a massive amount of wind generation combinations. At the same time, it is very difficult to anticipate the actual future distribution of wind turbines (WT) and solar PV. In order to deal with this, scenarios have been developed. Every scenario is characterized by the chosen pixels, the resulting area and installable capacities on the one hand, and the electrical characteristics which result from the aggregation of the pixels' time series on the other hand.

To account for the uncertainty regarding of how much capacity will actually be installed at which time in the future, the different scenarios described below are assessed for different shares of electricity supply from wind and solar PV energy, namely

- 40, 80 and 200 TWh of electricity per year generated from solar PV energy (see chapter 3.2.2), and
- 50, 100 and 250 TWh of electricity per year generated from wind energy.

An overview of the resulting scenarios and the shares of renewable energy in electricity are shown in Figure 18.

Figure 18: Different levels of electricity supply from wind and solar PV energy and the resulting shares of renewable energy in electricity generation

Wind and Solar Resource Aggregation Study
for South Africa

The main focus of this study lies on aggregation effects for wind energy in South Africa because wind shows a higher geospatial dependency than solar PV energy. For this reason the following wind energy scenarios were developed to investigate different ways of distributing wind turbines within the country:

- Uniform wind turbine distribution (chapter 4.1.1)
- All-in-one-place (chapter 4.1.2)
- High wind speeds wind turbine distribution (chapter 4.1.3)
- Minimal ramps resource distribution (chapter 4.1.4)
- EIA-focused wind turbine distribution (chapter 4.2.1)
- REDZs-focused wind turbine distribution (chapter 4.2.2)Current grid-focused wind turbine distribution (chapter 4.3)
- Future grid-focused wind turbine distribution (chapter 4.3)

The wind energy scenarios are divided in two parts. Some are developed for predefined areas taking into account existing regulations and plans (chapter 4.2), others are based on newly and scientifically defined areas (chapter 4.1).
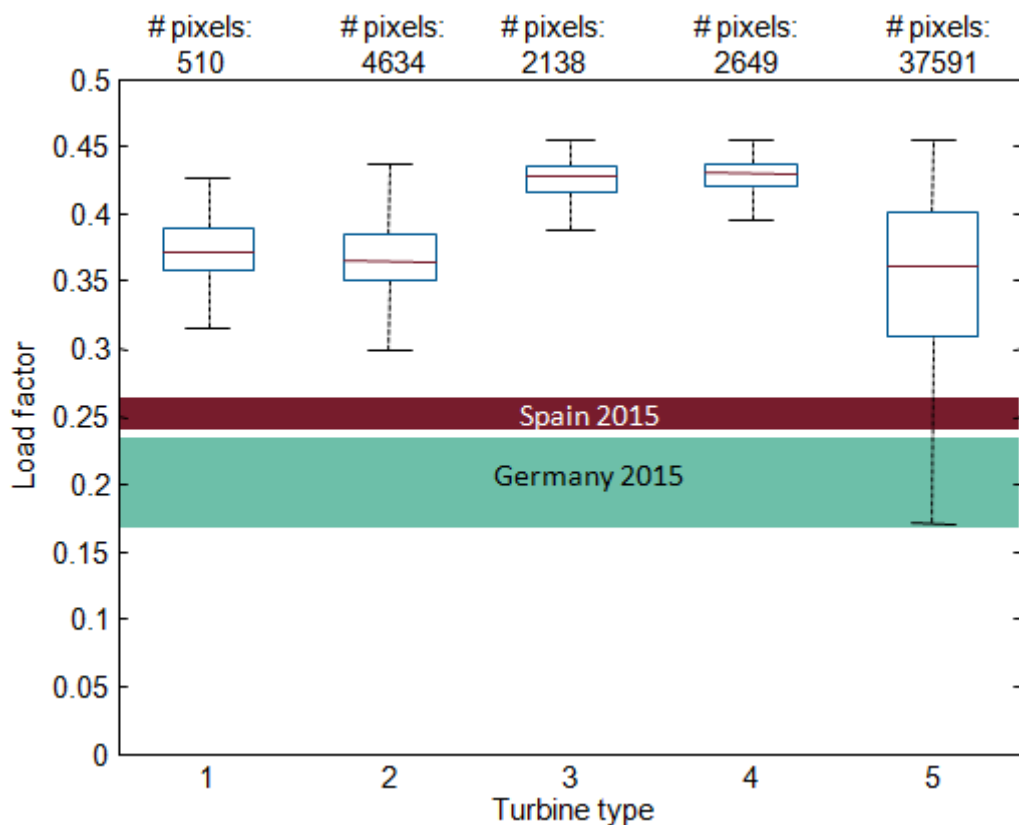
Figure 19: Quartiles of load factors (average load factors for the weather years 2009-2013 in South Africa) by turbine type, number of pixels selected for each turbine type indicated on top

Wind and Solar Resource Aggregation Study
for South Africa

4.1 Scientific scenarios

4.1.1 Uniform wind turbine distribution

4.1.1.1 Whole country

South Africa has an area of about 1,2 million square kilometres. Applying the space requirement of 0.1 km² per MW (see previous section), 12 200 GW of wind power capacity could be installed in South Africa (theoretically). According to the time series of the previous chapter, this would lead to a potential annual electricity generation of more than 38 000 TWh and very high load factors given the assumption that the entire area could be used for wind energy. The average load factor amounts to 0.36.
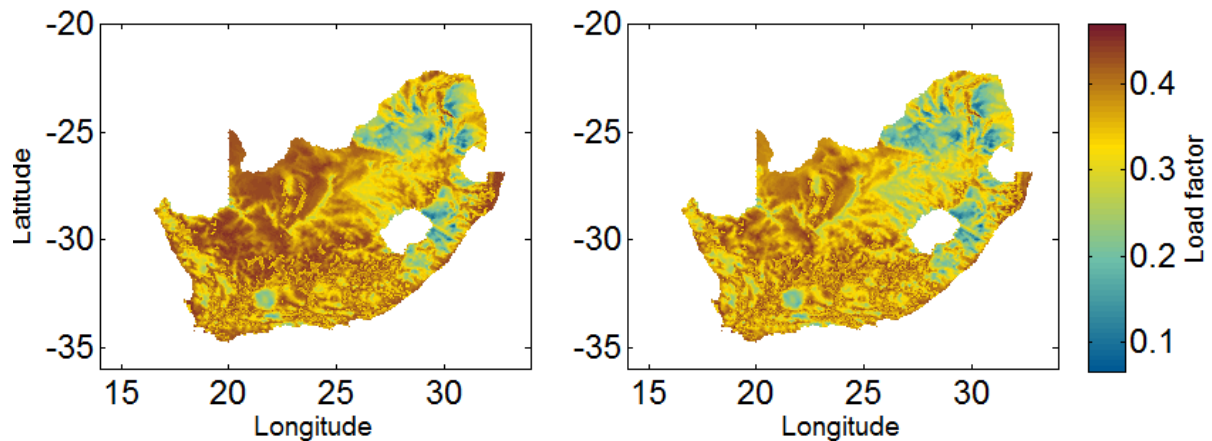
Figure 20: Load factors for turbine types no. 1-5 (left), turbine types no. 1-3 only (right)

Figure 20 reveals that in most parts of South Africa load factors exceed 0.3, large areas even offer load factors around 0.4. As can be seen from Figure 19 where the quartiles of the load factors by turbine type are shown, other countries with much higher installed capacities and an ongoing extension of RE are operating their wind fleet at significantly lower average load factors. Germany and Spain, for example, reached average load factors around 0.2 and 0.25 in 2015 with an installed capacity of 44 GW and 23 GW, respectively. This means that turbines can be operated in a cost-effective way in most regions of South Africa.

Even if it is not possible to install wind turbines at any location because of different restrictions, these results underline the extraordinary good conditions and the enormous potential of South Africa. An assessment of the potential regarding those areas where turbines can actually be built does not change this conclusion, as described in the following sub-section.

Wind and Solar Resource Aggregation Study
for South Africa

4.1.1.2 Whole country minus exclusion zones

To determine areas which are not eligible for the installation of either wind turbines or PV installations, an exclusion mask [15] was laid over the country, which was also applied in [18].
The designated areas with specific buffers are such as protected areas and threatened ecosystems, coastal areas and rivers, field crop boundaries, roads and railways, power lines and steep slopes. The result is shown in Figure 21 in the form of the installable capacity of wind power for each pixel.
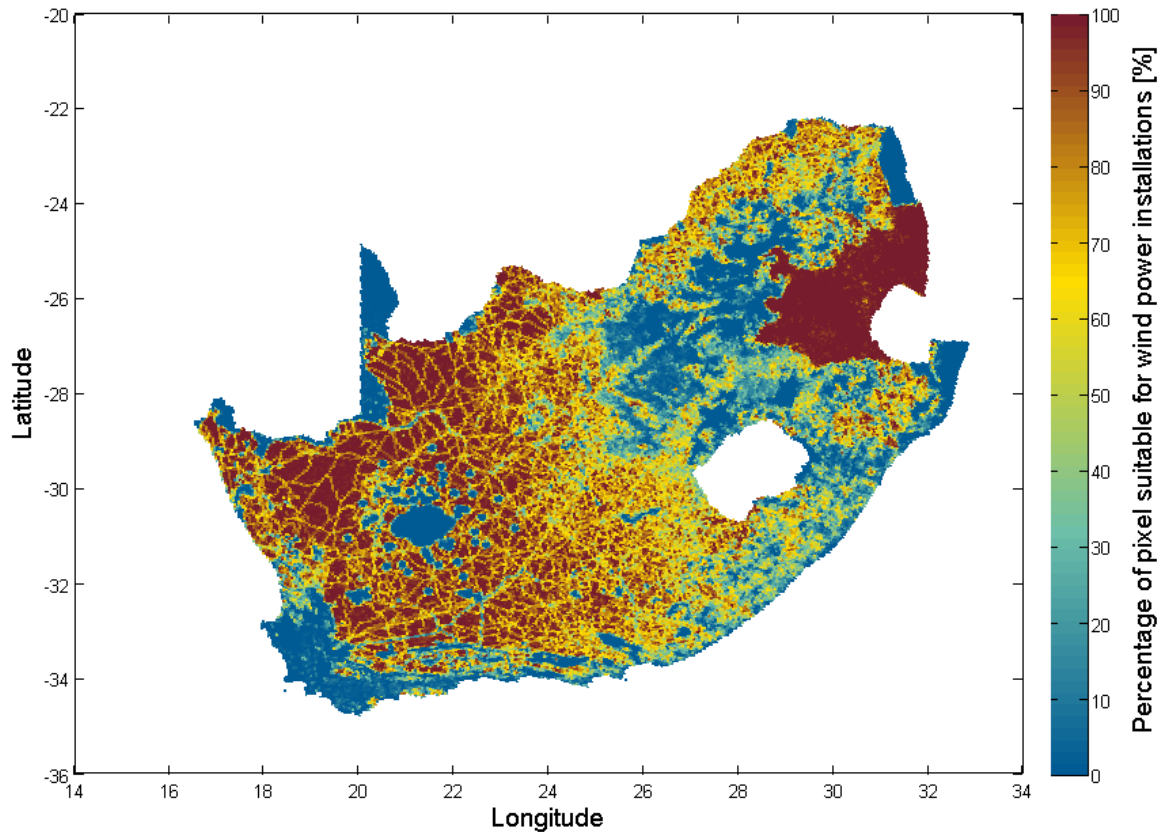
Figure 21: Share of each 5x5 km square suitable for the installation of wind turbines after excluding areas designated for other functions

A difference between Mpumalanga region in the East and the rest of the country is clearly visible in Figure 21. This results from incompleteness of the exclusion mask. Therefore larger areas are assumed to be suitable. In reality, more exclusion areas will be found. Due to the low wind resources in the Mpumalanga area the impact on the final results should be insignificant.

The areas remaining after applying the exclusion mask still offer space for an installable capacity of 6 787 GW of wind power (on 43113 pixels) which could produce nearly 22 000 TWh of electricity per year. This is a reduction of 43% of the theoretical potential, and yet it is almost 100 times the current demand (about 225 TWh, see chapter 3.2.1).
This high value makes it clear, that this scenario of wind energy in South Africa is still very theoretical, even if the exclusion zones mask infeasible areas. It is a rather scientific scenario and not very likely to happen in reality but it leads to interesting results, especially in comparison with other scientific scenarios included in this analysis. Since the wind turbines would be distributed evenly over the remaining areas of the whole country, this scenario will be referred as the **'uniform wind turbine distribution'**.

Figure 22 shows the energy yield per pixel of the uniform wind turbine distribution. The turbine types of Table 4 and the weather data from 2009 to 2013 are applied for this figure.

Wind and Solar Resource Aggregation Study
for South Africa
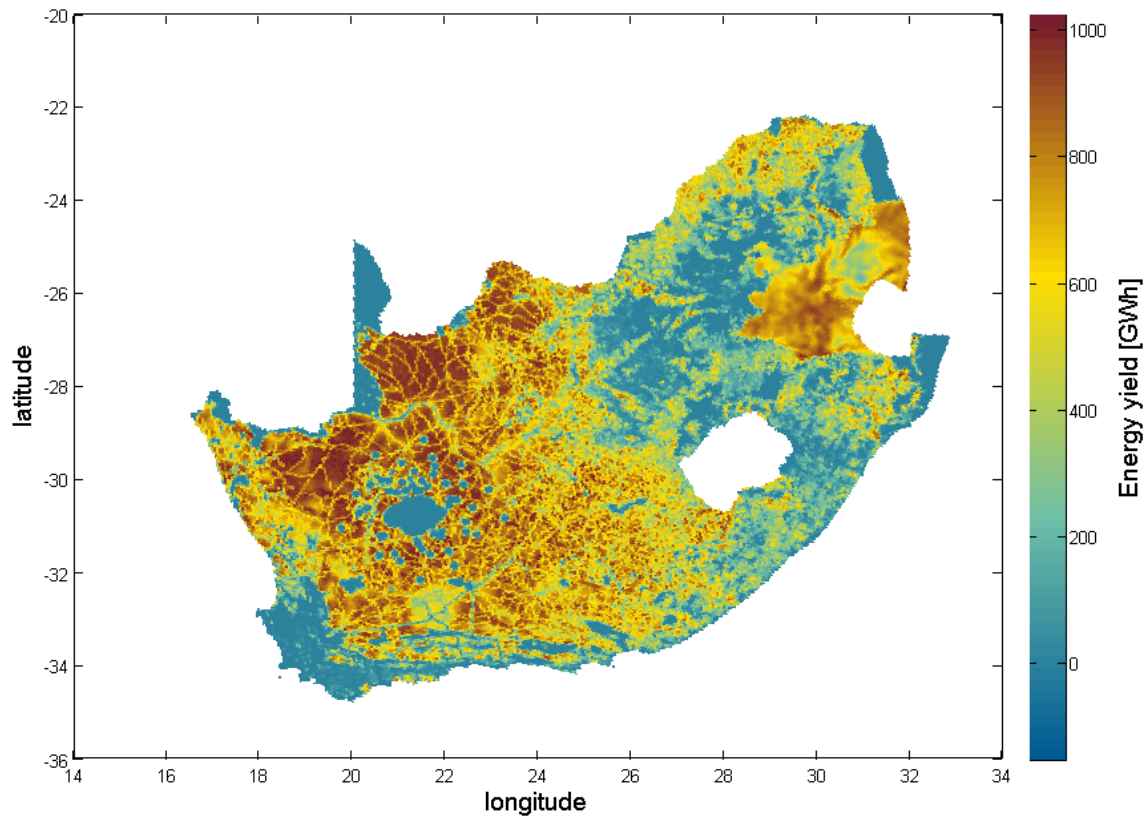
Figure 22: Annual wind energy yield of the uniform wind turbine distribution

Regarding the load factors, the exclusion areas even consist of mostly areas with relatively low load factors which leads to an increase of average load factors for the whole country relative to the case without exclusion zones. Figure 23 indicates which percentage of the remaining area can be used for building wind turbines to reach a certain load factor. For example, a load factor of at least 0.35 can be reached for 67.5% of the area considered feasible in this study for installing turbines no. 1 to 5. If only turbines 1 to 3 are supposed to be installed, a smaller area of 52% of the considered area can be used (example marked by red arrows in Figure 23).

Once again these curves underline the very good conditions for renewable electricity generation (specifically wind) and the available space in South Africa by showing a high share of the land mass can be used for typically feasible wind power projects. Installing turbine type 4 and 5 would cause higher costs (as a result of the height of the construction) but also increase load factors and electricity yield whilst using the same area.

In order to make the **'uniform wind turbine distribution'** comparable with other scenarios it was scaled down by a constant factor in order to achieve energy yields of 50, 100 and 250 TWh per year respectively. This downscaling does not change the uniform character of the distribution: the wind turbines are still uniformly distributed over the whole country but with a lower density. Table 5 makes this point clear.

Wind and Solar Resource Aggregation Study
for South Africa
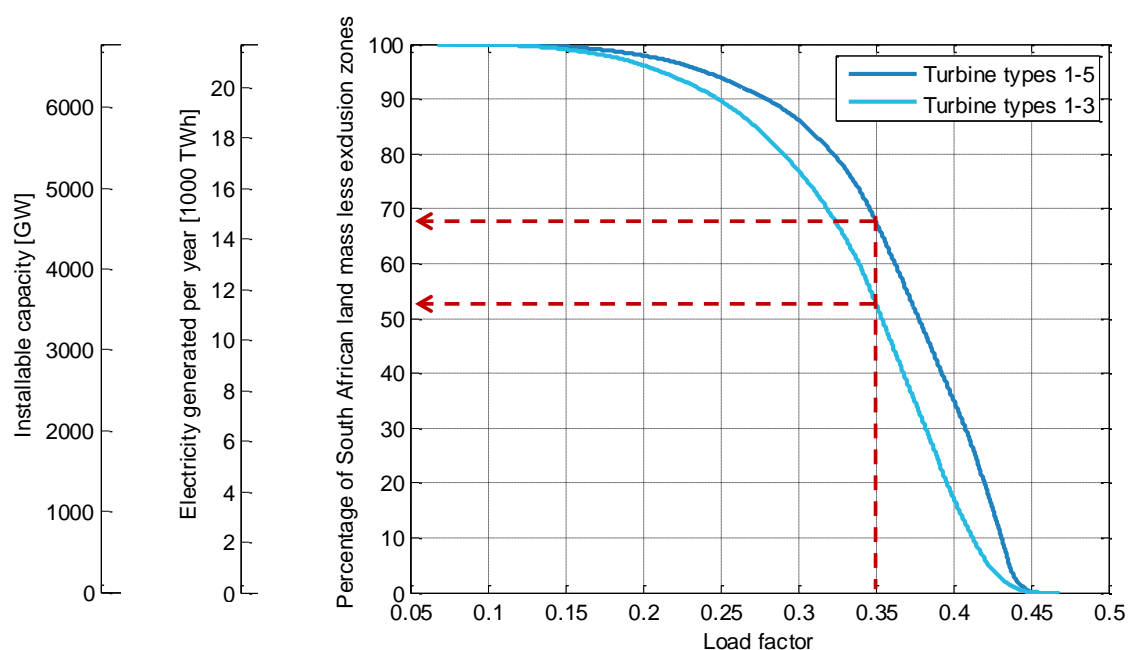
Figure 23: Share of South African land mass less exclusion zones and load factors to be reached accordingly

		Potential	50 TWh/yr	100 TWh/yr	250 TWh/yr	All in one place 100 TWh/yr
Capacity		6 787 GW	16 GW	31 GW	78 GW	32 GW
Minimum output		162 GW	0.4 GW	0.8 GW	1.9 GW	0 GW
Normalised wind power 15-min gradient	Max	4.2%	4.2%	4.2%	4.2%	92%
	Min	-4.3%	-4.3%	-4.3 %	-4.3 %	-90%
Residual load 15-min gradients (assuming 80 TWh of PV)	Max	291 GW	5.4 GW	5.3 GW	4.9 GW	30 GW
	Min	-285 GW	-3.2 GW	-3.3 GW	-3.6 GW	-30 GW
Daily energy	Max	119 449 GWh	274 GWh	549 GWh	1 374 GWh	708 GWh
	Mean	59 494 GWh	137 GWh	274 GWh	685 GWh	274 GWh
	Min	13 327 GWh	31 GWh	61 GWh	153 GWh	1 GWh
Load factor		0.37	0.37	0.37	0.37	0.35
Spatial spread		678 688 km²	678 688 km²	678 688 km²	678 688 km²	15.8 km²

Table 5: Statistics of aggregated wind output and residual load for the uniform wind turbine distribution

Figure 24 and Figure 25 show screenshots of animations made for this study. The left parts of the figures show maps, the right parts 4 time series of a specific day. In this case, 14 January 2012 was chosen as example, because this day has the highest standard deviation of wind power feed-in of all days considered The upper figures of the right parts show the normalised simulated feed-in of the whole day as blue lines. The lower figures show the 15-min gradients of the normalised feed-in. Figure 24 and Figure 25 differ in the number of pixels contributing to the simulated wind power feed-in. In the case of Figure 24 one and ten pixels were taken into account, in the case of Figure 25 100 and all pixels of the uniform wind turbine distribution. The positions of the pixels are shown on the maps which also display the wind speed at 100m above ground at quarter to midnight.
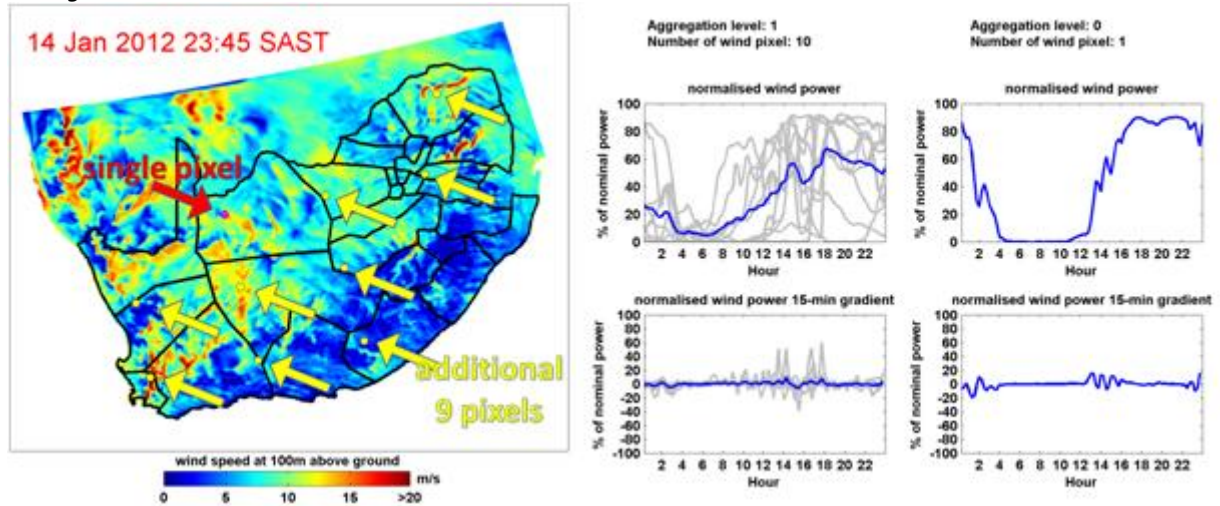
Figure 24: Screenshot of the animation of wind power feed-in of one and 10 pixels
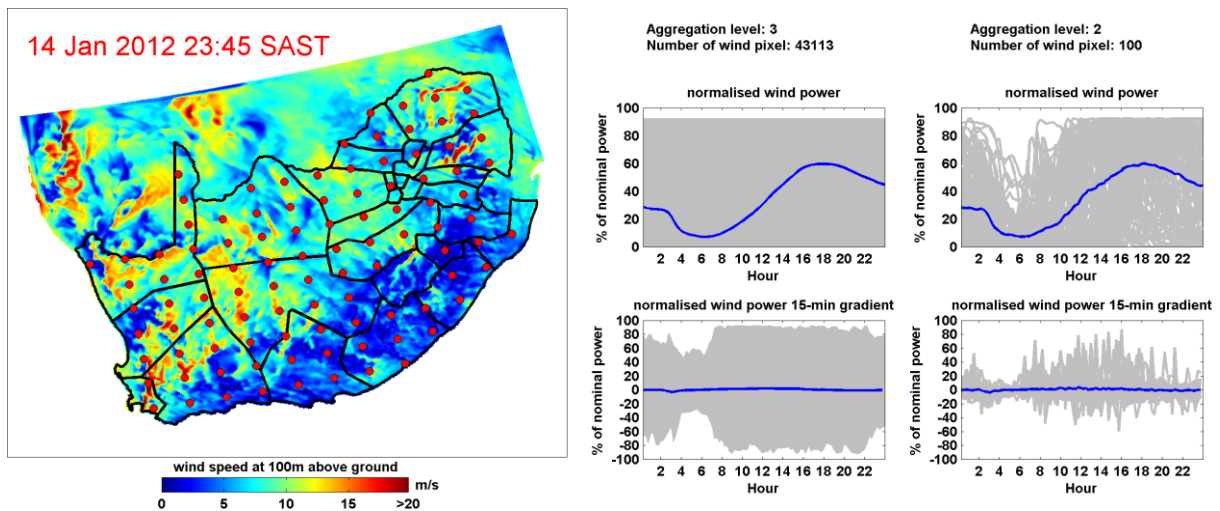
Figure 25: Screenshot of the animation of wind power feed-in of 100 and all pixels

The comparison of the feed-ins and the gradients of Figure 24 and Figure 25 cleary reveals the spatial aggregation effects. The feed-ins and the gradients are as smoother as higher the number of pixels considered.

Wind and Solar Resource Aggregation Study
for South Africa

4.1.2 All-in-one-place

As shown previously, it was assumed that all areas which remain after sorting out the exclusion zones (chapter 4.1.1.2) are suitable for installing wind turbines, and that wind turbines will be evenly distributed over the entire country. The extreme opposite to this **'uniform wind turbine distribution'** of chapter 4.1.1.2 is an installation of all electricity generation capacity in a single pixel (**'all-in-one-place'** scenario). Again, this scenario is very academic and not very likely to happen in reality but leads to interesting results for comparison with other scenarios.

The pixel was chosen according to the criteria of a central position in the country (see Figure 26) and medium load factor. Its load factor is 0.35, thus a little bit lower than the average of the whole country of 0.37. In spite of that only 158 MW can be installed and only 0,49 TWh can be achieved on this pixel, its feed-in is scaled up to 50, 100 and 250 TWh for the purpose of comparison with the other scenarios.

The high spatial concentration of wind power capacity on only one pixel results in high fluctuations of the feed-in. This scenario can be understood as the worst case of distributing wind power capacities over the country in terms of the smoothness of the feed-in. According to that, the gradients in Table 6 are the highest of all scenarios.
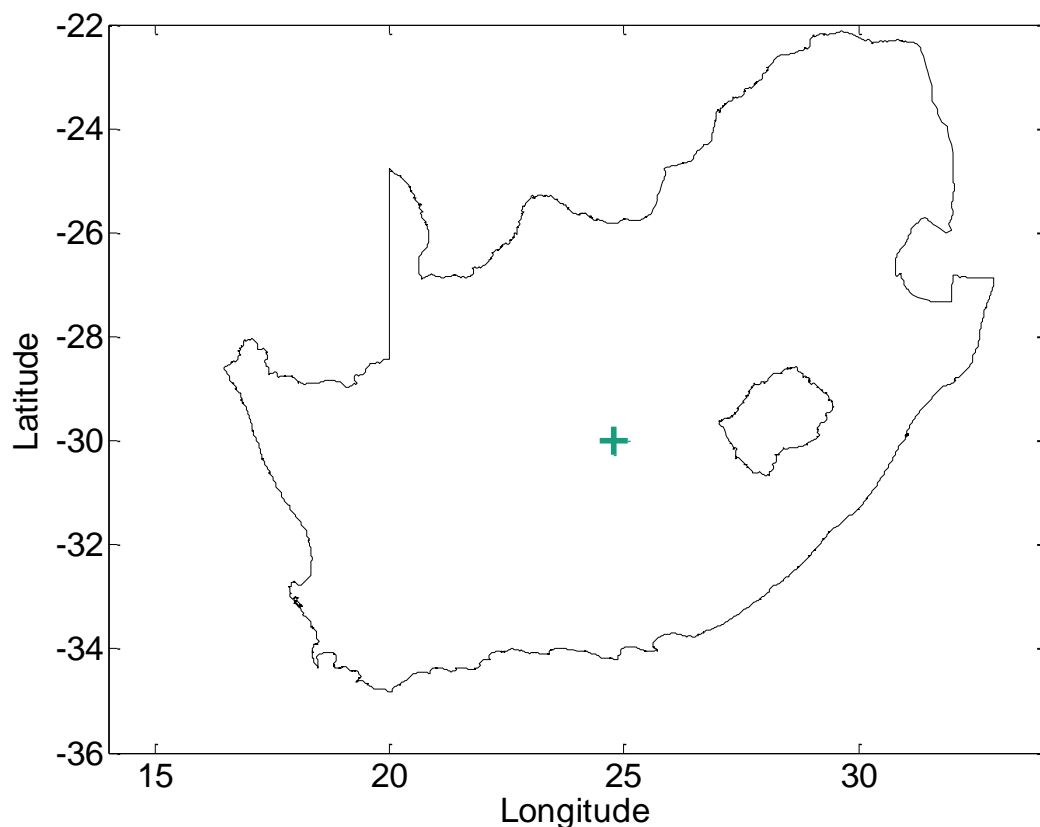
Figure 26: 'All-in-one-place' scenario

		Potential	50 TWh/yr	100 TWh/yr	250 TWh/yr
Capacity		0.16 GW	16 GW	32 GW	81 GW
Minimum output		0 GW	0 GW	0 GW	0 GW
Normalised wind power 15-min gradient	Max	92%	92%	92%	92%
	Min	-91%	-91%	-91%	-91%
Residual load 15-min gradients (assuming 80 TWh of PV)	Max	5.5 GW	15 GW	30 GW	74 GW
	Min	-3.1 GW	-15 GW	-30 GW	-74 GW
Daily energy	Max	3.5 GWh	354 GWh	708 GWh	1 769 GWh
	Mean	1.3 GWh	137 GWh	274 GWh	685 GWh
	Min	0 GWh	0.5 GWh	1.0 GWh	2.5 GWh
Load factor			0.35	0.35	0.35
Spatial spread		678 688 km²	15.8 km²	15.8 km²	15.8 km²

Table 6: Statistics of aggregated wind output and residual load for the 'all-in-one-place' wind turbine distribution

4.1.3 High wind speeds wind turbine distribution

For the **'high wind speeds wind turbine distribution'**, it is assumed that turbines will be built preferably at those locations with the highest average wind speeds. The mean wind speeds of the years 2009 to 2013 at 100m above ground level (see Figure 4) are used for the modelling of this distribution. The mean wind speeds of all pixels unless the pixels which are completely excluded (according to chapter 4.1.1.2) are considered and sorted. Beginning with the pixel with the highest mean wind speed further pixels are added to the distribution until the sum of their energy yields reach the total amount of 250TWh. The lower part of Figure 27 shows the resulting distribution. The upper and the middle figures one show the interim stage of 50 TWh and 100 TWh respectively.
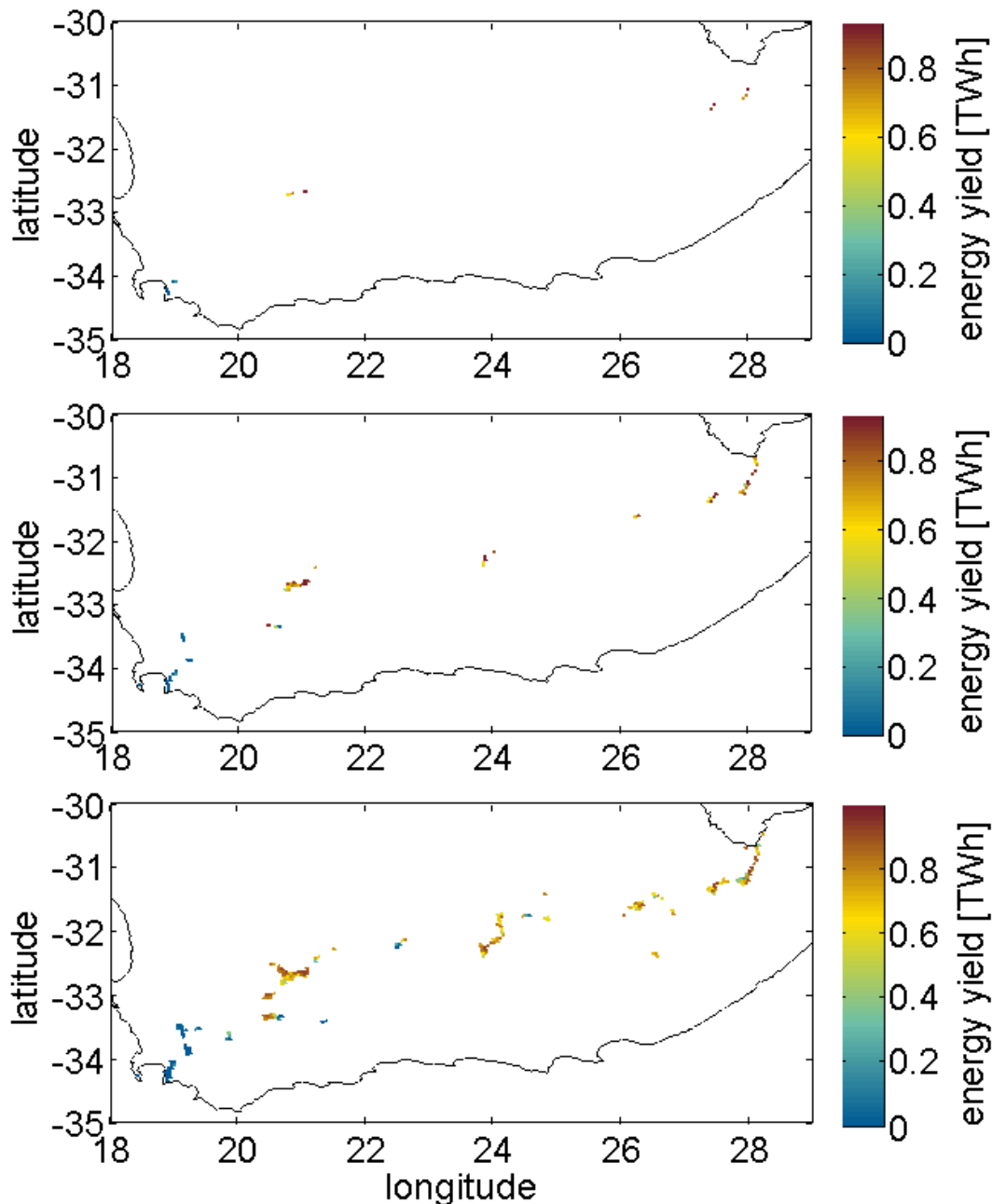
Figure 27: The high wind speeds wind turbine distribution for energy yields of 50 TWh (upper), 100 TWh (middle) and 250 TWh (lower)

The total installed capacity of the distribution for 250 TWh amounts to 76.25 GW. That is not much less than the installed capacity of 78.09 GW the uniform resource distribution needs for 250 TWh (see chapter 4.1.1.2).

Wind and Solar Resource Aggregation Study
for South Africa

This may be surprising since the highest wind speeds were used for this distribution promising high energy yields with relatively low installed capacities.

The bar diagram of Figure 28 reveals the reason for that. Every bar represents a pixel, given its mean wind speed in 100m above ground on the x-axis and its potential energy yield on the y-axis. The pixels are sorted according to their mean wind speed as described above. It becomes clear that the pixels with the highest mean wind speeds are not the one with the highest energy yields. The reason for that are the assumed turbine types of Table 4 in chapter 3.2.3. Apart from a few turbines of type no. 2, which are only selected for the 250TWh distribution, the high wind speeds wind turbine distribution consists throughout of turbines of type no. 1.
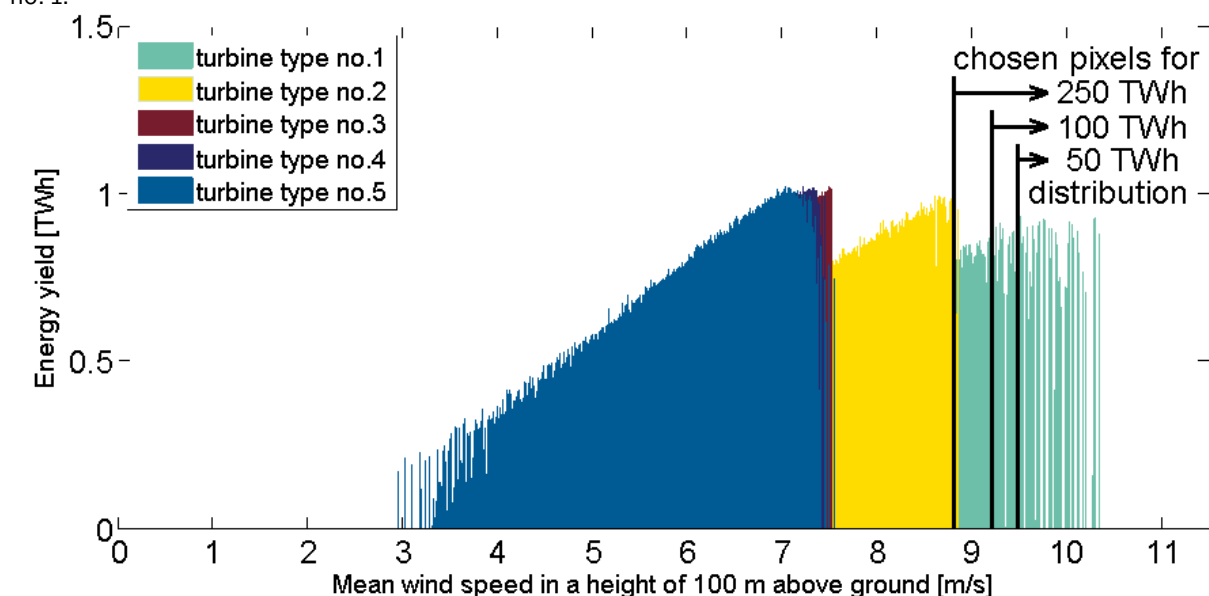
Figure 28: Energy yields of pixels sorted according to their mean wind speeds

		Potential	50 TWh/yr	100 TWh/yr	250 TWh/yr	All in one place 100 TWh/yr
Capacity		6 787 GW	15 GW	30 GW	76 GW	32 GW
Minimum output		162 GW	0.01 GW	0.04 GW	0.08 GW	0 GW
Normalised wind power 15-min gradient	Max	4.2%	16%	12%	8.4%	92%
	Min	-4.3%	-17%	-12%	-8.5%	-91%
Residual load 15-min gradients (assuming 80 TWh of PV)	Max	292 GW	5.4 GW	5.9 GW	9.0 GW	30 GW
	Min	-286 GW	-3.3 GW	-4.3 GW	-5.7 GW	-30 GW
Daily energy	Max	119450 GWh	301 GWh	603 GWh	1 539 GWh	708 GWh
	Mean	59 494 GWh	138 GWh	275 GWh	686 GWh	274 GWh
	Min	13 327 GWh	2.9 GWh	6.7 GWh	15 GWh	1 GWh
Load factor		0.37	0.4	0.39	0.37	0.35

Table 7: Statistics of aggregated wind output and residual load for the 'high-wind-speed' wind turbine distribution

Wind and Solar Resource Aggregation Study
for South Africa

4.1.4 Minimal ramps wind turbine distribution

The fluctuating nature of wind power is supposed to pose a major challenge on the power system. A possible way to quantify this challenge is to calculate the so-called 'ramps of the residual load' of a power supply scenario. The residual load usually corresponds to the electricity demand less the feed-in based on wind and solar PV. A ramp of the residual load is understood in this study as the change of the residual load from one time step to the next (having a temporal resolution of 15min). Thus, a main feature of a power supply scenario is the standard deviation or specific percentiles of the ramps of its residual load. In this context a power supply scenario with a minimal standard deviation or minimal percentiles would be preferable because it imposes minimal requirements on the flexibility of its components. It is important to note that the extent of the ramps depends on the spatial distribution of the wind turbines.

In this chapter so-called **'minimal ramps wind turbine distributions'** are determined which result in minimal ramps of the residual load. The 7 distributions differ in their optimisation criteria, constraints and additional processing steps as shown in Table 8.

Optimisation number		6	2	1	3	4	5	7
Optimisation criteria:	residual load's ramps should have:	minimal 5th and 95th percentiles			a minimal standard deviation			
Optimisation constrains:	minimal addable capacity per step [MW]			5	5			
	maximal addable capacity per step [MW]	50		15	15	50		10
	maximal installable capacity of the pixels [MW]			whole potential				
additional processing:		none		normalisation of residual load's ramps by the energy of added pixel		none		

Table 8: Criteria, constraints and additional processing steps for the minimal ramps wind turbine distributions

The 7 minimal ramps wind turbine distributions where obtained by an iterative process. At the beginning it is assumed, that none of the approximately 47500 pixel is equipped with wind power capacities. At each following step the specific pixel is determined whose wind power feed-in results in the minimal standard deviation (optimisation number 2, 3, 5 and 7) or in minimal 5th and 95th percentiles of the residual load's ramps (optimisation number 1 and 6). The 5th and 95th percentiles were weighted equally. Once a pixel is selected its wind power contributes to the residual load of all following aggregation steps. The optimisations differ in how much capacity is assumed to be installed in the pixels. Optimisation no. 2, 4, 5 and 6 assume that 50 MW are installed in the pixels step by step if there is enough area for this capacity. If not, the respective pixel was not considered. Optimisation no. 7 does the same assuming 10 MW. Optimisation no. 1 and 3 have a different approach. They assume that 15 MW are installed per step if there is enough eligible area on the specific pixel. If not, less than 15MW but at least more than 5MW are installed. A pixel can be chosen more than once in optimisation no. 1 and 3, if its influence on the residual load remains to be the 'best' in several optimisation steps. All in all the total installable wind power capacity of a pixel can be installed at a pixel. The optimisations do not only differ regarding the installed capacities per step and pixel and regarding the optimisation criteria (standard deviation or percentiles), but also whether an additional processing of the residual load's ramps is

performed or not. An additional processing is done for optimisation no. 1 to 5, namely a normalisation of the residual load's ramps by the energy of the added pixel. All optimisation are done for the weather data of the year 2010, 4 solar PV penetration levels (0, 40, 80 and 200TWh, see Figure 18) and until a total wind energy yield of 250TWh is reached.
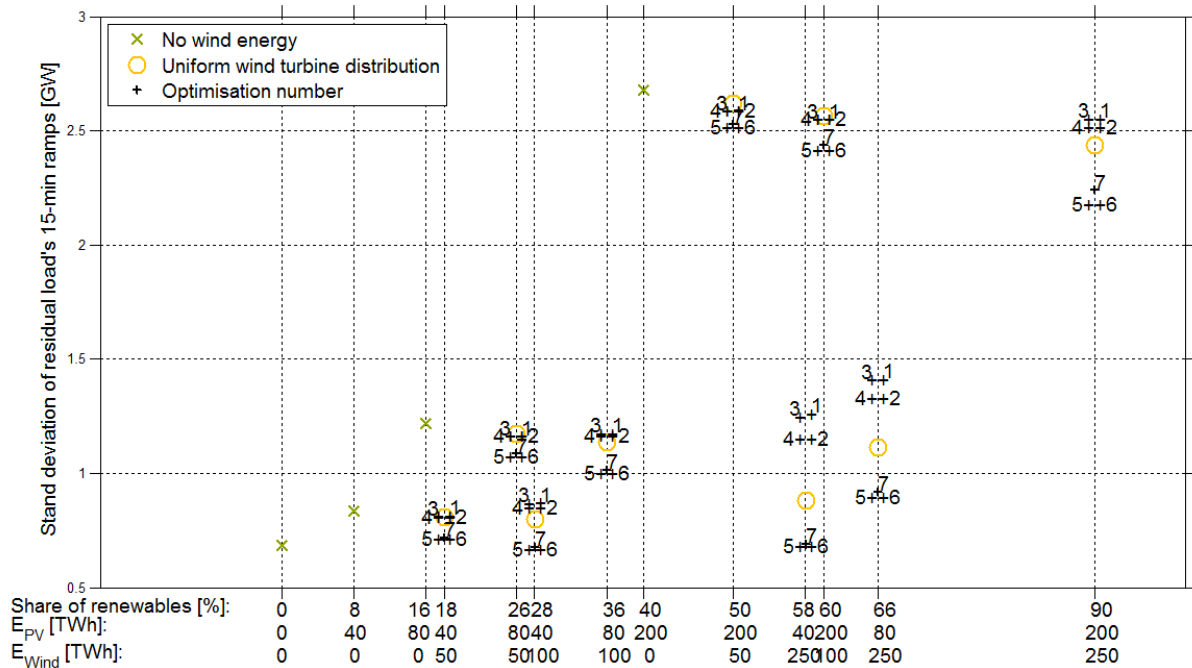

Figure 29: Standard deviation of residual load's ramps of different optimisations

Figure 29 offers a comparison of the optimisation results. It shows the standard deviations of the residual load's ramps in relation to the annual energy yield of wind power and PV as well as the annual share of RE in the electricity system. A similar method of presenting results is used and described in more detail in Figure 45. Figure 29 mainly serves to compare the optimisation results between themselves and between the uniform wind turbine distribution of chapter 4.1.1.2. The reason for comparing the optimisation results with the uniform wind turbine distribution is that the latter one can be expected as a nearly ideal in terms of guaranteeing relatively low ramps of the residual load because of the smooth character of its feed-in. However, some optimisation numbers managed to obtain better results than the uniform wind turbine distribution even if their spatial distribution of wind turbines is more concentrated. Optimisation number 5, 6 and 7 show lower standard deviations of the residual load's ramps for all shares of RE, the other optimisation numbers only for some. That leads to the conclusion that the additional processing was disadvantageous. It is clearly visible in Figure 29, that some optimisation numbers form pairs, namely number 1 and 3, number 2 and 4 and number 5 and 6. The standard deviations within the pairs do not differ more than 1% leading to the conclusion that the two different optimisation criteria do not have a significant influence on the results. However, a difference between optimisation number 7 and the pair of optimisation numbers 5 and 6 is noticeable. The restriction of optimisation number 7 to only 10MW installable capacity per pixel seems to result in a constrained utilization of pixels with beneficial properties. Those pixels seem to be selected preferably by optimisation number 5 and 6 and equipped with a higher installed capacity of 50MW. Thus, optimisation numbers 5 and 6 results in a relatively highly concentrated wind turbine distribution (see left part of Figure 30), which features even lower ramps of the residual load than more dispersed distributions as the one of optimisation number 7 (see right part of Figure 30) or the uniform resource distribution. The wind turbine distribution of optimisation number 5 will henceforth be referred to as the **'minimal ramps wind turbine distribution'**.

Table 9 shows main characteristics of this distribution.
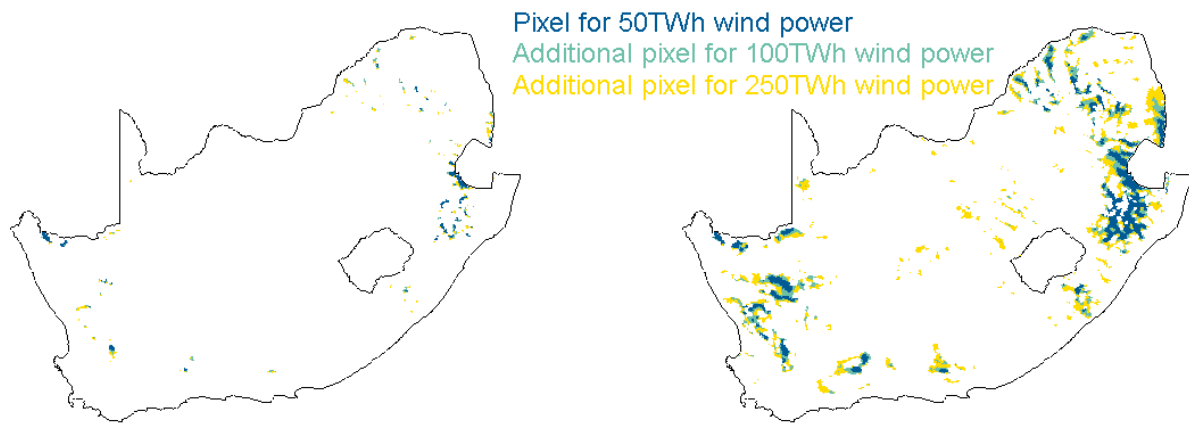
Figure 30: Location of the pixels selected by optimisation number 5 (left) and 7 (right) assuming 200TWh PV

Annual wind energy yield [TWh]	Assumed energy yield of PV [TWh]	Spatial spread [km²]	Installed capacity [GW]	Load Factor
50	40	1725	17.25	0.33
50	80	1660	16.6	0.34
50	200	1640	16.4	0.35
100	40	3360	33.6	0.34
100	80	3250	32.5	0.35
100	200	3205	32.05	0.36
250	40	8575	85.75	0.33
250	80	8165	81.65	0.35
250	200	8000	80	0.36

Table 9: Characteristics of the 'Minimal ramps wind turbine distribution'

		Potential	50 TWh/yr	100 TWh/yr	250 TWh/yr	All in one place 100 TWh/yr
Capacity		6 787 GW	16.6 GW	32.5 GW	81.65 GW	32 GW
Minimum output		162 GW	0.04 GW	0.16 GW	2.46 GW	0 GW
Normalised wind power 15-min gradient	Max	4.2%	9.84%	7.67%	4.46%	92%
	Min	-4.3%	-7.21%	-4.5812%	-3.77%	-91%
Residual load 15-min gradients (assuming 80 TWh of PV)	Max	292 GW	5.16 GW	4.97 GW	4.57 GW	30 GW
	Min	-286 GW	-2.98 GW	-2.91 GW	-3.29 GW	-30 GW
Daily energy	Max	119450 GWh	265 GWh	500 GWh	1198 GWh	708 GWh
	Mean	59 494 GWh	137 GWh	274 GWh	685 GWh	274 GWh
	Min	13 327 GWh	32 GWh	84 GWh	247 GWh	1 GWh

Table 10: Statistics of aggregated wind output and residual load for the 'minimal ramps wind turbine distribution' assuming 80 TWh of PV

4.2 Designated areas scenarios

4.2.1 EIA-focused wind turbine distribution

The South African Department for Environmental Affairs provides a database on spatial data for renewable energy applications for environmental authorisation, the so called Renewable Energy environmental impact assessment (EIA) applications (Department for Environmental Affairs 2015). It includes spatial and attribute information for both active (in process and with valid authorisations) and non-active (lapsed or replaced by amendments) applications. Data is captured and managed on a parcels level as well as aggregated to the project level. Only outer boundaries are provided in this release. The EIA for wind energy and solar PV energy applications are still labeled ambiguously, labels such as 'Wind energy', 'Onshore Wind and Solar PV', 'Solar CSP', 'Solar CSP and PV' or just 'Solar' can be found in the data set. The first two were interpreted as 'wind energy' applications in the following, the latter as 'solar PV energy' applications. But not only the labeling is ambiguous in this data set, some EIA applications are also overlapped and non-contiguous. Table 11 shows the characteristics of the EIA applications after splitting into contiguous areas and removing overlaps. In the case that wind and solar PV energy EIA were overlapped the predominant technology, i.e. the one with the larger area was preferred. Table 11 also shows the estimations of the possible capacities based on the assumptions for space requirements of chapter 3.2.2 and 3.2.3 as well as the capacities declared in the data set.

EIA	Wind energy	Solar PV energy
number	242	728
area	17852 km²	19035 km²
Number of contiguous areas without overlaps	244	519
Contiguous areas without overlaps	8894 km²	9874 km²
Resulting estimated capacity,	89 GW	329 GW
Contiguous areas without overlaps and exclusion zones	5665 km²	6584 km²
Resulting estimated capacity	57 GW	219 GW
declared capacity in data set	27.3 GW	35.96 GW

Table 11: Characteristics of the EIA applications (Department for Environmental Affairs 2015)

The unambiguously labelled, contiguous and non-overlapping EIA for wind and solar PV energy applications are shown in Figure 31.
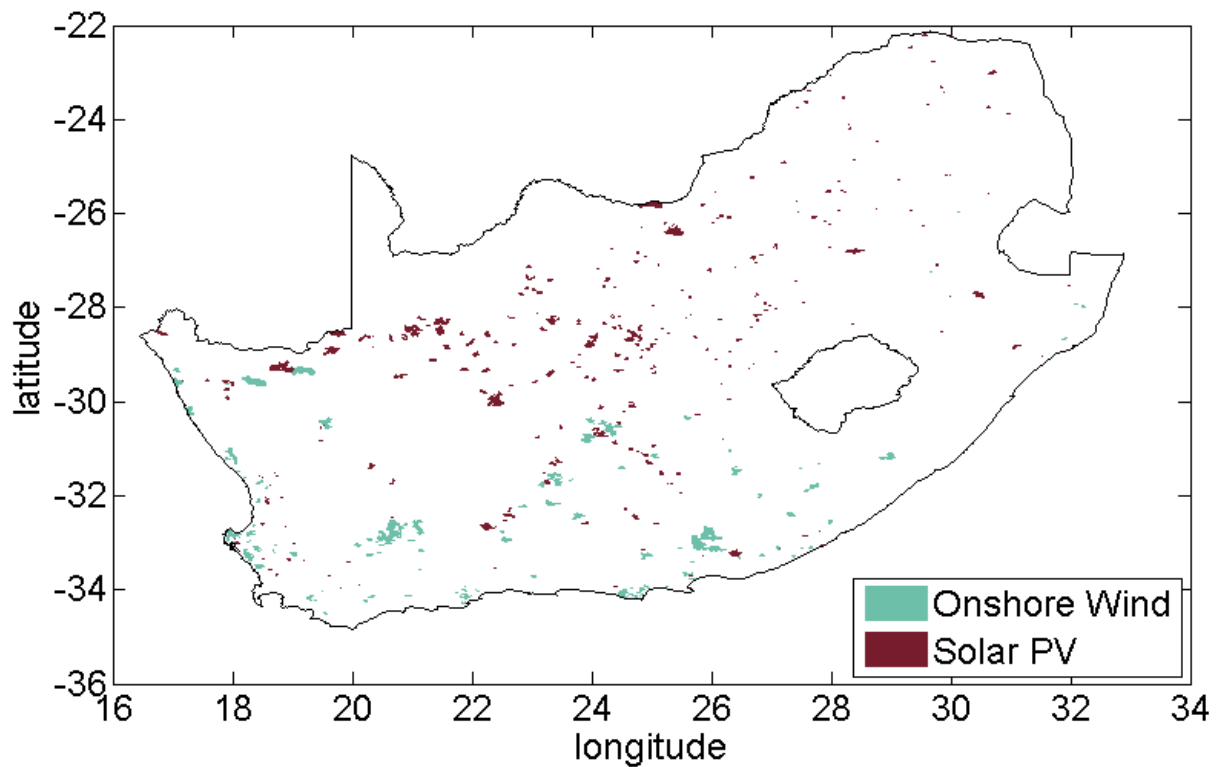
Wind and Solar Resource Aggregation Study
for South Africa

Figure 31: Renewable Energy EIA applications

By aggregating the feed-in time series of all 5km by 5km pixels within each EIA area, 244 time series of EIA wind power production and 519 time series of EIA PV production were obtained in a temporal resolution of 15min covering a period of 3 years (years 2010 to 2012) respectively. Taking into account the exclusion zones all wind energy EIA deliver together an annual energy yield of 192 TWh with an average load factor of 0.39. The PV EIA deliver 219 TWh with an average load factor of 0.22. The highest load factor of all 244 wind energy EIA amounts to 0.435, the lowest to 0.243. The highest load factor of all 519 PV EIA amounts to 0.237, the lowest to 0.178. The aggregation of all wind energy EIA will be henceforth referred to as **'EIA-focused wind turbine distribution'.**

Table 12 shows its main characteristics which result from scaling the energy yields to 50 TWh, 100 TWh and 250 TWh respectively. It should be noted that the scaling up to 250 TWh exceeds the potential which results from an assumed space requirement of 0.1 km²/MW. The wind turbines have to be placed more densely for 250 TWh namely with a space requirement of 0.07 km²/MW, which is still in a realistic range.

	Spatial spread [km²]	Installed capacity [GW]	Annual energy yield [TWh]	Load Factor
Potential	5665	56.65	192	0.39
Scaled to 50 TWh	5665	14.73	50	0.39
Scaled to 100 TWh	5665	29.46	100	0.39
Scaled to 250 TWh	5665	73.64	250	0.39

Table 12: Characteristics of the 'EIA-focused wind turbine distribution'

Wind and Solar Resource Aggregation Study
for South Africa

4.2.2 REDZ-focused wind turbine distribution

In [18] areas were identified where large scale wind and solar PV energy facilities can be developed in a manner that limits significant negative impacts on the environment, while yielding the highest possible socio-economic benefits to the country. These areas are referred to as Renewable Energy Development Zones (REDZs) and shown in Figure 32.
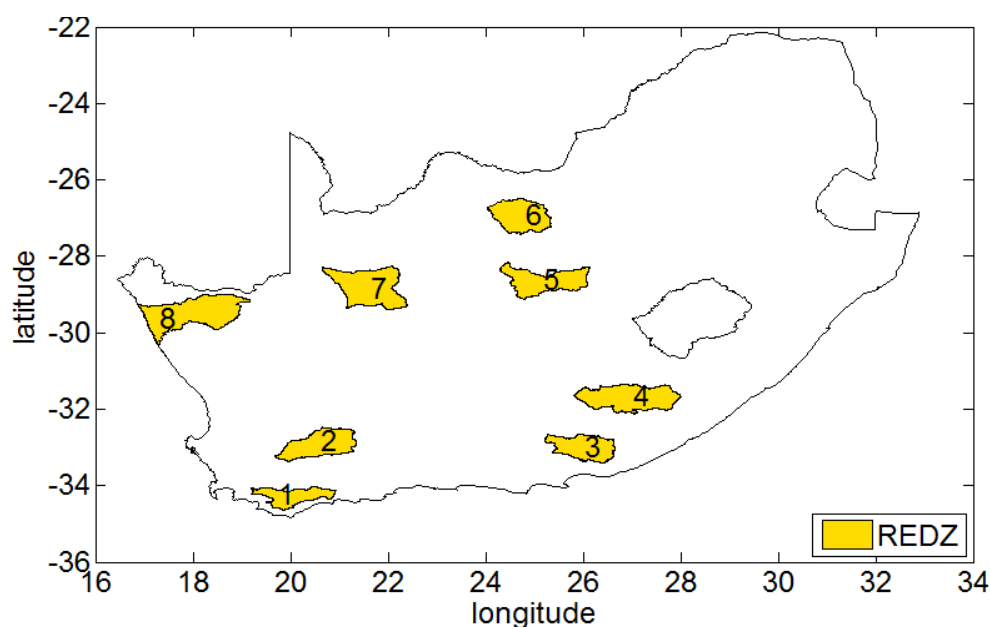
Figure 32: Renewable Energy Development Zones (REDZs)

The scenario of wind power generation on the whole REDZs areas minus exclusion will henceforth be referred to as **'REDZ-focused wind turbine distribution'**.
Table 13 shows the main characteristics of the **'REDZ-focused wind turbine distribution'**.

	Spatial spread [km²]	Installed capacity [GW]	Annual energy yield [TWh]	Load Factor
Potential	53472	535	1780	0.38
Scaled to 50 TWh	53472	15	50	0.38
Scaled to 100 TWh	53472	30	100	0.38
Scaled to 250 TWh	53472	75	250	0.38

Table 13: Characteristics of the 'REDZ-focused wind turbine distribution'

Table 14 gives some more information on every single REDZ.

Wind and Solar Resource Aggregation Study
for South Africa

4.2.3 EIA/REDZ overlaps

It is still undefined if a REDZ is more suitable to develop wind or PV energy facilities. A way to assess this suitability is to determine the overlaps of REDZs and EIA applications as done in Figure 34. The figure clarifies that some REDZs are rather designed for wind energy as REDZ no. 2 or 4 and other for PV as REDZ no. 5 and 7 for example.

Figure 33 gives an overview on this.

Table 14 indicates the areas of the REDZs for different subdivisions and also notes the electrical characteristics, which result from the simulation models of section 3.2.

Figure 33: Overlaps of REDZs and EIA

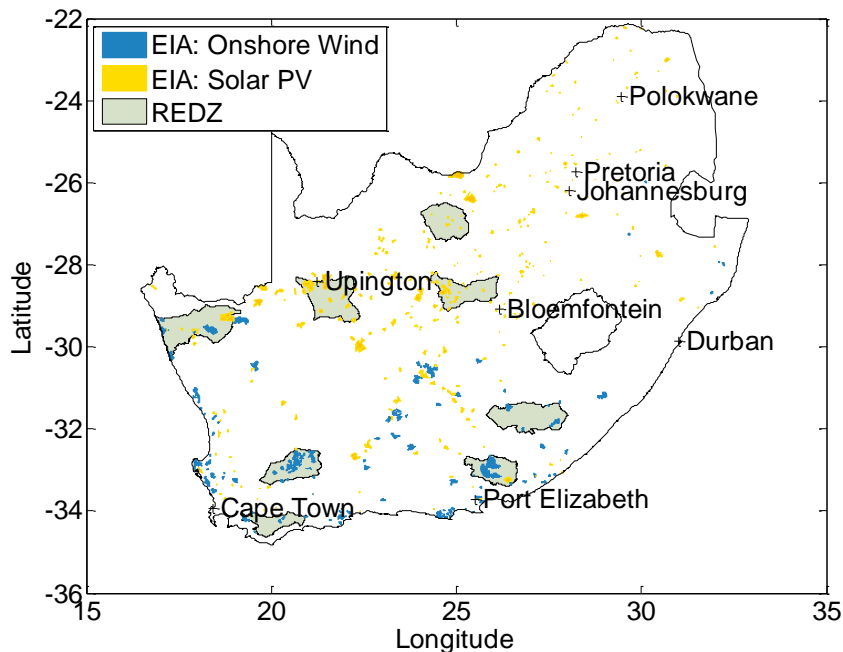|		REDZ no.	1	2	3	4	5	6	7	8	total
		Area [km²]	5271	8879	7356	12046	9561	9238	12830	15349	80530
Area minus exclusion		Area [km²]	236	7594	5351	6899	5070	5300	10537	12486	53472
	Wind energy	Capacity [GW]	2.4	75.9	53.5	69	50.7	53	105.4	124.9	534.7
		Energy [TWh]	8.1	245.3	174.9	229.7	163.7	177	356.8	425	1780
		Load factor	0.39	0.37	0.37	0.38	0.37	0.38	0.39	0.39	0.38
	PV	Capacity [GW]	7.9	253.1	178.4	230	169	176.7	351.2	416.2	1782.4
		Energy [TWh]	12.9	487.9	297.9	432.1	329.7	348.8	675.6	785.8	3370.6
		Load factor	0.19	0.22	0.19	0.21	0.22	0.23	0.22	0.22	0.22
EIA areas on REDZs minus exclusion	Wind energy	Area [km²]	3.1	1324.5	1623	285.9	0	0	0	1241	4477.5
		Capacity [GW]	0.03	13.25	16.23	2.86	0	0	0	12.41	44.77
		Energy [TWh]	0.1	43.8	54.1	9.5	0	0	0	45.2	152.8
		Load factor	0.4	0.38	0.38	0.38	0	0	0	0.42	0.39
	PV	Area [km²]	0	3.41	140.81	15.33	617.54	62.08	741.1	617.68	2197.95
		Capacity [GW]	0	0.11	4.69	0.51	20.58	2.07	24.7	20.59	73.27
		Energy [TWh]	0	0.2	7.7	0.9	39.8	4.1	47.5	39.5	139.7
		Load factor	0	0.23	0.19	0.2	0.22	0.22	0.22	0.22	0.22

Table 14: Characteristics of the REDZs and the overlaps of REDZs and EIA

Figure 34: EIA within REDZs

Wind and Solar Resource Aggregation Study
for South Africa
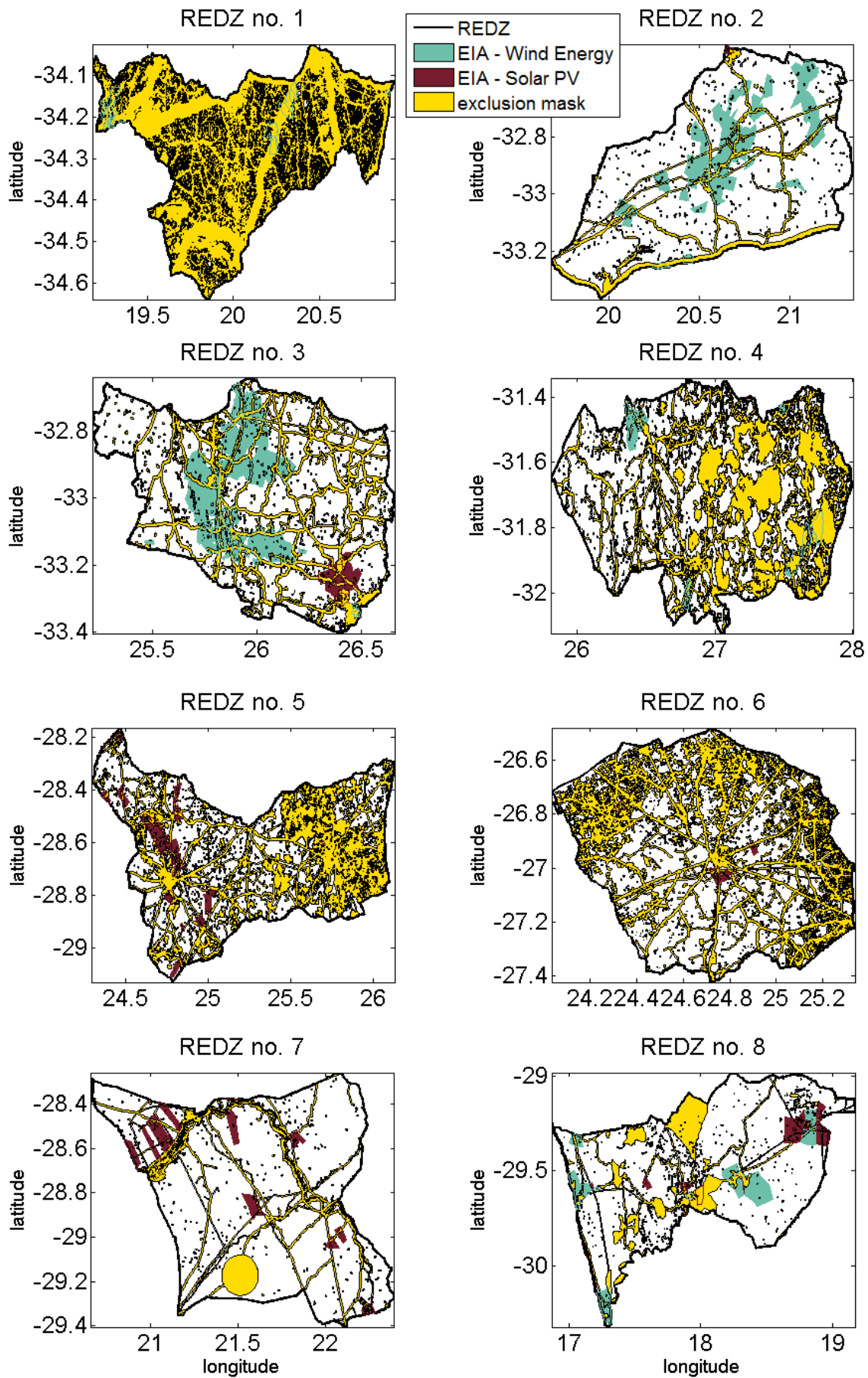
4.3 Grid-focused wind turbine distribution

A widespread concern with high shares of renewables in the electricity system deals with the ability of the grid to transport the possibly strongly fluctuating electricity. So a transmission level **'grid-focused wind turbine distributions'** are assessed in this chapter, including both the current grid and a future grid as it is planned today by the transmission development plan (TDP) 2024 [19]. Figure 35 shows the 233 locations of the substations and indicates whether the time series of the electricity demand are available in [9] or not. Those 126 time series were aggregated in order to obtain the electricity demand of the whole country as described in chapter 3.2.1. In [1], time series of solar and wind power feed-in are simulated for every of the 233 locations of Figure 35 in order to analyse how much RE capacities can be installed at the substations as a function of the required curtailments.
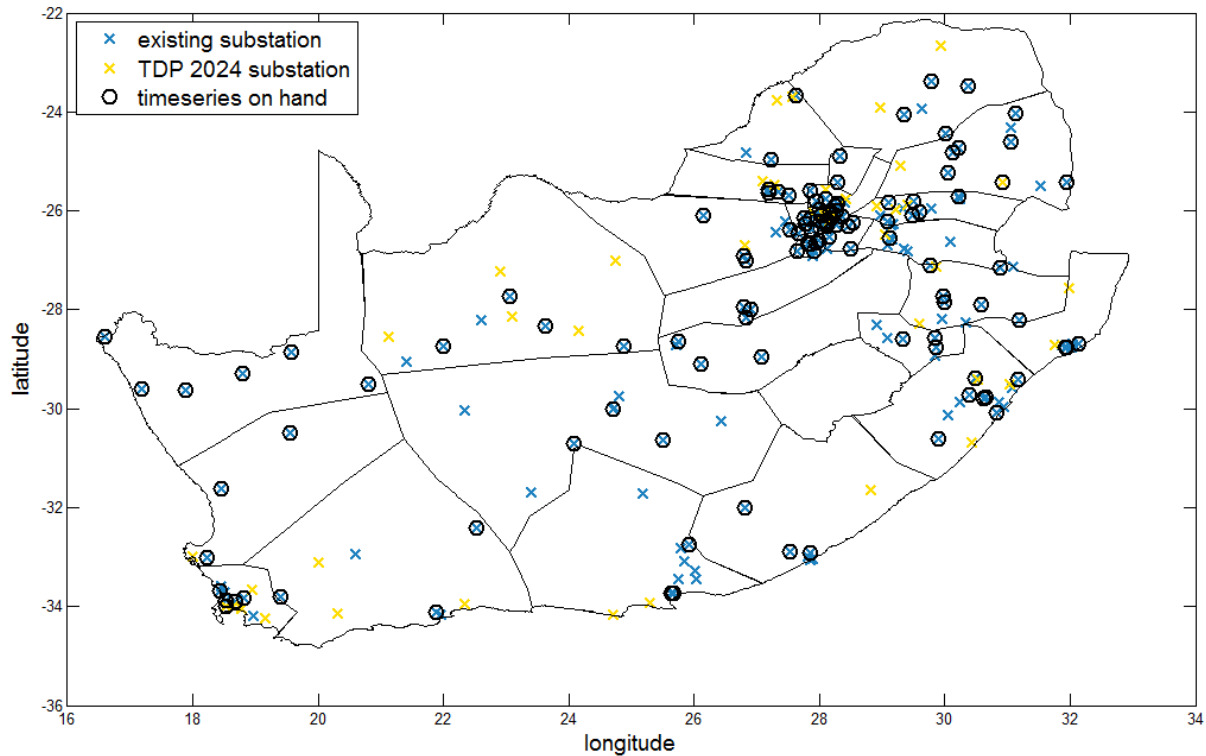

Figure 35: Locations of high voltage substations

The intention of the grid-focused wind turbine distributions is to determine pixels with low distances to the substation as well as high load factors. For this purpose all pixels with load factors lower than 0.4 are excluded in a first step. After that, the remaining pixels are sorted according to their distances to their nearest substation. As much sorted pixels are selected as are needed for 250TWh wind energy based on the uniform wind turbine distribution of Figure 22. This method is applied twice: on the existing substations on the one hand, on the existing substations and planned substation on the other hand. Thus, two grid-focused wind turbine distributions are derived. The first one will henceforth be referred to as **'present grid-focused wind turbine distribution'**, the latter as **'future grid-focused wind turbine distribution'**. Figure 36 and Figure 37 show the locations of the determined pixels for 250TWh..

It becomes clear, that there are plenty pixels with high energy yields very close to substations. The distances of a selected pixel to a substation are not longer than 13km. Most selected pixels are situated in the countryside. In urban areas the distances would have to be longer, thus no pixels are assigned to urban substations for the most part. The future gird-focused wind turbine distribution differs only very slightly from the present gird-focused one. Table 15 shows main characteristics of the two grid-focused wind turbine distributions.

Additional characteristics of the **'future grid-focused wind turbine distribution'** are given in Table 16
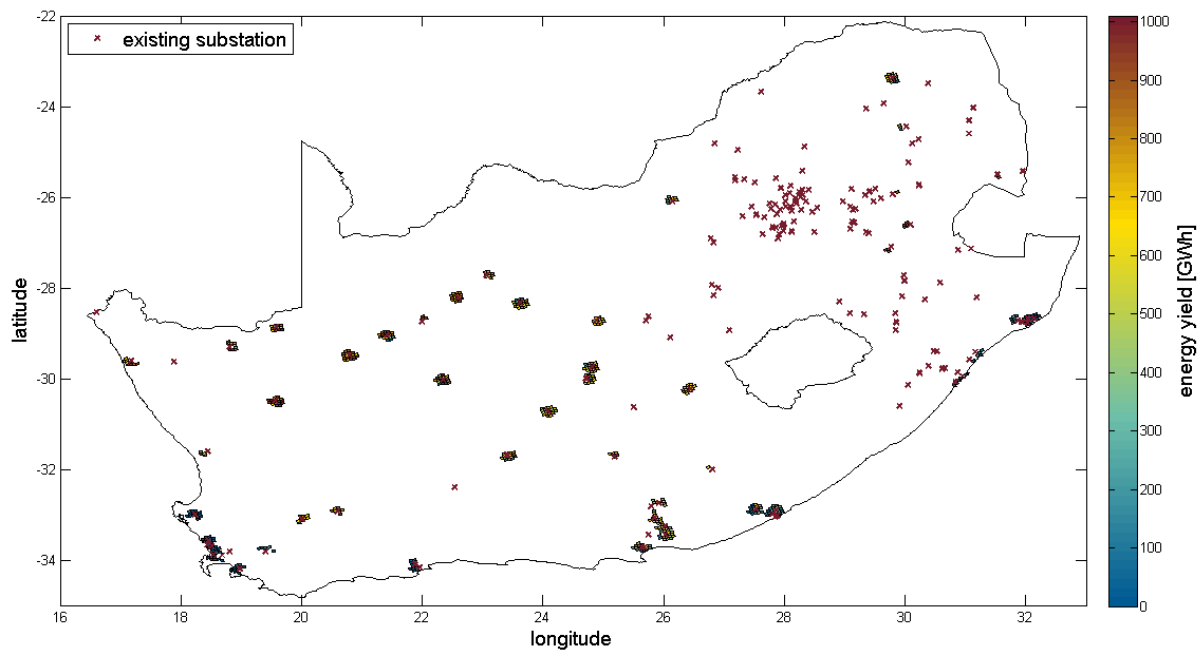
Figure 36: Locations of the 'present grid-focused wind turbine distribution' for 250TWh
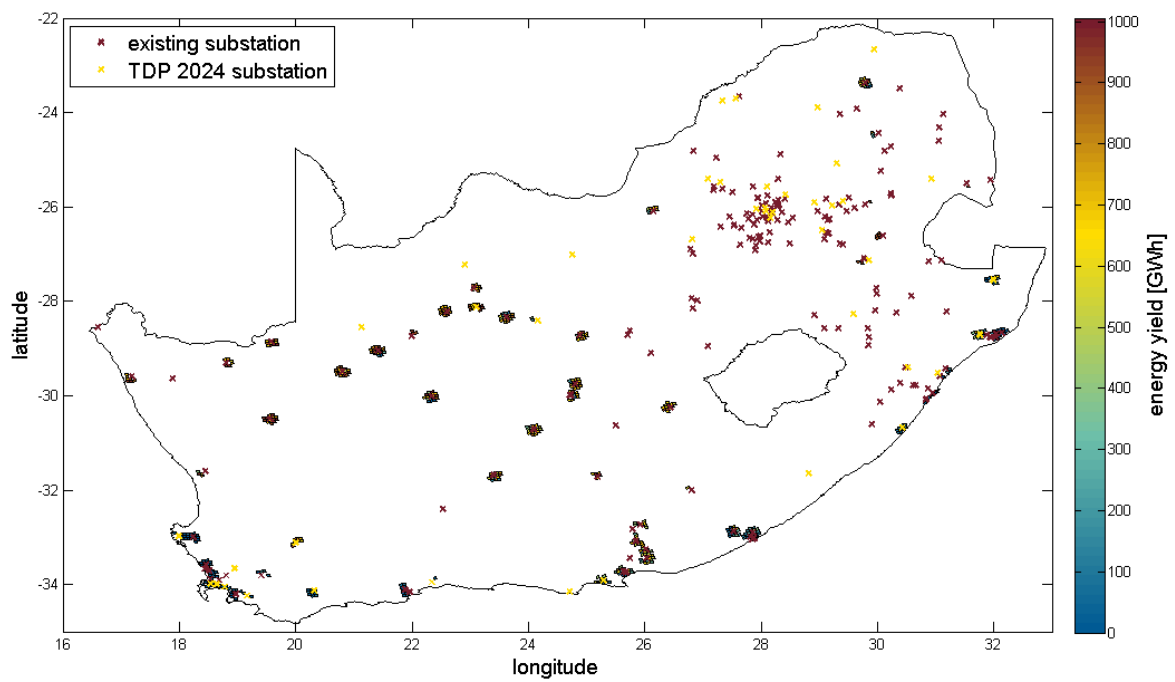
Figure 37: Locations of the 'future grid-focused wind turbine distribution' for 250TWh

Considered substations	Annual wind energy yield [TWh]	Spatial spread [km²]	Installed capacity [GW]	Load Factor
Existing	50	1365	13.65	0.42
Existing	100	2723	27.23	0.42
Existing	250	6769	67.69	0.42
Existing and planned	50	1368	13.68	0.42
Existing and planned	100	2711	27.11	0.42
Existing and planned	250	6762	67.62	0.42

Table 15: Characteristics of the 'Grid-focused wind turbine distributions'

		Potential	50 TWh/yr	100 TWh/yr	250 TWh/yr	All in one place 100 TWh/yr
Capacity		6 787 GW	13.68 GW	27.11 GW	67.62 GW	32 GW
Minimum output		162 GW	0.29 GW	0.47 GW	1.53 GW	0 GW
Normalised wind power 15-min gradient	Max	4.2%	12.9%	11.1%	8.29%	92%
	Min	-4.3%	-9.27%	-9.16%	-7.69%	-91%
Residual load 15-min gradients (assuming 80 TWh of PV)	Max	292 GW	5.53 GW	5.44 GW	6.49 GW	30 GW
	Min	-286 GW	-3.34 GW	-3.67 GW	-5 GW	-30 GW
Daily energy	Max	119450 GWh	258 GWh	512 GWh	1277 GWh	708 GWh
	Mean	59 494 GWh	139 GWh	275 GWh	686 GWh	274 GWh
	Min	13 327 GWh	30 GWh	57 GWh	143 GWh	1 GWh

Table 16: Statistics of aggregated wind output and residual load for the 'future grid-focused wind turbine distribution' assuming 80 TWh of PV

5. Results

This study focuses on the aggregation effects of wind energy in South Africa whilst taking into account the influence of solar PV as well. Different scenarios as described in chapter 4 are investigated.

5.1 Temporal characteristics of RE feed-in

The characteristics of the feed-in of electricity generated from wind and solar PV energy can be called advantageous: In the example of the 'grid-focused wind turbine distribution' as depicted in Figure 38 and Figure 39, it can be seen that there is hardly any seasonality in PV electricity generation. The wind feed-in shows a minimum at noon complementing the solar PV peak (see also Figure 38). In addition, the seasonal performance of the wind feed-in (Figure 39) matches demand very well.

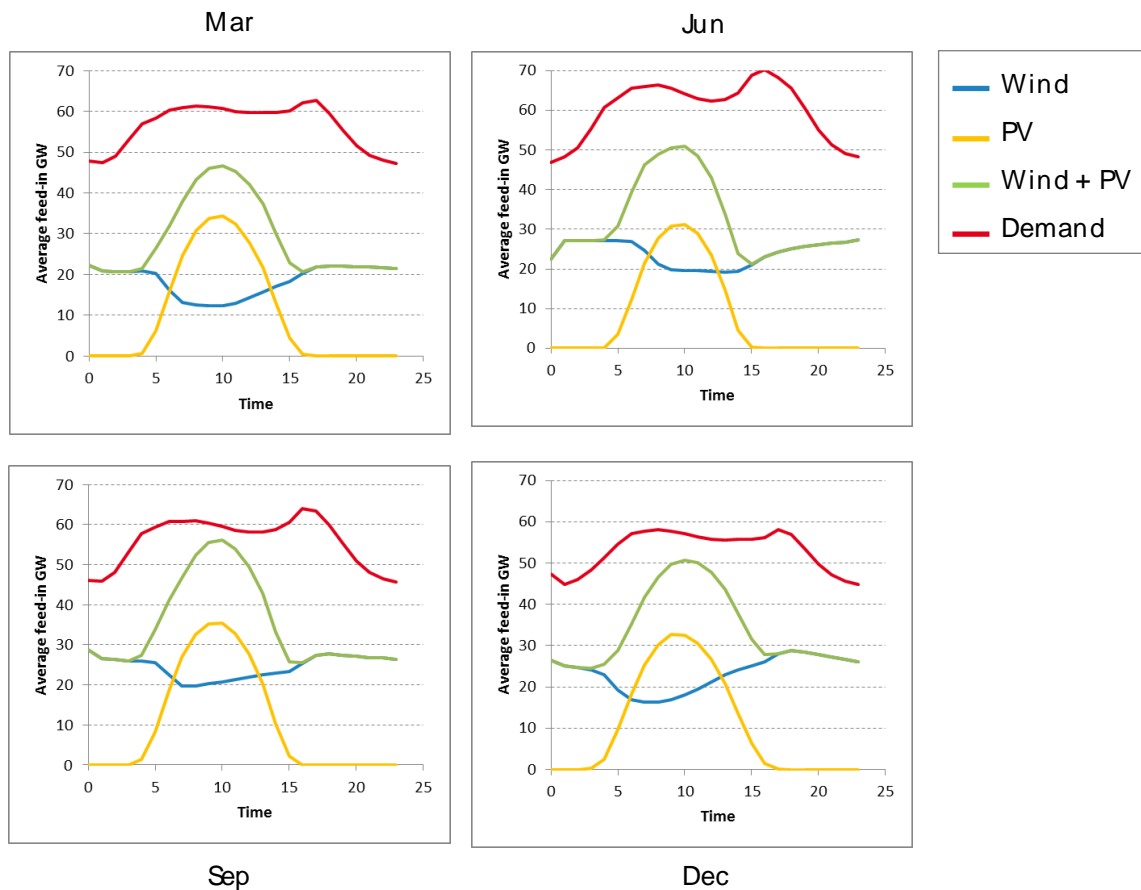**Figure 38: Average daily profiles of wind and PV feed-in and demand in the example of the 'grid-focused wind turbine distribution' (200 TWh/a wind, 80 TWh/a PV), daily average of 2010**
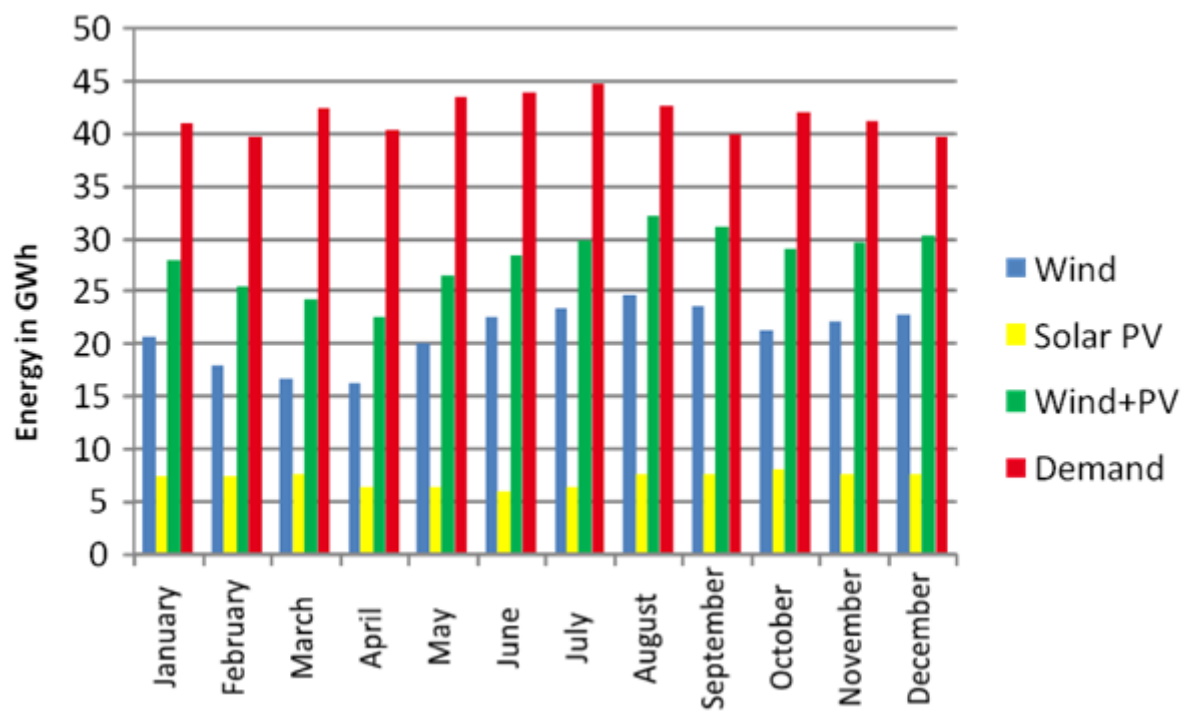
Wind and Solar Resource Aggregation Study
for South Africa

Figure 39: Seasonal profile of wind and PV feed-in and demand in the example of the 'grid-focused wind turbine distribution' (200/a TWh wind, 80 TWh/a PV)

5.2   Key performance indicators of the scenarios

In the following, the scenarios are analysed and compared based on key performance indicators dealing for example with the behaviour of the residual load and electricity surpluses.

The different scenarios cover a variety of possibilities of how to distribute wind turbines. Aiming for an electricity generation of 500 TWh according to the expected future demand with varying steps of wind power yields leads to the installed capacities shown in Figure 40.
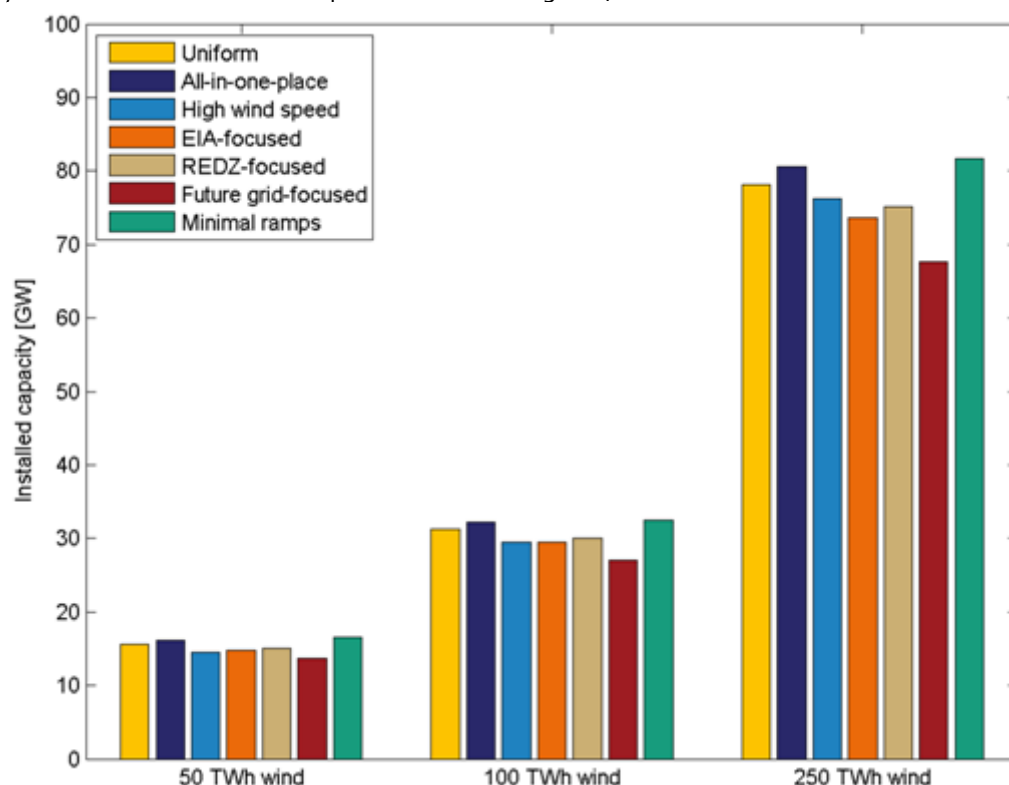
Figure 40: Installed capacity of wind power of different scenarios

The capacities to install differ by location and accordingly by the selected type of turbines (see section 3.2.3). To generate 50 TWh of electricity about 15 GW of wind power has to be installed. Assuming a specific required area of 0.1 km² per MW installed capacity, this would require only 1500 km² (≈0.1% of the South African landmass. Scenarios where 250 TWh of electricity is generated from wind power would need around 75 GW of installed capacity on average and thus consume ≈0.6% of South African landmass or 7500km². Actually, the consumed area would be much smaller as shown in Table 17.

	% of the wind farm area	**% of South African land mass** *(for a 75 GW wind fleet that yields 250 TWh/yr)*
Wind farm area	100%	0.61% *(7 500 km²)*
Ways, foundation during construction	3%	0.018% *(225 km²)*
Permanently used	2%	0.012% *(150 km²)*
Wind turbine foundations	0.1%	0.0008% *(10 km²)*

Table 17: Illustration of land required during operation of a wind farm

Wind and Solar Resource Aggregation Study
for South Africa

The capacity to install for each scenario is directly related to the average load factors of each scenario, which are shown in Figure 41. The load factors are remarkably high for all scenarios. This confirms the fact that the conditions for wind energy in South Africa are extraordinarily good, which also explains why the load factor does not change much even with higher installed capacity.
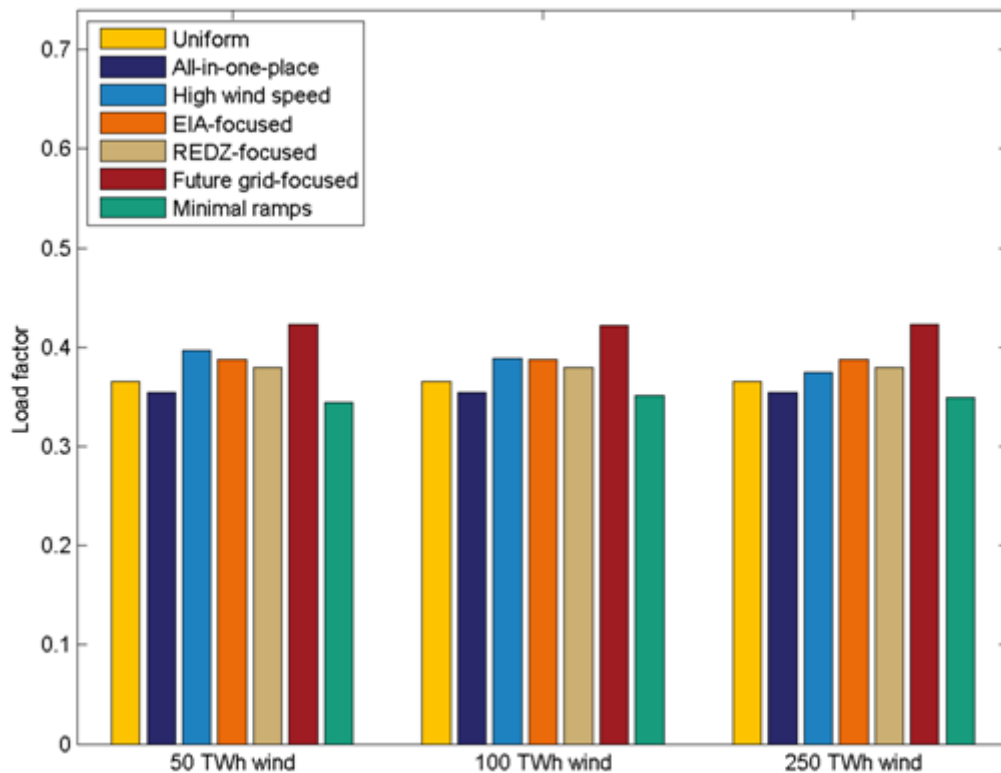

Figure 41: Load factors of wind power for different scenarios and different installed capacities of wind power

Comparing the scenarios, for the **'all-in-one-place'** scenario the selected pixel happens to offer conditions a little below average. The selection of another pixel could result in either a better or a worse load factor. The **'future grid-focused distribution'** of wind power considers only those pixels with the lowest distance to grid nodes and high load factors, so the high values for this scenario are not a coincidence. For the the **'minimal ramps wind turbine distribution'**, on the other hand, wind turbines have to be placed in areas with relatively low average load factors. Therefore, this scenario's installed capacity is the highest.

All in all it can be noted that wind turbines can be operated with high load factors almost everywhere in the country. Nevertheless, a wider distribution will lead to a steadier operation of the turbines. This effect can be seen in Figure 42 where the aggregated wind power duration curves of different scenarios with 250 TWh of electricity generated from wind power are shown.

Those scenarios with a wider distribution of turbines result in smoother curves while the distribution of turbines according to the highest wind speeds shows a steeper course. Furthermore, the locations of the **'high wind speed'** scenario are relatively close to each other (even more so for an installation of all turbines in one place, i.e. a single pixel) while those of the other scenarios are widely spread over the country which causes stronger aggregation effects. The case of South Africa a wide distribution leads to the benefit of zero hours with no feed-in at all. At any time step of 15 min there is electricity generated from wind energy at some location in South Africa for any scenario but **'all-in-one-place'**.

Wind and Solar Resource Aggregation Study
for South Africa
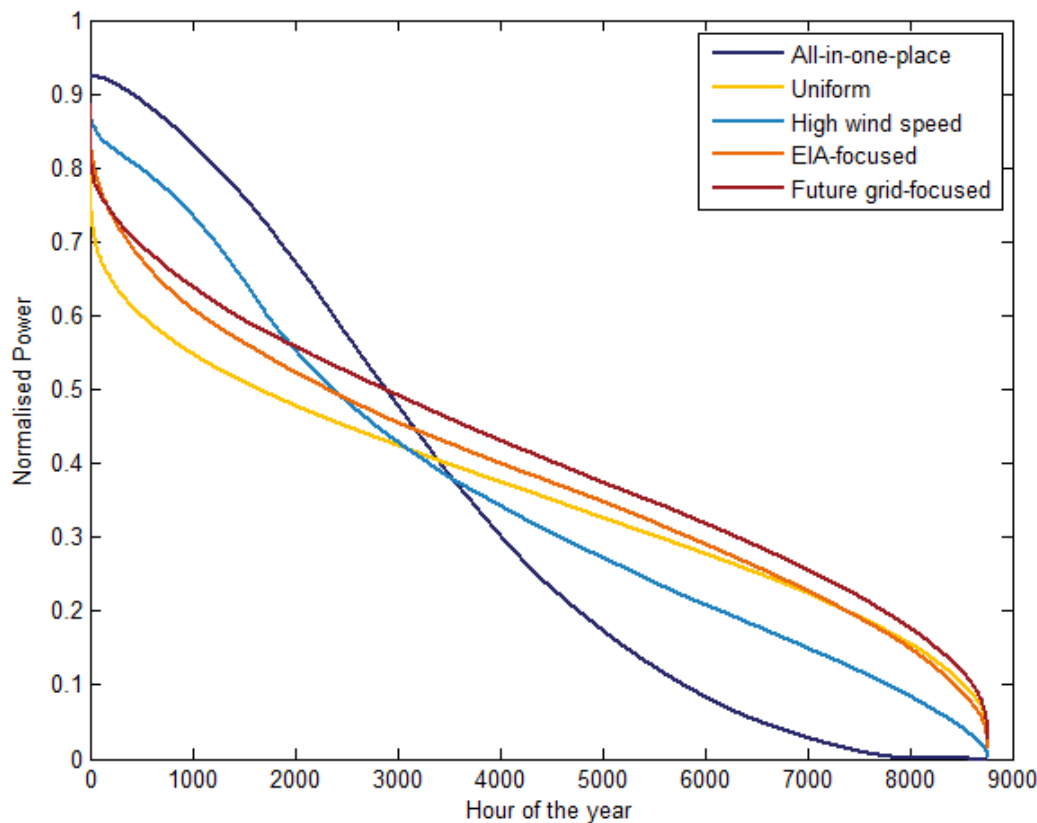
Figure 42: Aggregated wind power duration lines of different scenarios with 250 TWh of electricity generated from wind power, years: 2010-2012

Figure 43, showing the maximum residual load of different scenarios assuming 80 TWh of PV, underlines the positive effects of an even distribution of wind turbines over the country. Furthermore, a higher installed capacity of wind power would decrease the residual load. While the residual load reaches a maximum value of about 76 GW in case of the **'all-in-one-place'** scenario, this value would be 71 to 76 GW for an installation of turbines according to high average wind speeds. Those scenarios with more even distribution methods (**'uniform'**, **'EIA-focused'** and **'future grid-focused'**) lie between 67 and 75 GW, the **'uniform wind turbine distribution'** leads to the lowest values. The lowest values of all scenarios are reached by the **'minimal ramps'** scenario. This scenario shows a residual load of about 60 GW at 250 TWh of electricity generation from wind energy. In comparison the maximum load of the system is about 77 GW.

The results do not change remarkably with installed capacity of solar PV. A reasonable explanation would be an occurrence of maximum residual loads mainly at night when the demand is high and no solar irradiation arises.

Wind and Solar Resource Aggregation Study
for South Africa

Figure 43: Maximum residual load for different scenarios and different installed capacities of wind assuming 80 TWH of PV

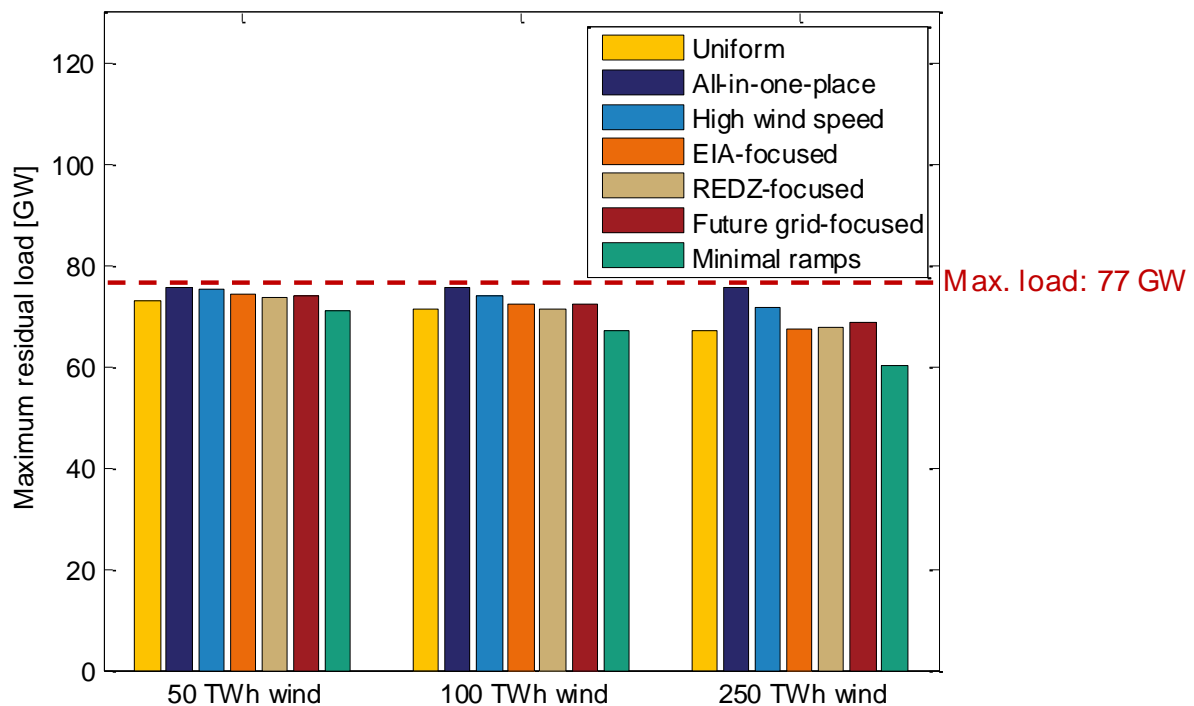The relative frequency of residual load of different scenarios (Figure 44) illustrates clearly how fluctuations influence strongly the feed-in of electricity when wind farms are not distributed over a larger area. For example, the 15 min power increments of the extreme scenario **'all-in-one-place'** with 100 TWh of electricity from wind energy and 40 TWh from solar PV vary between nearly -30 GW and 30 GW. These values can be reduced massively to -2 GW and 2.8 GW for the 'minimal ramps wind turbine distribution'. The **'uniform wind turbine distribution'** and the **'future grid-focused wind turbine distribution'** show low values, too, while the **'high wind speed wind turbine distribution'** leads to modestly higher values around roughly +/-4.5 GW.

Figure 45 offers a comprehensive comparison of all scenarios. It shows the standard deviation of their residual load's 15min ramps in relation to the annual energy yield of wind power and solar PV as well as the annual share of RE in the electricity system. The values for an electricity generation without any wind energy are included, too.

This figure shows how much of an effect well informed placements of wind power generation can have. An installation of turbines in only one area as for the **'all-in-one-place wind turbine distribution'** would be the only scenario leading to a higher standard deviation than without any building of wind turbines having solar PV energy in the system. As long as wind turbines are distributed over larger areas, up to roughly 30% of RE will not increase ramps and fluctuations significantly (except for the **'all-in-one-place'** scenario).

Solar PV is the main driver for high standard deviation. The best results, i.e. minimal standard deviations, can be reached with a balanced combination of wind and solar PV. This effect can be derived from observing the relation between the energy generated annually from wind and PV. On the one hand, those scenarios with 200 TWh of electricity from solar PV (and thus higher shares of PV) show clearly high standard deviations, as can be seen from the upper group of scenarios in Figure 45. On the other hand, adding wind energy to a system with solar PV causes no increase in the standard deviation. This can be detected from a comparison of the green crosses ('no wind energy') and the relevant groups of scenarios with the same amount of solar PV energy where the standard deviation stays at about the same level. Higher overall shares of RE can be realized with low standard deviations as well but show a stronger dependency on the ratio of wind to solar PV. To determine an optimal share of wind and PV and an optimal distribution investigation is needed.
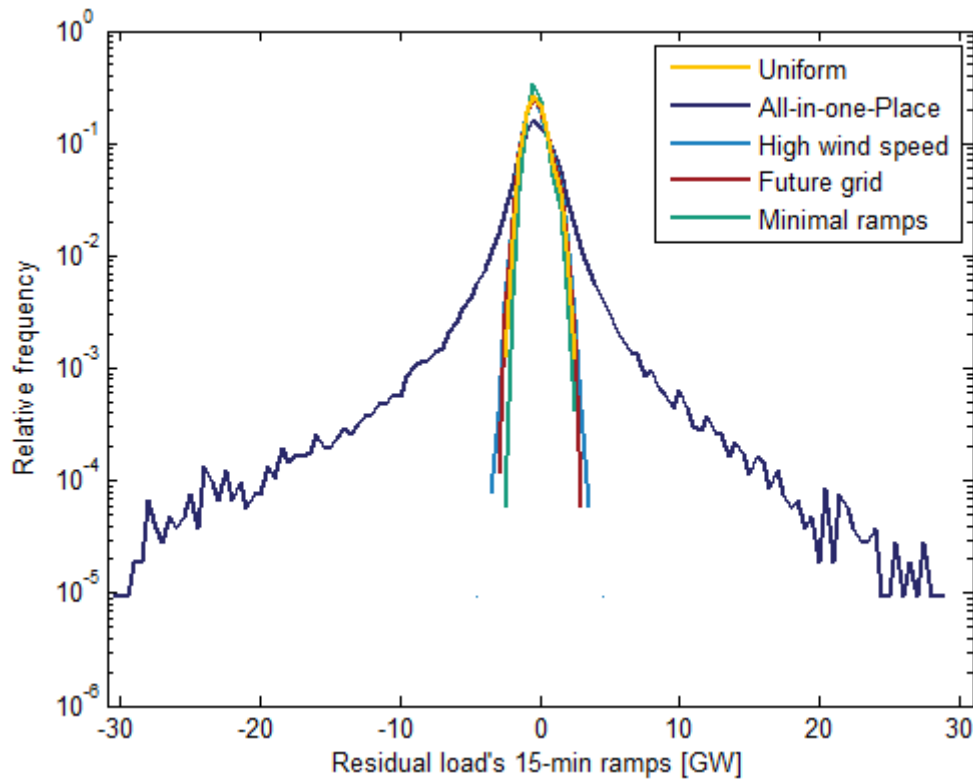
Figure 44: Relative frequency of residual load of different scenarios with 100 TWh of electricity from wind energy and 40 TWh from PV as a function of 15min power increments
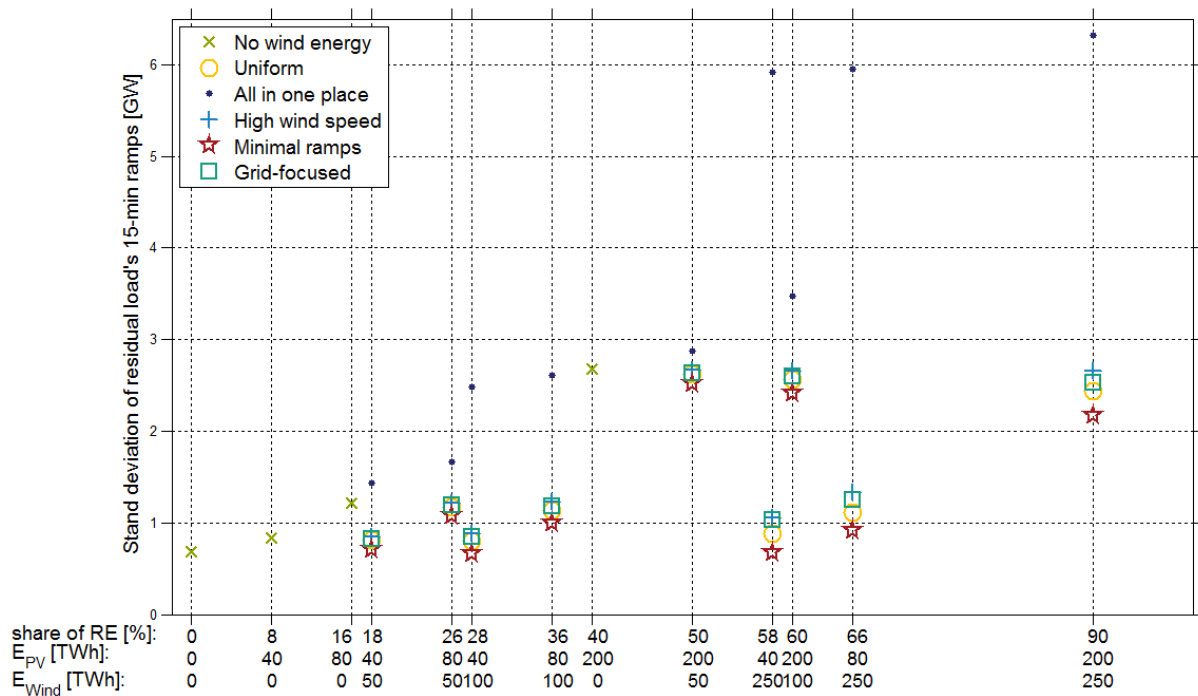
Figure 45: Standard deviation of residual load with 15min ramps of different scenarios

The fluctuating feed-in of electricity generated from wind and solar PV will lead to times with excess electricity as well as deficits. While the latter can be compensated by flexible power plants (operated with either renewable or fossil fuels), excess electricity must be either stored or curtailed. Figure 46 illustrates the

Wind and Solar Resource Aggregation Study
for South Africa

electricity surpluses and deficits, which occur during a week in a scenario of 500TWh demand, 80 TWh PV and 250 TWh wind energy. Surpluses and deficits are equivalent to a negative and a positive residual load, respectively.
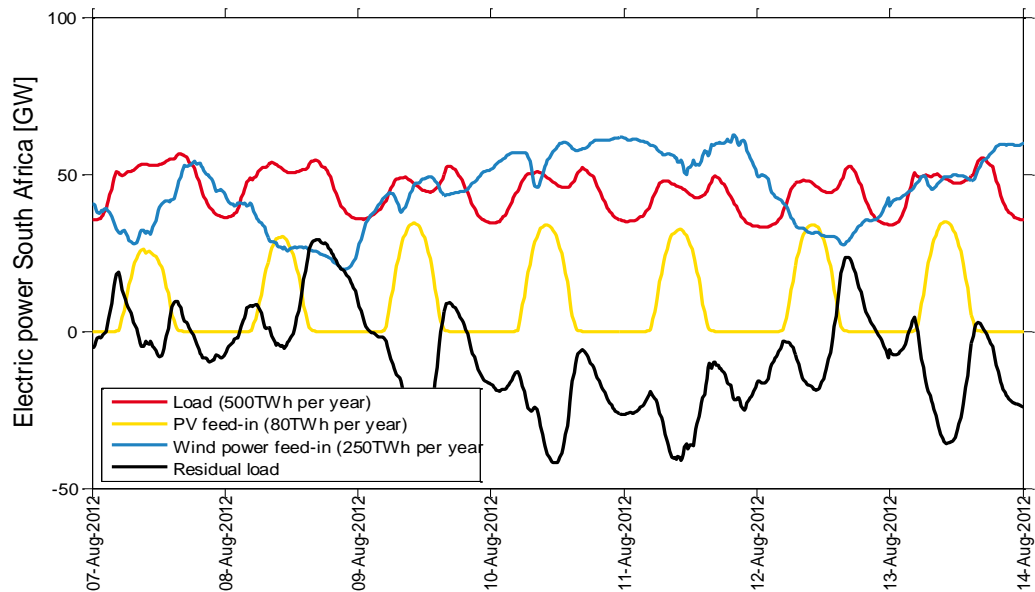
Figure 46: Illustration of electricity surplusses and deficits

In terms of the storage option, it is important whether short-term or long-term storage would be needed. In order to answer this question the durations of continuous periods with electricity excesses and surpluses only are determined as shown in Figure 47.

.
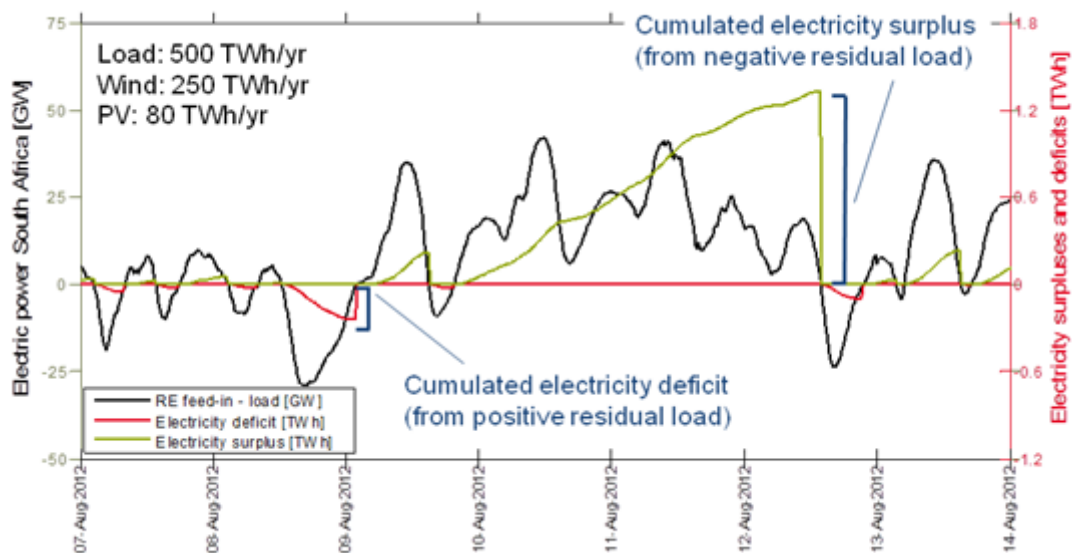
Figure 47: Determination of bulk storage needs

The maximum duration of periods where more electricity than needed is generated is evaluated as a function of the share of renewables in Figure 48.

Wind and Solar Resource Aggregation Study
for South Africa
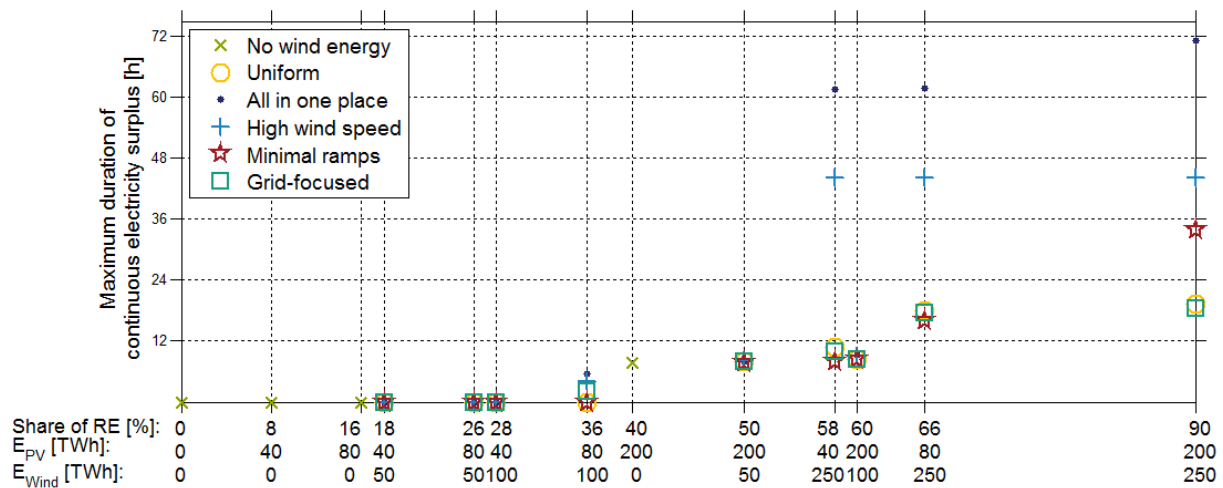
Figure 48: Electricity surpluses: Maximum duration by scenario

It can be derived that electricity storage will only be needed at high shares of renewables: Maximum surplus situations only occur if there are over 40% of wind and solar PV in the system. Aggregation effects can limit the duration of continuous surplus situations to less than 2 days.

5.3 Economic application of RE

As shown with the help of Figure 23, installing wind turbines type 4 and 5 (see section 3.2.3) will cause higher costs but also increase load factors and electricity yield whilst consuming the same area as turbines 1 to 3. The actual decision on which wind turbine to build will be cost-driven in the end. Since a comprehensive cost analysis does not lie not in the scope of this study, the widely applied 'levelised cost of energy' (LCOE) approach is evaluated in a slightly modified manner. The method is illustrated in the example of turbine type 5 in Figure 49.
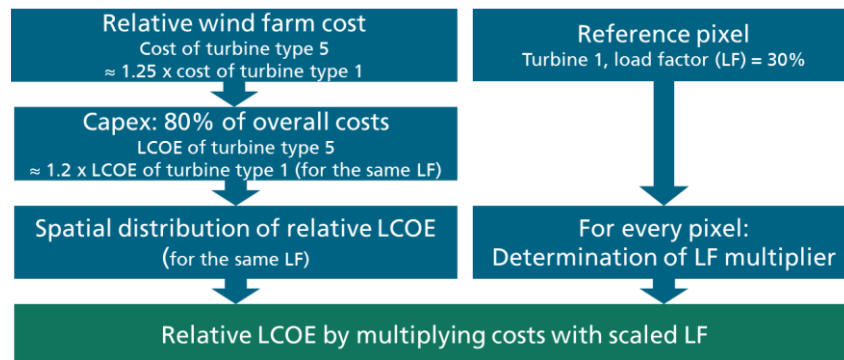
Figure 49: Method and assumptions for calculating relative levelised cost of energy (LCOE) in the example of turbine type 5 (LF: load factor, Capex: capital expenditure)

The LCOE method used is based on the two assumptions; (1) the cost for wind turbine 5 is approximately 25% higher than the cost of turbine type 1 and (2) it is assumed that the capital expenditure (Capex) makes about 80% of the overall cost. This leads to a factor of 1.2 for turbine type 5 compared to the LCOE of turbine type 1 with the same load factor (LF). This factor would be 1.05 for turbine type 2, 1.1 for turbine type 3, and 1.15 for turbine type 4. Taking into account the spatial distribution of the LCOE, the latter get multiplied with a scaled load factor determined in reference to a pixel where turbine type 1 with a load factor of 30% is installed. This way relative LCOE are determined for every pixel.
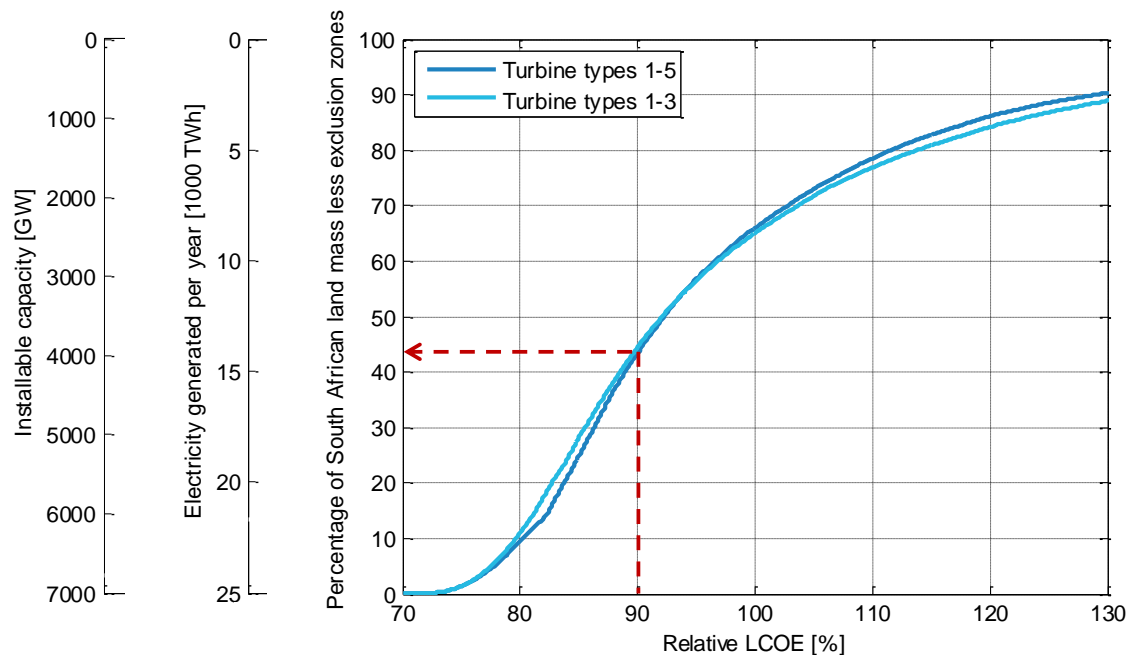
Figure 50: Share of South African land mass less exclusion zones and relative LCOEs to be reached accordingly

Figure 50 indicates the percentage of the South African land mass less exclusion zones that can be used for installing wind turbines to reach a certain relative LCOE. If, for example, a maximum relative LCOE of 90% is supposed to be reached, up to 44% of the land mass can be used. At the same time, wind turbines with a capacity of about 4000 GW could be installed within this area. For the relative LCOE, it does not make a big difference if turbine types 1 to 5 or 1 to 3 only are installed.

Figure 51 shows the map of the relative LCOE assuming turbine types 1 to 5 to be installed. Figure 52 assumes turbine types 1 to 3 only.
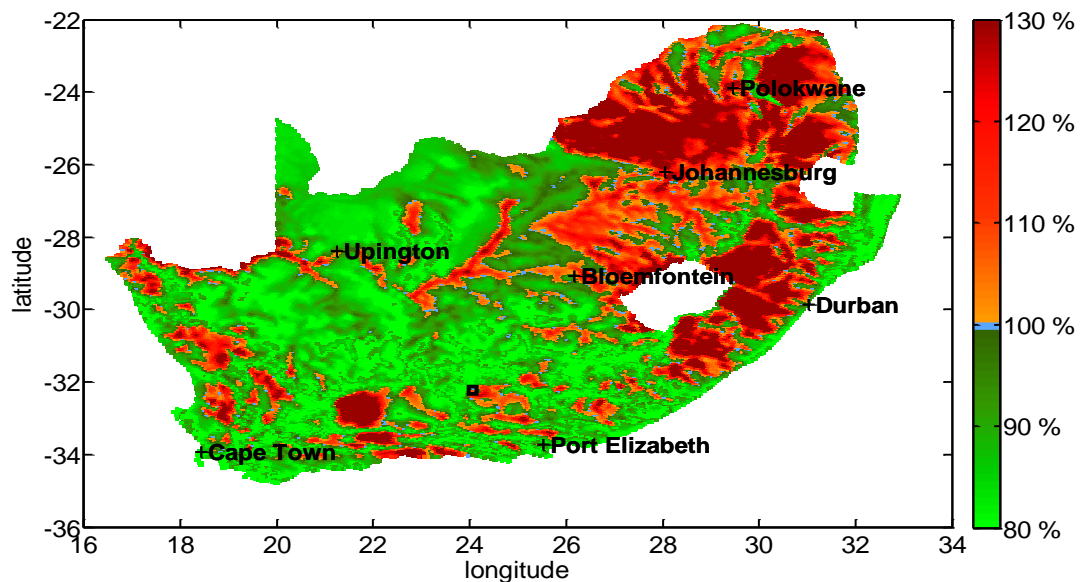
Figure 51: Relative LCOE across South Africa when installing turbine types 1 to 5
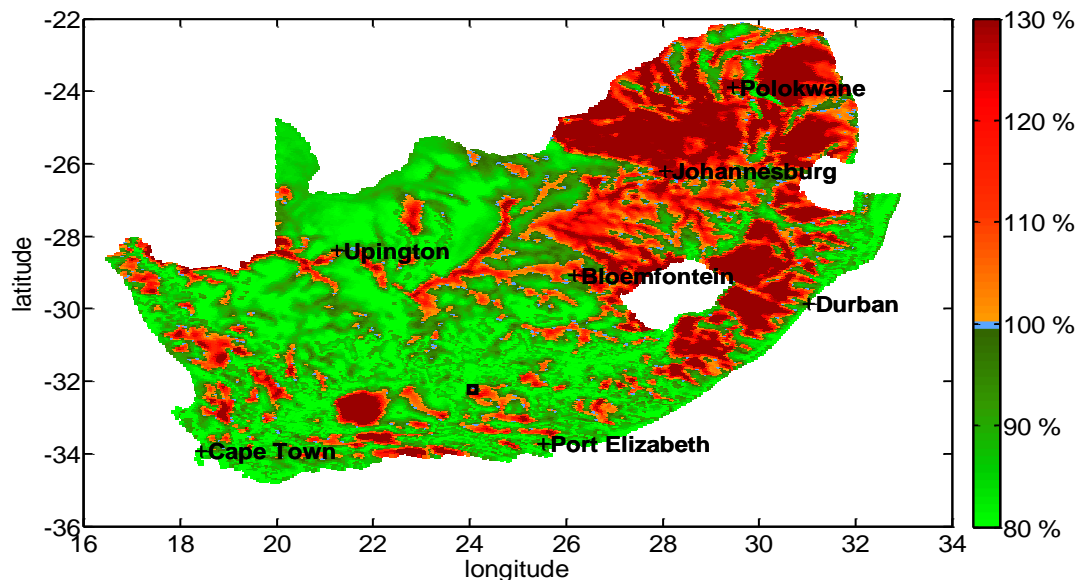
Figure 52: Relative LCOE across South Africa when installing turbine types 1 to 3 only (i.e. type 3 at 4/5 pixels)

Wind and Solar Resource Aggregation Study
for South Africa

5.4 Predictability of wind supply

Worldwide, there are several tools for forecasting wind power on different turbine aggregation levels, ranging from single turbines and wind farm portfolios to regional and nationwide production. Their errors are often summarized with conventional error statistics - max, min, mean, mean square or mean absolute error - whose amplitudes result from different factors. The main drivers of the forecast accuracy can be divided into three classes:

i. **Forecast horizon (or lead time):** It is obvious that in general the quality of a forecast decreases with increasing *forecast horizon*. Figure 53 shows the results of a large-scale German forecast error evaluation. The results have been averaged over a large number of wind farm, portfolio and regional forecasts that are based on 20 individual numerical weather forecasts (NWPs). The forecast error in terms of the root-mean-square-error (RMSE) clearly increases with increasing forecast horizon. The strong decrease of the RMSE for horizons of about 1 to 5 hours results from the assimilation of recent wind farm measurements in addition to NWP data into the forecast models. Consequently, a reduction of the forecast horizon from 48 hours to 1 hour leads to an average improvement of the RMSE of more than 50%.
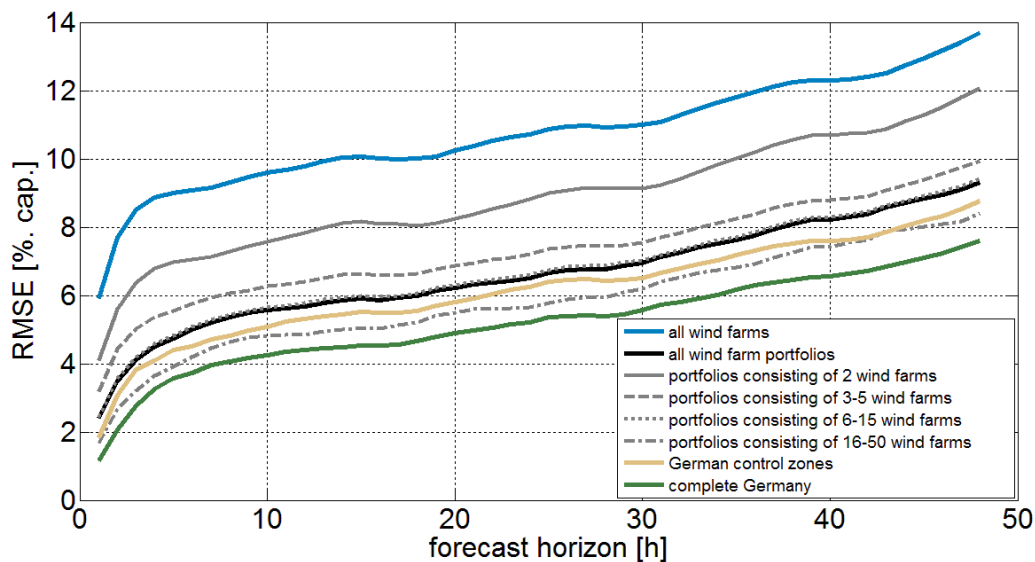
**Figure 53: Forecast accuracy in terms of the RMSE (in percent of the considered capacity) as a function of the forecast horizon. The lines present different aggregation levels ranging from single wind farms (blue) up to all of Germany (green). The forecast accuracy has been averaged over all relevant wind farms, wind farm portfolios, and with over 20 individual numerical weather forecasts [20].**

ii. **Wind complex:** The class *wind complex* regards all local and spatial information of the considered wind turbines, farms, and wind farm portfolios or regions with respect to spatial smoothing effects, orographic and terrain effects, wind farm layout and technology, as well as local or regional wind characteristics. Figure 54 shows the forecast error in terms of the RMSE for different aggregation levels ranging from single wind farms up to nationwide. The results show an error reduction of more than 5% in RMSE for regions ranging from aggregations of single wind farms to large regions (here Germany). In [20], it was shown that the class *wind complex* can be represented by the variability of the wind power feed-in. Aggregation leads to a smoothed feed-in. Different local wind characteristics lead to individual characteristics of the wind power variability. Moreover different wind farm power

curves and wind farm layout and technology have an impact on the wind farm power curves and therefore on the transformation of wind to power and consequently also on the variability. Figure 54 shows a close to linear dependency between predictability (in terms of the RMSE) and variability of the target wind power time series. The RMSE increases with increasing variability of the wind power time series that must be forecasted. The correlation is almost R=0.97. Within this study, the presented dependency is used to estimate the day-ahead wind power forecast errors for two different aggregation scenarios in South Africa.
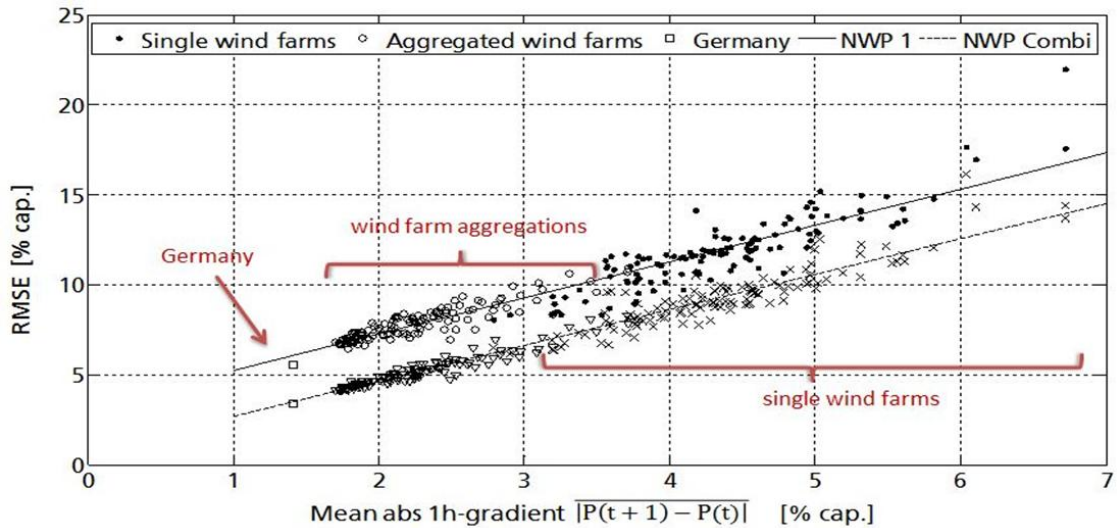
Figure 54: Dependency between forecast errors of single wind farms, wind farm aggregations and all of Germany on the variability of the respective measurements in terms of the mean absolute 1h-gradients. The results are based on a single NWP wind power forecast with lead times of 5 to 30 hours and on a combination of different NWPs [20].

iii. **Model:** The class *model* describes the performance of the applied physical or statistical model including the learning algorithm, the used numerical weather forecasts and other datasets like online measurements of the power feed-in or anemometer wind speeds of representative wind farms. With respect to forecast horizons $> \sim 5$ hours, the wind power forecast quality mainly depends on the quality of the used NWP. Figure 54 shows the RMSE values of different wind farm and portfolio forecasts based on a single NWP (upper line) and a combination of different NWPs (lower line). It is clearly visible that an adequate usage and combination of different weather forecasts lead to a clear forecast improvement. Aside from the NWP data, it was shown in Figure 53 that the addition of online power measurements has the highest impact on the forecast quality for short forecast horizons of up to 5 hours.

Within this study two approaches are applied to estimate the wind power forecast errors for two different wind energy installation scenarios in South Africa. In the first scenario it is assumed that all wind power is installed at a single location (all in one place). In the second scenario the wind power is equally distributed over all potential areas in South Africa (uniform).

I. In the first estimation approach, the forecast errors of lead times ranging from 1 to 48 hours are estimated based on the existing knowledge about the main drivers of wind power forecast errors as listed above. With respect to the identified main drivers, a model was developed in [20] to estimate the average forecast error in terms of the RMSE for different sized wind farms, portfolios and regions. The model was constructed based on experience gathered within a large-scale wind power forecast

Wind and Solar Resource Aggregation Study
for South Africa

error analysis of German wind energy installations. In general, the model is based on a statistical dependency between variability and predictability as shown in Figure 54. The dependency was investigated for each lead time separately. Within the present study, the model is used to estimate the forecast error in terms of the RMSE for South Africa. As input for the model, the variability of the simulated time series of both scenarios (see previous sections) has been used. The variability is calculated in terms of the mean absolute (1h) power gradients (increments) within the analysed time period ranging from 2009 to 2013 and based on a time resolution of one hour.
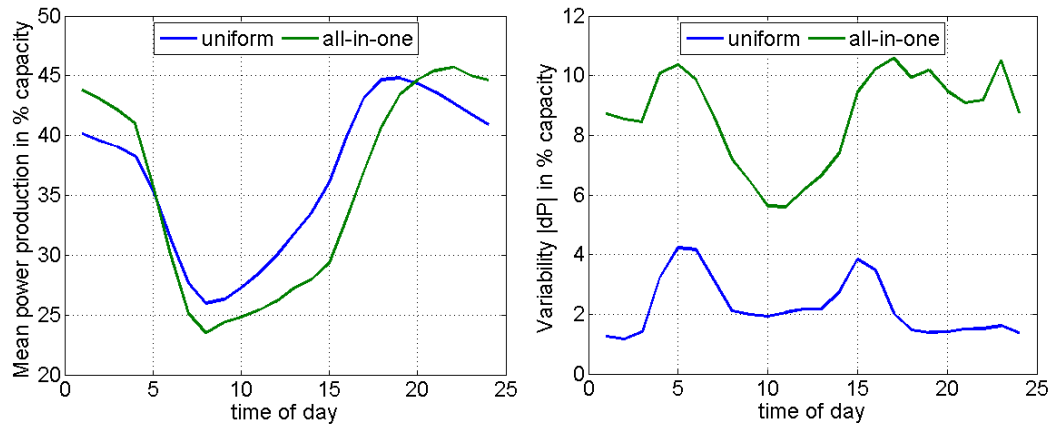
Figure 55: Mean wind power production (left) and variability (one-hour increments, right) as a function of the time of day for two simulated installation scenarios for South Africa (uniform, all in one place)

Figure 55 shows the mean wind power production and variability as a function of the time of day for the two simulated installation scenarios. It is clearly visible that the wind power production in South Africa is on average much higher in the evening and nighttime (4 pm to 4 am). This characteristic also explains the temporal trend in the variability. The distinct differences between night and day lead to an increase of the variability during the time when the average wind speed is decreasing (about 5 am) and increasing again (about 3 pm). Averaged over all hours, the all-in-one-place scenario leads to a variability value of 8.6% of the installed capacity. Due to the spatial smoothing effects, the uniform scenario shows a reduced variability of about 2.2% of the installed capacity. Based on the investigated variability of the simulated wind power time series and the model described in [20], the forecast error in terms of the RMSE has been estimated for lead times of 1 to 48 hours and for both scenarios. The left plot in Figure 56 presents the results. On one hand it is clearly visible that the uniform scenario has a significantly lower RMSE than the all-in-one-place scenario due to spatial smoothing effects, leading to a reduced variability and hence RMSE. On the other hand, the RMSE of both scenarios varies with the time of day aside from the general increase with the time horizon. At about 10 am, the RMSE is clearly reduced due to the lower average wind speeds, as the power production and variability (see Figure 55).

II.   The second approach for estimating the wind power forecast error for South Africa is based on the evaluation of the wind power prediction time series produced using a typical time series model. The individual simulated wind power time series for both installation scenarios for South Africa serve as a basis for the time series model in this study. As several studies have shown that recent wind power measurements have the highest information content for forecast horizons of one to about three to five hours (compare Figure 53), it seem only appropriate to use the simulated feed-in time series as inputs for forecasting the first few hours, without additional data from numerical weather forecasts. Nevertheless, it is clear that additional weather forecast would increase the forecast quality significantly for horizons larger than three to five hours. On this assumption, wind power forecasts

Wind and Solar Resource Aggregation Study
for South Africa

with lead times of one to five hours have been derived using a common time series model that only uses the simulated time series of the wind power feed-in as input (see also [21]). In principle, the used model is a common linear regression model considering different characteristics of the simulated time series, like trends and gradients on different time scales. The resulting forecast errors in terms of the RMSE are shown in the right plot in Figure 56. On the one hand, it is visible that the uniform scenario leads again to clearly reduced forecast errors. On the other hand, the RMSE values of horizons of about one to two hours show the same error magnitude as estimated by the first approach.

Figure 56: Estimated wind power forecast error for two installation scenarios in South Africa (all in one place, uniform). The left plot shows the estimated RMSE for lead times of one to 48 hours based on an estimation approach described in [21] that is only based on the feed- in characteristics in form of the variability. The right plot presents the RMSE for lead times of one to eight hours that has been calculated out of a wind power forecast time series that has been generated using a common time series model and the time series of the simulated wind power feed-in.

This latter mentioned fact can be interpreted as an additional quality check on the reliability of the results. The larger increase of the RMSE for horizons of up to eight hours is expected, given that additional weather forecasts are not considered.

Summary and Conclusion: Figure 57 shows a bar plot with the final estimated RMSE values for a one-hour and day-ahead (24-48h) wind power forecast for the all-in-one-place and uniform wind power scenarios for South Africa, based on the years 2009 to 2013. It is obvious that the RMSE increases with the forecast horizon. Moreover, uniformly distributed wind energy leads to a forecast error improvement of ~85% for the day-ahead and ~60% for the intra-day as compared to an installation in one place. Within the uniform scenario the forecast error in terms of the RMSE is about 1.6% of the total capacity for the one-hour horizon forecast and about 7.8% for the day-ahead forecast.

Compared to e.g. Germany, the estimated RMSE values are clearly higher, while the considered area in South Africa is larger, which lead in general to larger smoothing effects and smaller errors. The higher values of especially the day-ahead forecast for South Africa can be explained by two reasons. One reason is that the RMSE is estimated by assuming that only a single NWP model with moderate quality has been used, due to the unknown quality of weather forecasts available for the South African regions. With respect to an optimized day-ahead forecast that is based on a combination of different high-quality weather forecasts, an additional improvement of about 20 to 30% can be

Wind and Solar Resource Aggregation Study
for South Africa

expected [20]. The other reason can be explained by the wind characteristics. As shown in Figure 55, South Africa has a comparably high mean wind power production rate of 25 to 45% of the installed capacity, in addition to a high temporal variability of about 3% on average. By comparison, the mean wind power production of Germany is smaller than 20% of the installed capacity and the mean absolute variability amounts to about 1.5%. Both parameters impact the average forecast quality in terms of the RMSE, as illustrated in Figure 54 with respect to the variability. Moreover, the distinctive steep mean wind power gradients at 5 am and 3 pm lead to more frequent phase errors.

To summarize, a reduction of the wind power variability results in a reduction of the average forecast quality.

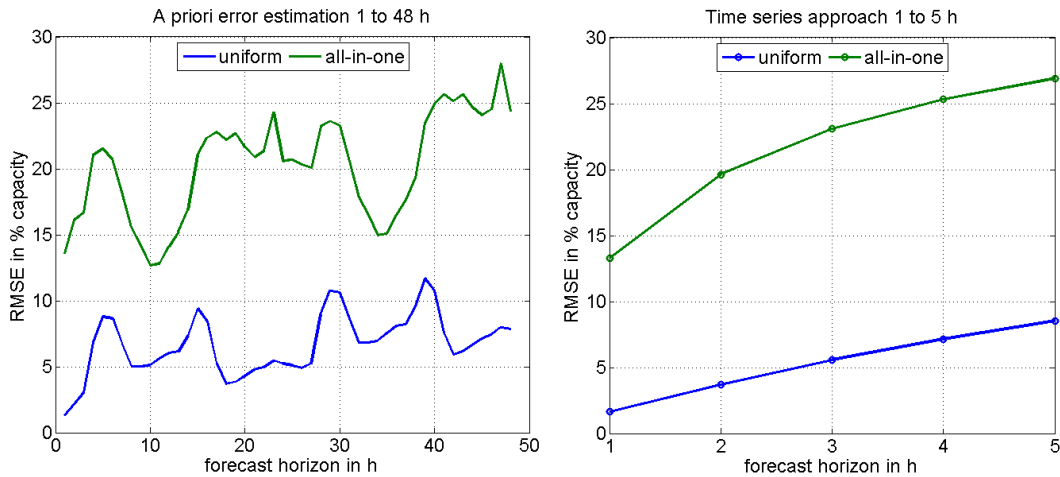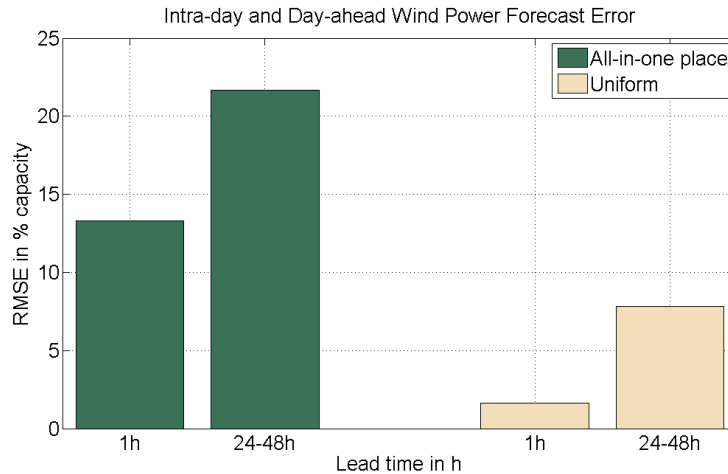**Figure 57: Estimated wind power forecast error for two installation scenarios in South Africa (all-in-one-place, uniform). The bars represent RMSE forecast errors of one-hour forecast horizons and of day-ahead forecasts.**

Wind and Solar Resource Aggregation Study
for South Africa

6. Conclusions

The primary findings of the study include the following:

- The wind resource potential in South Africa is extremely good as solar PV. These potentials exceed the current and the expectable future demand by far. Wind turbines could be operated with extraordinarily high load factors above 0.3 in locations all over the country, large areas even offer load factors around 0.4. In other words, **more than 80% of South Africa's land mass has enough wind resources for low cost wind energy**. Furthermore, South Africa is a large country with a low population density and much space.
- **REDZ are a good starting point** for the larger implementation of wind energy in South Africa. When expanding the REDZ further, the wind resource should not be the limiting factor but only environmental considerations.
- **The low seasonality in wind conditions and solar irradiation** allows a steady electricity supply from renewable enegies compared to the rest of the world. This makes integration of wind and solar PV easier, no seasonal storage is required in particular.
- The existing wide spread interconnected electricity system enables spatial aggregation as investigated in this study. Comparisons of the scenarios taking into account different ways of distributing wind turbines lead to the result that the more distributed wind turbines are being installed, the stronger the aggregation effects. Short term gradients in the aggregated wind power feed-in are significantly reduced by wide spatial distributions of turbines. Where an individual wind farm's power output can fluctuate by +/- 90% of its installed capacity within 15 minutes, a widespread wind fleet's 15-minutes-fluctuations are reduced to +/- 4% of installed capacity. A share of **50% wind energy in South Africa's electricity supply does not increase the short-term (intra-hour) gradients** if the wind fleet is widely distributed; no negative impact on reserve requirements.
- **Up to 20 to 30% energy share of variable renewable energies (wind and solar) does not increase ramps and fluctuations in the system significantly** if there is a balanced combination of wind and PV in the system.
- As determined in [1], at least 20% overcapacity of wind and solar PV power can be installed per substation without any curtailment of wind and solar PV power. If a curtailment of 5% in average is acceptable, the overcapacity could amount 40%. The overcapacity can be much higher, if the load substation is taken into account as well [1] .
- **Distributing wind turbines widely also leads to an improvement in the forecast error of about 85 % for day-ahead** and 60% for intra-day compared to putting all wind turbines in one place.
- The magnitude and cost competeiveness of wind power in South Africa is on par with solar PV. **Solar and wind energy are very low-cost bulk energy providers in South Africa.**

To conclude, South Africa has perfect conditions to introduce a very large amount of variable renewables into the electricity system in a cost-effective way.

7. Outlook

Further research is required that builds on the results achieved in this study. That would be:
- The creation of virtual power plant platforms to balance variable renewable energies.
- The development of forecast models for solar PV and wind feed-in for South Africa.
- The development of a concept for reserve provision from variable renewable energies.
- The determination of the optimal mix of solar PV and wind energy for South Africa.

A study on sector links would be of great interest as well. South Africa could invest into Power-to-Liquid to make the competitive advantage solar/wind resources an export article for a global CO_2-neutral-fuels market.

An extension of the study to the Southern African Power Pool could lead to further revealing findings.

Data and results of this study will be made publically available.

8. Publication bibliography

[1]   S. Bofinger, K. Knorr, and B. Zimmermann, "Analysis of the curtailments needed to integrate wind and solar PV power into substations of the South African transmission grid," Jul. 2016.

[2]   Department of Energy (DoE) South Africa, "Integrated Resource Plan for electricity (IRP) 2010-2030," 2013. [Online] Available: http://www.energy.gov.za/IRP/irp.html.

[3]   C. Mushwana *et al,* "Smoothing out the volatility of South Africa's wind and solar photovoltaic energy resources," *CSIR Science Scope*, vol. 8, no. 2, pp. 28–29, http://reference.sabinet.co.za/document/EJC180012, 2015.

[4]   Eskom, "Transmission development plan 2015-2024," Oct. 2014.

[5]   A. N. Hahmann *et al,* "Mesoscale modeling for the Wind Atlas of South Africa (WASA) project," DTU Wind Energy, Feb. 2015. [Online] Available: http://orbit.dtu.dk/files/107110172/DTU_Wind_Energy_E_0050.pdf. Accessed on: Jan. 13 2016.

[6]   B. Gschwind, L. Ménard, M. Albuisson, and L. Wald, "Converting a Successful Research Project into a Sustainable Service: The Case of the SoDa Web Service," vol. 21, pp. 1555–1561, 2006.

[7]   W. Skamarock *et al,* "A description of the advanced research WRF version 3: NCAR/TN–475+STR," NCAR - National Center for Atmospheric Research, Jun. 2008. [Online] Available: http://www2.mmm.ucar.edu/wrf/users/docs/arw_v3.pdf. Accessed on: Jan. 13 2016.

[8]   N. G. Mortensen *et al, Wind Atlas for South Africa (WASA): Station and Site Description Report.* [Online] Available: http://stel-apps.csir.co.za/wasa-data/docs/WASA_Station_and_Site_Description_Report_%28April_2014%29.pdf. Accessed on: May 19 2016.

[9]   Eskom, "Transmission metering data 2008-2012," 2012.

[10]   M. Suri *et al,* "Cloud cover impact on photovoltaik power production in South Africa," http://geomodelsolar.eu/_docs/papers/2014/Suri-et-al--SASEC2014--Cloud-cover-impact-on-PV-power-production-in-South-Africa.pdf, 2014.

[11]   S. Bofinger, "Rolle der Solarstromerzeugung in zukünftigen Energieversorgungsstrukturen - Welche Wertigkeit hat Solarstrom: Studie im Auftrag des Bundesministeriums für Umwelt, Naturschutz und Reaktorsicherheit," Berlin, 2008.

[12]   Klucher T.M, "Evaluation of models to predict insolation on tilted surfaces," Jan. 1979. [Online] Available: http://ntrs.nasa.gov/search.jsp?R=19790069478. Accessed on: Jan. 14 2016.

[13]   H. Schmidt and Sauer D.U, "Wechselrichter-Wirkungsgrade," *Sonnenenergie 4*, pp. 43–47, 1996.

[14]   H. G. Beyer, G. Heilscher, and S. Bofinger, "A robust model for the MPP performance of different types of PV-modules applied for the performance check of grid connected systems," *EUROSUN 2004 (ISES Europe Solar Congress)*, Jan. 2004.

[15]   Department for Environmental Affairs, *EGIS South Africa.* [Online] Available: http://egis.environment.gov.za/. Accessed on: Jun. 11 2015.

[16]   International Electrotechnical Commission, "EC 61400-1: Wind turbines part 1: Design requirements," 2005.

[17]   K. Knorr *et al,* "Kombikraftwerk 2 - Final report," Aug. 2014. [Online] Available: http://www.kombikraftwerk.de/fileadmin/Kombikraftwerk_2/Abschlussbericht/Abschlussbericht_Kombikraftwerk2_aug14.pdf. Accessed on: Jan. 13 2016.

[18]   CSIR and Department for Environmental Affairs, RSA, *Renewable Energy Development Zones (REDZs).* [Online] Available: https://redzs.csir.co.za. Accessed on: April 2015.

[19]   R. Marais, "Transmission development plan 2015-2024," 2014.

[20]   J. Dobschinski, "How good is my forecast?: Comparability of wind power forecast errors," Proceedings of the 13th International Workshop on Large-Scale Integration of Wind Power into Power Systems as well as on Transmission Networks for Offshore Wind Power Plants, 2014. Accessed on: Jan. 14 2016.

[21]   A. Braun and J. Dobschinski, "Error Reduction of Regional Wind Power Forecast by Integrating Spatio-temporal Information into an Artificial Intelligence Model," Berlin, Germany, Proceedings of the 13th International Workshop on Large-Scale Integration of Wind Power into Power Systems as well as on Transmission Networks, 2014.

9.   Annex

9.1   Wind power correlation between supply areas

The South African transmission grid is divided into 27 supply areas (see Figure 58). Each supply area comprises several grid nodes. The size of the supply areas is determined by the grid topology and location of the total customer load. Supply areas with load centres usually include a high number of nodes in a small area.
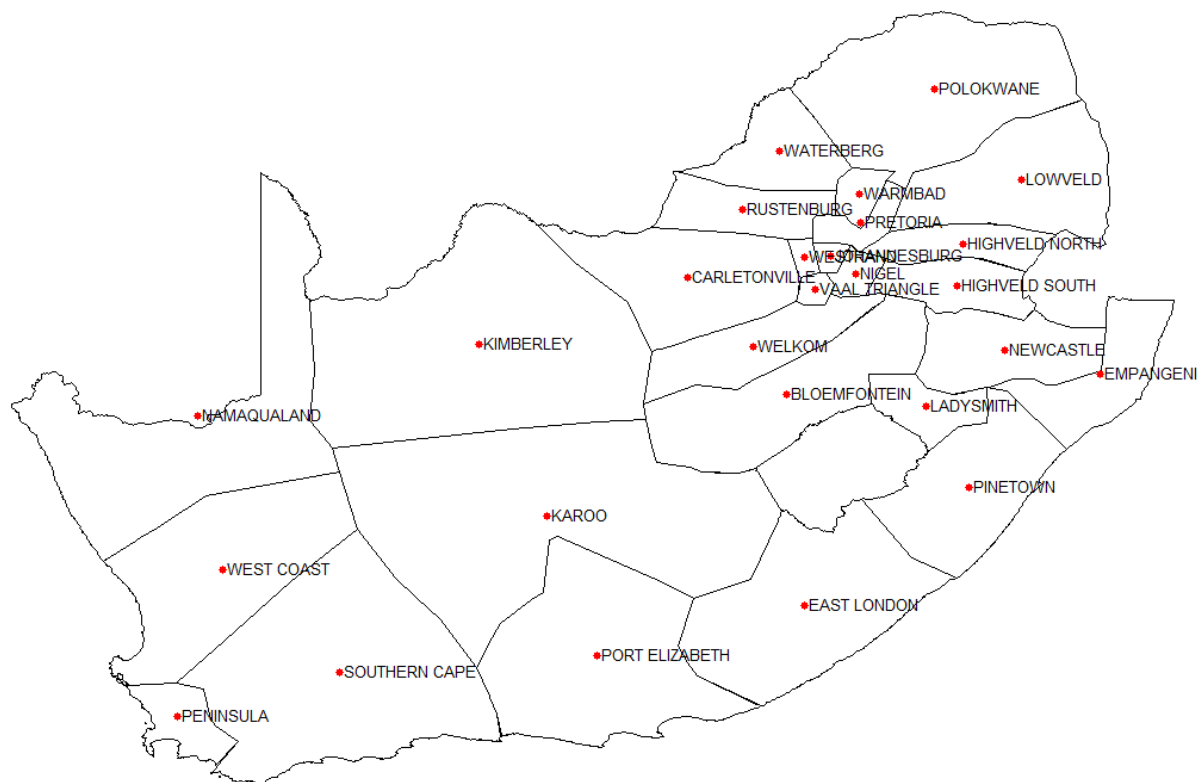
Figure 58: The 27 supply areas of South Africa

In order to assess the correlation between potential wind power feed-ins of supply areas, wind power feed-in was simulated by aggregating all 5 km by 5 km wind power feed-ins of each supply area while applying the exclusion mask (as described in chapter 4.1.1.2). The resulting 27 time series of wind power feed-in of the supply areas with a temporal resolution of 15 minutes and covering a period of 5 years, were analysed in terms of their correlation coefficients:

As can be seen in Table 18 the correlation coefficients between different supply areas range between 0.89 and -0.12. This means that the wind power feed-in for some supply areas are very correlated, others are relatively uncorrelated while some are negatively correlated. A low correlation coefficient is beneficial for spatial aggregation at power system level because it involves low fluctuations. It can be assumed that, apart from the different weather conditions, the distance between supply areas is the main reason for low correlation coefficients. In order to assess the distances between the supply areas there centroids were determined To measure the distances between the supply areas the distances between their centroids were used regardless of whether a centroid is located within its supply area or not (as in the case of Namaqualand). The centroids are shown as red dots in Figure 58.

Figure 59 shows the correlation coefficients of wind power feed-in for supply areas as a function of their respective distances from each other. It is obvious that the further two wind farms are away from each other, the lower the correlation between their wind power-production profiles

Wind and Solar Resource Aggregation Study
for South Africa

The correlation coefficients between the 15min and 1h wind power gradients as shown in Figure 60 and Figure 61 respectively show similar results.

JOHANNESBURG	NIGEL	WESTRAND	VAAL TRIANGLE	NEWCASTLE	PINETOWN	EMPANGENI	WEST COAST	PENINSULA	SOUTHERN CAPE	EAST LONDON	PORT ELIZABETH	KAROO	WATERBERG	POLOKWANE	WARMBAD	RUSTENBURG	WELKOM	BLOEMFONTEIN	HIGHVELD NORTH	HIGHVELD SOUTH	PRETORIA	CARLETONVILLE	KIMBERLEY	LADYSMITH	LOWVELD	NAMAQUALAND	
1.00	0.84	0.89	0.80	0.41	0.29	0.25	0.11	0.14	0.17	0.17	0.14	0.22	0.59	0.45	0.60	0.68	0.70	0.63	0.65	0.60	0.67	0.58	0.25	0.25	0.46	0.13	JOHANNESBURG
	1.00	0.77	0.85	0.46	0.28	0.25	0.13	0.16	0.21	0.16	0.15	0.26	0.59	0.49	0.63	0.60	0.77	0.69	0.72	0.72	0.67	0.56	0.26	0.28	0.49	0.16	NIGEL
		1.00	0.80	0.33	0.25	0.19	0.10	0.12	0.15	0.14	0.10	0.24	0.65	0.47	0.57	0.74	0.73	0.65	0.55	0.51	0.59	0.69	0.30	0.18	0.40	0.13	WESTRAND
			1.00	0.41	0.27	0.26	0.14	0.18	0.21	0.13	0.13	0.30	0.58	0.46	0.54	0.62	0.86	0.74	0.60	0.60	0.54	0.66	0.31	0.29	0.45	0.16	VAAL TRIANGLE
				1.00	0.65	0.74	0.12	0.25	0.34	0.49	0.41	0.32	0.13	0.08	0.17	0.20	0.38	0.48	0.67	0.81	0.28	0.25	0.17	0.78	0.42	0.06	NEWCASTLE
					1.00	0.69	0.08	0.17	0.25	0.59	0.36	0.33	0.14	0.08	0.13	0.19	0.29	0.39	0.37	0.46	0.20	0.24	0.20	0.61	0.23	0.05	PINETOWN
						1.00	0.15	0.18	0.23	0.34	0.26	0.28	0.07	0.04	0.07	0.15	0.26	0.31	0.39	0.45	0.15	0.18	0.16	0.55	0.33	0.13	EMPANGENI
							1.00	0.43	0.64	0.09	0.36	0.50	0.12	0.22	0.17	0.16	0.20	0.22	0.15	0.10	0.15	0.15	0.39	0.08	0.24	0.83	WEST COAST
								1.00	0.69	0.22	0.44	0.38	0.10	0.13	0.13	0.11	0.21	0.27	0.22	0.23	0.13	0.13	0.17	0.28	0.19	0.23	PENINSULA
									1.00	0.46	0.78	0.66	0.09	0.13	0.15	0.13	0.25	0.34	0.27	0.31	0.15	0.16	0.35	0.37	0.20	0.43	SOUTHERN CAPE
										1.00	0.77	0.46	-0.01	-0.12	-0.02	0.06	0.15	0.28	0.25	0.37	0.04	0.16	0.26	0.51	0.04	0.00	EAST LONDON
											1.00	0.61	0.00	0.00	0.06	0.06	0.15	0.27	0.25	0.33	0.09	0.10	0.30	0.45	0.12	0.22	PORT ELIZABETH
												1.00	0.21	0.17	0.20	0.24	0.42	0.55	0.24	0.29	0.19	0.38	0.73	0.31	0.18	0.48	KAROO
													1.00	0.70	0.73	0.76	0.60	0.51	0.39	0.34	0.65	0.64	0.34	-0.01	0.33	0.20	WATERBERG
														1.00	0.74	0.59	0.49	0.43	0.45	0.29	0.66	0.42	0.23	-0.04	0.61	0.29	POLOKWANE
															1.00	0.63	0.54	0.49	0.50	0.39	0.90	0.43	0.23	0.02	0.45	0.24	WARMBAD
																1.00	0.65	0.58	0.47	0.37	0.62	0.70	0.35	0.08	0.45	0.22	RUSTENBURG
																	1.00	0.90	0.55	0.54	0.52	0.76	0.47	0.28	0.46	0.23	WELKOM
																		1.00	0.56	0.58	0.48	0.69	0.51	0.41	0.45	0.23	BLOEMFONTEIN
																			1.00	0.88	0.62	0.35	0.17	0.43	0.73	0.15	HIGHVELD NORTH
																				1.00	0.50	0.36	0.20	0.57	0.54	0.09	HIGHVELD SOUTH
																					1.00	0.41	0.20	0.10	0.52	0.22	PRETORIA
																						1.00	0.61	0.16	0.27	0.19	CARLETONVILLE
																							1.00	0.09	0.14	0.49	KIMBERLEY
																								1.00	0.26	-0.03	LADYSMITH
																									1.00	0.25	LOWVELD
																										1.00	NAMAQUALAND

Table 18: Correlation coefficients of wind-power production of supply areas

JOHANNESBURG	NIGEL	WESTRAND	VAAL TRIANGLE	NEWCASTLE	PINETOWN	EMPANGENI	WEST COAST	PENINSULA	SOUTHERN CAPE	EAST LONDON	PORT ELIZABETH	KAROO	WATERBERG	POLOKWANE	WARMBAD	RUSTENBURG	WELKOM	BLOEMFONTEIN	HIGHVELD NORTH	HIGHVELD SOUTH	PRETORIA	CARLETONVILLE	KIMBERLEY	LADYSMITH	LOWVELD	NAMAQUALAND	
0	49	37	65	299	463	435	1015	1222	1013	638	796	616	204	339	121	151	197	260	189	187	75	206	520	306	305	929	JOHANNESBURG
	0	80	64	251	419	388	1025	1225	1012	609	781	615	249	355	146	199	196	240	161	144	94	238	545	261	291	953	NIGEL
		0	62	329	479	467	984	1196	989	636	781	592	196	358	139	123	179	253	226	222	102	170	485	322	339	895	WESTRAND
			0	288	419	427	962	1164	953	577	732	555	257	403	186	179	135	196	224	200	139	182	482	264	354	890	VAAL TRIANGLE
				0	253	140	1140	1299	1075	539	785	698	483	486	352	450	351	313	202	135	309	465	733	149	312	1122	NEWCASTLE
					0	274	1020	1136	909	310	588	578	667	726	556	597	394	302	442	367	506	547	725	158	564	1064	PINETOWN
						0	1248	1388	1163	584	854	803	608	569	472	586	486	436	305	257	436	604	866	248	371	1247	EMPANGENI
							0	275	244	783	525	449	1087	1323	1117	975	833	834	1180	1134	1086	833	541	1003	1314	284	WEST COAST
								0	228	854	564	614	1320	1545	1333	1205	1030	1009	1371	1317	1296	1059	792	1154	1511	551	PENINSULA
									0	630	342	398	1126	1343	1127	1010	818	789	1155	1098	1088	863	628	929	1296	507	SOUTHERN CAPE
										0	291	385	829	957	754	728	479	386	693	619	703	620	653	399	831	895	EAST LONDON
											0	265	953	1133	916	839	604	542	902	835	869	702	591	637	1046	697	PORT ELIZABETH
												0	740	949	731	623	420	397	760	706	691	477	327	557	901	512	KAROO
													0	250	138	118	358	444	312	352	174	265	553	509	349	950	WATERBERG
														0	219	351	535	594	286	360	265	492	798	578	206	1197	POLOKWANE
															0	169	380	174	218	52	288	604	399	232	1012	WARMBAD
																0	251	344	319	334	169	148	447	443	400	852	RUSTENBURG
																	0	100	349	307	272	156	383	265	485	780	WELKOM
																		0	368	310	331	255	439	194	512	815	BLOEMFONTEIN
																			0	76	151	394	705	300	144	1112	HIGHVELD NORTH
																				0	179	381	679	224	214	1082	HIGHVELD SOUTH
																					0	265	582	348	241	992	PRETORIA
																						0	317	409	506	728	CARLETONVILLE
																							0	632	822	411	KIMBERLEY
																								0	434	1005	LADYSMITH
																									0	1230	LOWVELD
																										0	NAMAQUALAND

Table 19: Distances between supply areas [km]

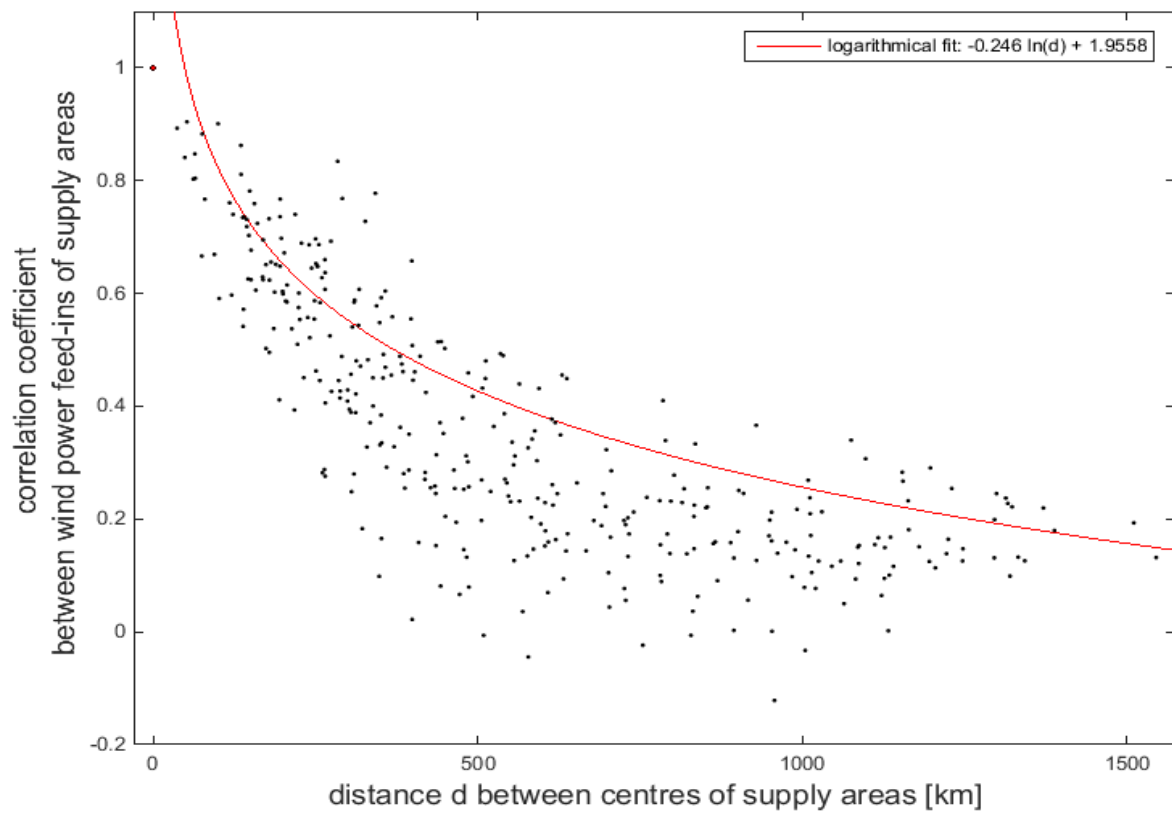Wind and Solar Resource Aggregation Study
for South Africa

Figure 59: Correlation coefficients of wind-power production of supply areas as a function of their distances
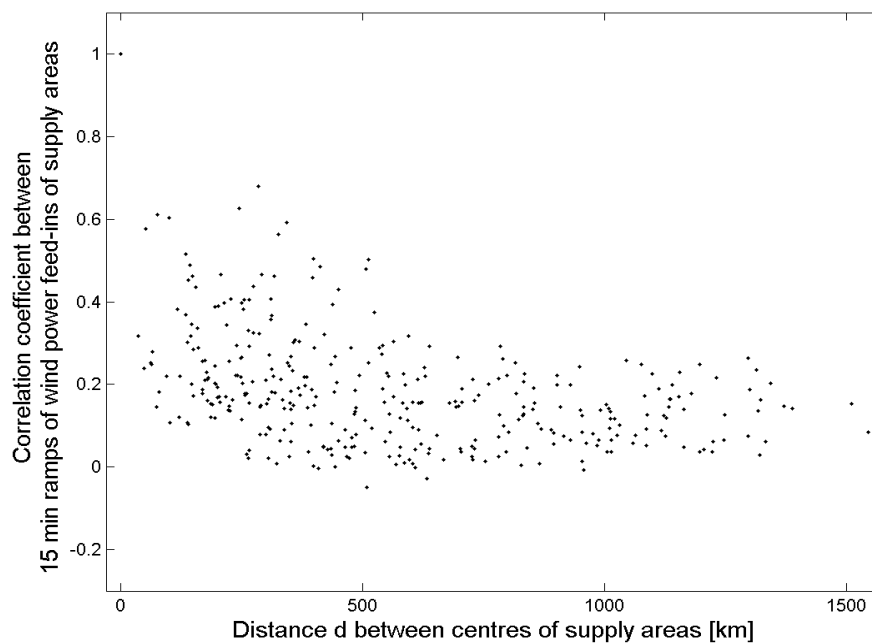

Figure 60: Correlation coefficients of 15min wind-power gradients of supply areas as a function of their distances
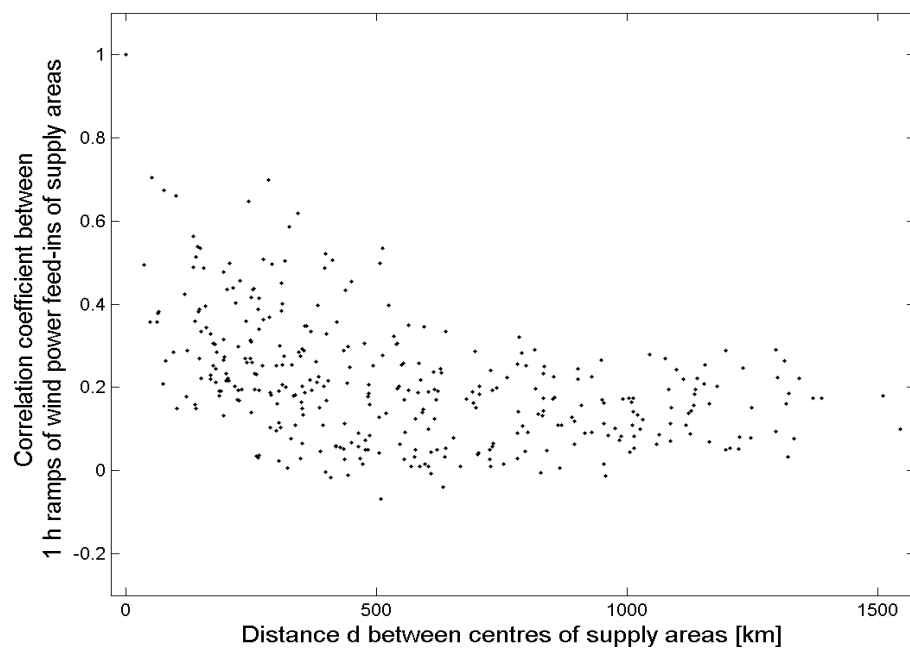
Figure 61: Correlation coefficients of 1h wind-power gradients of supply areas as a function of their distances

Wind and Solar Resource Aggregation Study
for South Africa